

NASA Contract Report 165833

NASA-CR-165833  
19820011121

---

Cabin Noise Control  
For Twin Engine  
General Aviation Aircraft

R. Vaicaitis and M. Slazak

**Modern Analysis Inc.**  
**Ridgewood, New Jersey**

**CONTRACT NAS1-16117**  
**February 1982**

LIBRARY COPY

1 5 1982

LANGLEY RESEARCH CENTER  
HAMPTON, VIRGINIA  
10703, VIRGINIA

**NASA**

National Aeronautics and  
Space Administration

**Langley Research Center**  
Hampton, Virginia 23665



NF01355

---

NASA Contract Report 165833

# Cabin Noise Control For Twin Engine General Aviation Aircraft

R. Vaicaitis and M. Slazak

**Modern Analysis Inc.  
Ridgewood , New Jersey**

**CONTRACT NAS1-16117  
February 1982**

**NASA**

National Aeronautics and  
Space Administration

**Langley Research Center**  
Hampton Virginia 23665

*N82-18995 #*

NASA Contract Report 165833

CABIN NOISE CONTROL FOR TWIN  
ENGINE GENERAL AVIATION AIRCRAFT

R. Vaicaitis and M. Slazak

MODERN ANALYSIS INC.  
RIDGWOOD, NEW JERSEY

CONTRACT NAS1-16117

February 1982

## TABLE OF CONTENTS

<u>Section</u>		<u>page</u>
1.0	SUMMARY	1
2.0	INTRODUCTION	2
3.0	ANALYTICAL MODEL	4
3.1	Acoustic Model	4
3.2	Response of Sidewall Panels	7
3.3	Natural Frequencies and Modes of Sidewall Panels	10
3.4	Acoustic-Structural Model	13
3.5	Acoustic Absorption	16
3.6	External Pressure Field	17
3.7	Total TL Including Add-On Treatment	18
4.0	INTERIOR NOISE OPTIMIZATION	24
5.0	NUMERICAL RESULTS	26
5.1	Baseline Aircraft	26
5.2	Modes and Frequencies	27
5.3	Noise Levels in Baseline Aircraft	28
5.4	Sidewall Treatment With Honeycomb Panels	29
5.5	Damping Tape and Mass Addition	32
5.6	Honeycomb and Damping Tape Treatment	34
5.7	Additional Noise Losses Due to Acoustic Blankets, Septum and Trim Panels	35
5.8	Noise Transmission Through Windows	38
5.9	Noise Optimization in the Aircraft	38

<u>Section</u>	<u>page</u>
6.0 CONCLUSIONS	41
REFERENCES	44
APPENDIX A Elements of Transfer Matrices	128
APPENDIX B List of Symbols	132

LIST OF TABLES

<u>Table</u>		<u>page</u>
1	Material and Geometric Properties of Stiffeners	47
2	Natural Frequencies of Sidewall Panels (n = 1,3,5)	48
3	Natural Frequencies of Stiffened Panels for AeroCommander Sidewall With Honeycomb Add-On Treatment (First Frequency Band)	49
4	Fundamental Frequencies of the Stiffened Panel Units With Different Damping Tape Add-On Treatments	50

## LIST OF FIGURES

<u>Figure</u>		<u>page</u>
1	Twin-Engine Aircraft Used in the Noise Optimization Study	51
2	Structural Features of a Twin-Engine Light Aircraft	52
3	Simplified Geometry of Aircraft Cabin Model	53
4	Aircraft Sidewall Used for Noise Transmission Study	54
5	A Multispanned Skin-Stringer System	55
6	Geometry of a Double Wall Window Construction	56
7	Propeller Noise Input (Panel Unit No. 1)	57
8	Propeller Noise Input (Panel Unit No. 2)	58
9	Propeller Noise Input (Panel Unit Nos. 3 and 7)	59
10	Propeller Noise Input (Panel Unit Nos. 4, 9 and 10)	60
11	Propeller Noise Input (Panel Unit No. 5)	61
12	Propeller Noise Input (Panel Unit No. 6)	62
13	Propeller Noise Input (Panel Unit No. 8)	63
14	Geometry of Sidewall Treatment	64
15	Flow Diagram for Computation of Interior Noise	65
16	Details of Skin-Stringer Construction	66
17	Mode Shapes of a Stiffened Panel for the First Frequency Band (Panel No. 6)	67
18	Sound Levels in the Aircraft Cabin	68
19	Noise Reduction for a Stiffened Panel With and Without Cross-Modal Terms	69
20	Interior Noise Levels With and Without Convection	70
21	Interior Noise Levels With Honeycomb Treatment (Panel No. 1)	71
22	Interior Noise Levels With Honeycomb Treatment (Panel No. 2)	72

<u>Figure</u>		<u>page</u>
23	Interior Noise Levels With Honeycomb Treatment (Panel No. 3)	73
24	Interior Noise Levels With Honeycomb Treatment (Panel No. 4)	74
25	Interior Noise Levels With Honeycomb Treatment (Panel No. 6)	75
26	Interior Noise Levels With Honeycomb Treatment (Panel No. 10)	76
27	Interior Noise Levels With Honeycomb Treatment (Sidewall)	77
28	Interior Noise Levels With Heavy Honeycomb Treatment (Panel Nos. 1 and 2)	78
29	Interior Noise Levels With Heavy Honeycomb Treatment (Panel No. 3)	79
30	Interior Noise Levels With Heavy Honeycomb Treatment (Panel No. 4)	80
31	Interior Noise Levels With Heavy Honeycomb Treatment (Panel No. 6)	81
32	Interior Noise Levels With Heavy Honeycomb Treatment (Sidewall)	82
33	Interior Noise With Damping Tape Treatment (Panel No. 1)	83
34	Interior Noise With Damping Tape Treatment (Panel No. 2)	84
35	Interior Noise With Damping Tape Treatment (Panel No. 3)	85
36	Interior Noise With Damping Tape Treatment (Panel No. 4)	86
37	Interior Noise With Damping Tape Treatment (Panel No. 6)	87
38	Interior Noise With Damping Tape Treatment (Panel No. 9)	88
39	Interior Noise With Damping Tape Treatment (Sidewall)	89
40	Interior Noise With Damping Tape and Mass Treatment (Panel No. 1)	90
41	Interior Noise With Damping Tape and Mass Treatment (Panel No. 2)	91
42	Interior Noise With Damping Tape and Mass Treatment (Panel No. 4)	92
43	Interior Noise With Damping Tape and Heavy Mass Treatment (Panel No. 4)	93

<u>Figure</u>		<u>page</u>
44	Interior Noise With Damping Tape and Heavy Mass Treatment (Panel No. 6)	94
45	Interior Noise With Damping Tape and Heavy Mass Treatment (Panel No. 6, Add-On = 3.28 lb/ft <sup>2</sup> )	95
46	Interior Noise With Honeycomb-Damping Tape Treatment (Panel No. 1)	96
47	Interior Noise With Honeycomb-Damping Tape Treatment (Panel No. 2)	97
48	Interior Noise With Honeycomb-Damping Tape Treatment (Panel No. 3)	98
49	Interior Noise With Honeycomb-Damping Tape Treatment (Panel No. 4)	99
50	Interior Noise With Honeycomb-Damping Tape Treatment (Panel No. 6)	100
51	Interior Noise With Honeycomb-Damping Tape Treatment (Panel No. 10)	101
52	Interior Noise With Honeycomb-Damping Tape Treatment (Sidewall)	102
53	Interior Noise Levels With Heavy Honeycomb-Damping Tape Treatment (Panel No. 3)	103
54	Additional Transmission Losses for Acoustic Blankets and Semi-Rigid Materials ( $\mu_5 = 0.01$ lb/ft <sup>2</sup> )	104
55	Additional Transmission Losses for Acoustic Blankets and Semi-Rigid Materials ( $\mu_5 = 0.358$ lb/ft <sup>2</sup> )	105
56	Additional Transmission Losses for Acoustic Blankets and Semi-Rigid Materials ( $\mu_5 = 1.0$ lb/ft <sup>2</sup> )	106
57	Additional Transmission Losses for Acoustic Blankets and Semi-Rigid Materials ( $\mu_3 = 1.0$ lb/ft <sup>2</sup> )	107
58	Additional Transmission Losses for Acoustic Blankets and Semi-Rigid Materials ( $d_2 = d_4 = 0.167$ ft)	108
59	Additional Transmission Losses for Different Trim Panel Surface Densities	109
60	Additional Transmission Losses for Add-On Treatment ( $\mu_1 = 1.15$ , $\mu_5 = 0.01$ )	110

<u>Figure</u>		<u>page</u>
61	Additional Transmission Losses for Different Distances Between the Elastic Panel and the Trim Panel	111
62	Additional Transmission Losses for a Light Septum and Different Distances Between the Elastic Panel and the Septum	112
63	Additional Transmission Losses for Different Distances Between the Elastic Panel and the Septum	113
64	Interior Noise Transmitted by a Window (Panel No. 5)	114
65	Interior Noise Transmitted by a Window (Panel No. 7)	115
66	Interior Noise Transmitted by a Window (Panel No. 8)	116
67	Optimized Interior Noise (Panel No. 1)	117
68	Optimized Interior Noise (Panel No. 2)	118
69	Optimized Interior Noise (Panel No. 3)	119
70	Optimized Interior Noise (Panel No. 4)	120
71	Optimized Interior Noise (Panel No. 6)	121
72	Optimized Interior Noise (Panel No. 9)	122
73	Optimized Interior Noise (Panel No. 10)	123
74	Optimized Interior Noise (Sidewall)	124
75	Interior Sound Pressure Levels vs. the Ratio of Treated/Untreated Weight	125
76	Distribution of Surface Density	126
77	The Final Configuration of Add-On Treatment for the AeroCommander Aircraft	127

## 1. Summary

An analytical model has been developed to predict the noise transmission into the cabin of a twin-engine G/A aircraft. This model is then used to optimize the interior A-weighted noise to an average level of 85 dBA. The basic concept of the analytical model is that of modal analysis wherein the acoustic modes in the cabin and the structural modes of the sidewalls are accounted for.

The noise input pressure due to propeller blade passage harmonics is expressed in the form of a propagating pressure field wherein noise spectral levels measured under static test conditions are used. The cabin interior is treated as a rectangular enclosure. The sidewalls of the aircraft are modeled by several discretely stiffened panel units. Transfer matrix techniques are used to calculate the natural frequencies and normal modes of the skin-stringer panels. The additional noise losses due to cabin sidewall treatments which do not have a direct effect on the structural dynamic characteristics of the skin-stringer panels are estimated by the impedance transfer method.

To reduce the average noise levels in the cabin from about 105 dBA (baseline) to 85 dBA (optimized), add-on treatments which do not involve changes in the fuselage primary structure are used. The add-on treatments considered in this optimization study include lightweight aluminum honeycomb panels, constrained layer damping tapes, porous acoustic blankets, septum barriers and limp trim panels. The added weight of the noise control treatment is about 1.1% of the total gross take-off weight of the aircraft.

## 2. Introduction

Significant advances in the theoretical formulation and analysis of noise transmission into aircraft have been made in the recent past [1 - 15]. Some of these analytical models have been validated by experiments ranging in complexity from a simple box with one elastic side [9, 12] to full-scale tests measuring the noise transmission through one sidewall of the G/A aircraft under a white noise input [12]. Preliminary noise transmission studies [4, 15] have shown that a satisfactory agreement between theory and experiment can be achieved for built-up sidewalls consisting of a stiffened elastic panel, acoustic blankets, septum barriers and trim panel. In many of these studies, however, the main emphasis was placed on establishing correct and valid mathematical models of noise transmission, and not enough effort was devoted to deriving practical recommendations for the detailed and systematic evaluations of various methods of add-on treatment for reducing cabin noise to acceptable levels while adding the least amount of weight to the aircraft. In the present paper, a detailed analytical study of noise control with add-on treatments for a twin engine G/A aircraft is presented.

The basic concept of the analytical model is that of modal analysis wherein the acoustic modes in the cabin and the structural modes of the sidewall are accounted for [10 - 14]. The resonant and non-resonant response characteristics of the acoustic cavity and the sidewall panels are estimated by performing a narrow band analysis for frequencies up to 1122 Hz. In order to provide an analytical model which does not have very extensive computational requirements, various assumptions and simplifications are incorporated. The nearly flat floor, sidewalls and ceiling of the aircraft considered in this study of a 680 AeroCommander suggest that the cabin interior may be treated

as a rectangular enclosure. The rectangular shape allows for a simple representation of the acoustic modes rather than the more unwieldy finite element representations of the actual cabin shape. The sidewalls of the aircraft are modeled by several discretely stiffened panel units. The stiffeners and frames are included in the structural model either as discrete elements for the skin-stringer panels or as flexible boundaries for the selected stiffened panel unit. Transfer matrix techniques [12, 16, 17] are used to calculate the natural frequencies and normal modes of the skin-stringer panels. The dynamic characteristics of the double and single wall curved plexiglass windows are determined by performing an analysis on the windows with a dynamically "equivalent" single and flat plexiglass panel. The results from theoretical studies of double wall window constructions [18] are utilized for this purpose.

To estimate the noise losses due to add-on treatments such as acoustic blankets, septum barriers and trim panels, an analytical procedure based on the impedance transfer method is used [19, 20]. A reasonable agreement between these analytical predictions and experimental measurements has been achieved [15]. Differing add-on treatments lend differing amounts of noise reduction and differing amounts of weight to the aircraft. To optimize cabin noise for the least amount of added weight, a sensitivity analysis of the interior noise with respect to the different add-on treatments is performed. The add-on treatments considered in this noise optimization study include damping tape, acoustic blankets, septum barriers, honeycomb panels and trim panels.

To predict the amount of noise transmitted into the aircraft, the external excitation pressure field has to be defined. The noise input due to propeller blade passage harmonics can be expressed in terms of noise spectra levels, correlations and spatial pressure distributions. The surface pressure data corresponding to ground test conditions [21 - 23] are used for the analytical

study.

### 3. Analytical Model

The basic concept of the analytical model is that of modal analysis. This approach has been used for many noise transmission related problems [1, 6, 9-15]. For resonant acoustic cavities, lightly damped structural components and narrow band inputs such as propeller noise due to blade passage harmonics, modal analysis seems to be an attractive and efficient method to use.

#### 3.1 Acoustic Model

Consider that the interior space of the aircraft shown in Figs. 1 and 2 can be approximated by a rectangular enclosure occupying a volume  $V = abd$  as shown in Fig. 3. It is assumed that the main contribution to the interior noise is transmitted by the sidewalls at  $z = 0, d$  (shown by a dashed line in Fig. 2), and that the remaining surfaces are acoustically rigid. Figure 2 suggests that the floor members are of a heavy construction, which together with the greater distance from the propeller tips (Fig. 1) suggests that the floor transmits a relatively small amount of noise when compared to the airborne noise transmitted by the sidewalls. A similar assumption is invoked for the ceiling. The interior walls at  $z = 0, d$  are taken to be absorbent while the remaining walls are assumed to be acoustically hard. The contribution to noise losses due to absorption at these walls is included in the expression for the "equivalent" acoustic damping. Taking the perturbation pressure  $p$  to be at rest prior to the motions of the flexible sidewalls, the pressure inside the enclosure satisfies the acoustic wave equation

$$\nabla^2 p + \beta \frac{\partial p}{\partial t} = \frac{1}{c^2} \partial^2 p / \partial t^2 \quad (1)$$

where

$$\nabla^2 = \partial^2/\partial x^2 + \partial^2/\partial y^2 + \partial^2/\partial z^2 \quad (2)$$

and  $\beta$  is the acoustic damping coefficient. The boundary conditions to be satisfied are

$$\partial p/\partial z = -\rho \partial p/\partial t/Z_A \quad \text{at } z = d \quad (3a)$$

$$\partial p/\partial z = -\rho \partial p/\partial t/Z_A - \rho \partial^2 w/\partial t^2|_{S_F} \quad \text{at } z = 0 \quad (3b)$$

$$\partial p/\partial n = 0 \quad \text{otherwise} \quad (3c)$$

where  $\partial p/\partial n$  is the normal derivative at the wall surface,  $Z_A$  is the absorbent wall impedance assumed to be uniformly distributed over the wall surface and  $w$  is the displacement of the flexible wall  $S_F$ .

Taking the Fourier transformation of Eqs. 1 - 3 and writing the solution for the acoustic pressure in terms of orthogonal acoustic modes corresponding to hard walls at  $x = 0, a$  and  $y = 0, b$ , yields

$$\bar{p}(x, y, z, \omega) = \sum_{i=0}^{\infty} \sum_{j=0}^{\infty} \phi_{ij}(z, \omega) X_{ij}(x, y) \quad (4)$$

where  $\phi_{ij}$  are the modal coefficients and  $X_{ij}$  are the acoustic modes of the rectangular enclosure

$$X_{ij}(x, y) = \cos \frac{i\pi x}{a} \cos \frac{j\pi y}{b} \quad (5)$$

where a bar indicates a transformed quantity. By expanding the transformed flexible wall motions,  $\bar{w}$ , in terms of the acoustic modes and utilizing the

transformed boundary conditions given by Eq. 3, it can be shown that

$$\begin{aligned} \Phi_{ij}(z, \omega) = & \{G_{ij}(\omega)/(\lambda_{ij} - \rho^2\omega^2/Z_A^2\lambda_{ij}) \sin \lambda_{ij}d\} \\ & \cdot \{\cos \lambda_{ij}(d - z) + (i\rho\omega/Z_A\lambda_{ij}) \sin \lambda_{ij}(d - z)\} \end{aligned} \quad (6)$$

where

$$\lambda_{ij} = \{\omega^2 - \omega_{ij}^2 - 2i\xi_{ij}\omega_{ij}\omega\}^{1/2}/c \quad (7)$$

in which  $\omega_{ij} = c\{(i\pi/a)^2 + (j\pi/b)^2\}^{1/2}$  and  $\xi_{ij} = \beta c^2/2\omega_{ij}$ . In the present

study, the quantity  $\beta c^2$  is taken to be equal to  $2\omega_{10}\xi_0$  where  $\xi_0$  is the "equivalent" acoustic damping coefficient and  $\omega_{10}$  is the lowest modal frequency in the enclosure. The acoustic-structural coupling is reflected in the term  $G_{ij}$  where

$$G_{ij}(\omega) = \frac{\rho\omega^2 e_{ij}}{ab} \int_{a_0}^{a_0+L_x} \int_{b_0}^{b_0+L_y} \bar{w}(x, y, \omega) X_{ij}(x, y) dx dy \quad (8)$$

and

$$e_{ij} = \begin{cases} 1 & i = 0, j = 0 \\ 2 & \text{either } i \neq 0 \text{ or } j \neq 0 \\ 4 & i \neq 0, j \neq 0 \end{cases} \quad (9)$$

The solution for the perturbation pressure given in Eqs. 4 - 9 is in terms of the flexible wall motions  $\bar{w}(x, y, \omega)$ . Thus, the response characteristics of the flexible elastic panels must be determined next.

### 3.2 Response of Sidewall Panels

The flexible portion of the aircraft sidewalls shown in Figs. 1 and 2 is composed of an external skin which is stiffened by stringers and frames, thermal and acoustic insulation, acoustic barriers, trim panels and several single- and double-wall window units. While it is possible to model a sidewall by a single panel unit, it is much more feasible to break the sidewall down into smaller units. Such a segmentation offers significant advantages for noise transmission path identification and interior noise optimization. Due to the rapid spatial decay of the amplitude of the external noise pressure and the very stiff boundary conditions of some of the panel units, such an approximation seems to be justified for this type of fuselage construction. The details of a segmented sidewall are shown in Fig. 4.

The governing equation of motion for a single elastic panel located at  $z = 0$ ,  $a_0 \leq x \leq a_0 + L_x$ ,  $b_0 \leq y \leq b_0 + L_y$ , can be written in the frequency domain as

$$D\nabla^4\bar{w} + i\omega\zeta\bar{w} - m_s\omega^2\bar{w} = \bar{p}^r(x,y,\omega) - \bar{p}(x,y,0,\omega) \quad (10)$$

where  $D$  is the plate stiffness,  $\zeta$  is the structural damping coefficient,  $m_s$  is the panel mass per unit area,  $\bar{p}^r$  is the random external noise pressure,  $\bar{p}(x,y,0,\omega)$  is the cavity back pressure acting on the interior surface of the panel, and  $\nabla^4$  is the biharmonic operator. In the present analysis it is assumed that the viscous damping coefficient can be expressed as a linear combination of the mass and stiffness so that the resulting modal equations will not be coupled through the structural damping term. Furthermore, it is assumed that the acoustic blankets, septum barriers and trim panels have no direct effect on the response of the elastic panels. The noise reduction due to these treatments is estimated separately.

The solution for the panel deflection  $\bar{w}$  is expressed in terms of the panel modes:

$$\bar{w}(x,y,\omega) = \sum_{m=1}^{\infty} \sum_{n=1}^{\infty} \bar{q}_{mn}(\omega) Y_{mn}(x,y) \quad (11)$$

where  $\bar{q}_{mn}$  are generalized coordinates and  $Y_{mn}$  are orthogonal panel modes. In the remainder of this work, the indices  $m$  and  $n$  will be used to denote quantities related to the plate motion, and  $i,j$  will refer to the fluid motion. Substitution of Eq. 11 into Eq. 10 and utilization of the orthogonality principle yields

$$\bar{q}_{mn} = H_{mn} \left[ P_{mn}^r - \frac{\rho\omega^2}{abM_{mn}} \sum_{i=0}^{\infty} \sum_{j=0}^{\infty} Z_{ij}(0,\omega) \sum_{r=1}^{\infty} \sum_{s=1}^{\infty} \bar{q}_{rs} L_{ijrs} L_{ijmn} \right] \quad (12)$$

where the frequency response function of the panel is

$$H_{mn} = [\omega_{mn}^2 - \omega^2 + 2i\zeta_{mn}\omega_{mn}\omega]^{-1} \quad (13)$$

and

$$Z_{ij}(z,\omega) = \{e_{ij}/(\lambda_{ij} - \rho^2\omega^2/Z_A^2\lambda_{ij}) \sin \lambda_{ij}d\} \{ \cos \lambda_{ij}(d-z) + (i\rho\omega/Z_A\lambda_{ij}) \sin \lambda_{ij}(d-z) \} \quad (14)$$

in which  $\zeta_{mn} = \zeta_0(\omega_{11}/\omega_{mn})$  where  $\zeta_0$  is the damping coefficient and  $\omega_{mn}$  are modal frequencies. The generalized random forces due to external noise pressure are

$$P_{mn}^r = \frac{1}{M_{mn}} \int_{a_0}^{a_0+L_x} \int_{b_0}^{b_0+L_y} \bar{p}^r(x,y,\omega) Y_{mn}(x,y) dx dy \quad (15)$$

The response of a stiffened panel can be obtained from Eqs. 11-15 by replacing the modes  $Y_{mn}$  and the frequencies  $\omega_{mn}$  by those corresponding to a stiffened panel. Then, the generalized mass  $M_{mn}$  can be written as

$$M_{mn} = m_s \int_{a_0}^{a_0+L_x} \int_{b_0}^{b_0+L_y} Y_{mn}^2(x,y) dx dy + \sum_{k=1}^N m_k \int_{a_0}^{a_0+L_x} Y_{mn}^2(x,y_k) dx \quad (16)$$

in which  $m_k$  is the mass per unit length of the k-th stringer, and  $y_k = \sum_{i=1}^k b_i$  where  $b_i$  is the distance between the i-1 and i-th stringers. The quantities  $L_{ijmn}$  of Eq. 12 are parameters which couple the panel vibration modes to the acoustic cavity modes and are defined as

$$L_{ijmn} = \int_{a_0}^{a_0+L_x} \int_{b_0}^{b_0+L_y} Y_{mn}(x,y) X_{ij}(x,y) dx dy \quad (17)$$

In order to completely determine the panel motion and the acoustic pressure inside the cabin, the coupled system of Eqs. 12 must be solved for  $\bar{q}_{mn}$ . It should be noted that Eq. 12 is general and accounts for all the coupling effects between the panel and the cavity. However, some simplifying assumptions, suggested by previous work [24 - 29] can circumvent the lengthy numerical solution of the coupled system for  $\bar{q}_{mn}$ . For cases where the cavity is sufficiently deep and the panel is sufficiently stiff, the coupling terms in Eq. 12 due to back-up acoustic pressure can be neglected and the structural modal coefficients  $\bar{q}_{mn}$  can be computed explicitly in terms of the generalized random forces  $P_{mn}^r$ . Then, from Eqs. 11 and 12, the panel response can be expressed as

$$\bar{w}(x,y,\omega) = \sum_{m=1}^{\infty} \sum_{n=1}^{\infty} H_{mn}(\omega) P_{mn}^r(\omega) Y_{mn}(x,y) \quad (18)$$

The cross-spectral density of the panel deflection response  $S_w(x_1, x_2; y_1, y_2; \omega)$  can be obtained by taking the mathematical expectation of Eq. 18 and then using the spectral decomposition presented in Ref. 17. By setting  $x_1 = x_2 = x$ ,  $y_1 = y_2 = y$ , the spectral density of the panel deflection response is

$$S_w(x, y, \omega) = \sum_{m=1}^{\infty} \sum_{n=1}^{\infty} \sum_{r=1}^{\infty} \sum_{s=1}^{\infty} H_{mn}(\omega) H_{rs}^*(\omega) S_{mnrs}^r(\omega) \cdot Y_{mn}(x, y) \cdot Y_{rs}(x, y) \quad (19)$$

where the cross-spectral density of the generalized random input forces is

$$S_{mnrs}(\omega) = \frac{1}{M_{mn} M_{rs}} \int_{a_0}^{a_0+L_x} \int_{a_0}^{a_0+L_x} \int_{b_0}^{b_0+L_y} \int_{b_0}^{b_0+L_y} S^e(\bar{x}, \bar{y}, \omega) \cdot Y_{mn}(x_1, y_1) \cdot Y_{rs}(x_2, y_2) dx_1 dx_2 dy_1 dy_2 \quad (20)$$

in which  $S^e$  is the cross-spectral density of the random input noise pressure  $p^r$  and  $\bar{x} = x_2 - x_1$ ,  $\bar{y} = y_2 - y_1$ . The asterisk in Eq. 19 denotes a complex conjugate. To complete the solution for panel deflections and subsequently for the interior acoustic pressure, the natural frequencies and normal modes of the elastic panels are needed.

### 3.3 Natural Frequencies and Normal Modes of Sidewall Panels

In the present study, we seek the natural frequencies and normal mode shapes of the two-dimensional stiffened panels shown in Fig. 5 and double wall curved window constructions shown in Fig. 6. These results are used in Eqs. 11 - 17 to calculate the deflection response. The natural frequencies,  $\omega_{mn}$ , and normal modes,  $Y_{mn}$ , of the stiffened panel unit shown in Fig.

5 are determined by using transfer matrix methods [12, 16, 17]. A brief description of this procedure will now be given. The stiffened panel No. 6 shown in Figs. 4 and 5 is assumed to be simply supported along the frames at  $x = a_0$  and  $x = a_0 + L_x$ . Then, the normal modes corresponding to the direction along the stringers are  $\sin \{(\pi/L_x)(x - a_0)\}$ . Substitution of this relation into Eq. 10 and setting  $\bar{p}^r$  and  $\bar{p}(x, y, 0, \omega) = 0$  results in a fourth order homogeneous differential equation for each  $n$ . Utilizing the characteristic roots, the solution for this equation can be written in a state vector form:  $\{W_n\} = \{\delta_n, \theta_n, M_n, V_n\}$  where  $\delta_n, \theta_n, M_n$  and  $V_n$  are the components of deflection, slope, moment and shear, respectively. A transfer matrix  ${}^r_N[T]_0^L$  can then be constructed which transfers the state vector from the left side of station 0 to the right side of station N (see Fig. 5). Then, we can write

$$\{W_n\}_N^r = {}^r_N[T]_0^L \{W_n\}_0^L \quad (21)$$

where

$${}^r_N[T]_0^L = [G]_N [F]_N [G]_{N-1} \dots [F_1] [G]_0 \quad (22)$$

The point matrix  $[G]$  transfers the state vector across a stringer and the field matrix  $[F]$  transfers the state vector across a panel. The detailed expressions for these transfer matrices can be found in Appendix A. Utilizing the natural boundary conditions at  $y = b_0$  and  $y = b_0 + L_y$  in Eq. 21 yields an equation which can then be solved for the natural frequencies  $\omega_{mn}$ . For the purpose of illustration, assume simply supported boundaries at the end stations 0 and N for which  $\{W_n\}_0^L = \{0, \theta_n, 0, V_n\}_0^L$  and  $\{W_n\}_N^r = \{0, \theta_n, 0, V_n\}_N^r$ . Then, from Eq. 21, we obtain

$$\begin{bmatrix} 0 \\ 0 \end{bmatrix} \begin{matrix} r \\ N \end{matrix} = \begin{matrix} r \\ N \end{matrix} \begin{bmatrix} t_{12} & t_{14} \\ t_{32} & t_{34} \end{bmatrix}^{\ell} \begin{bmatrix} \theta_n \\ V_n \\ 0 \end{bmatrix}^{\ell} \quad (23)$$

where  $t_{ij}$  are the elements of the transfer matrix  ${}^r_N[T]_0^{\ell}$ . For a non-trivial solution, the determinant of the coefficient matrix in Eq. 23 vanishes, resulting in a transcendental frequency equation which is solved numerically. Due to ill-conditioning of the field transfer matrix  $[F]$  (hyperbolic functions with large arguments) and large stiffness from the stringers, numerical difficulties can arise in calculating the natural frequencies. These difficulties can be circumvented by dividing each panel between two stringers into several segments. Now the field transfer matrix can be written as  $[F] = [F(\ell_1)][F(\ell_2)] \dots [F(\ell_M)]$  where  $\ell_i$  is the length of a segment and  $M$  is the total number of selected segments. By calculating the products of these matrices, the large arguments of the hyperbolic functions are avoided.

The mode shapes,  $Y_{mn}$ , are obtained from

$$Y_{mn}(x, y_q) = \begin{matrix} r \\ q \end{matrix} \begin{bmatrix} t_{11} & t_{12} & t_{13} & t_{14} \\ 0 & 0 & 0 & 0 \end{bmatrix}^{\ell} \begin{bmatrix} 0 \\ \theta_n \\ 0 \\ V_n \\ 0 \end{bmatrix}^{\ell} \cdot \sin \frac{m\pi(x-a_0)}{L_x} \quad (24)$$

where  $y_q$  is the local co-ordinate locating an arbitrary point on the stiffened panel. From Eq. 23, the slopes  $\theta_n$  can be expressed in terms of the shears  $V_n$  at the natural frequencies  $\omega_{mn}$ .

In the present study, the natural frequencies and normal modes of the stiffened panels shown in Fig. 4 were estimated for flexible supports at the stringer boundaries, i.e., at stations 0 and  $N$ . For panel No. 6, these sup-

ports are along the x-boundary, while for panel Nos. 1-4, the flexible supports are along the y-boundary. Such a condition is believed to be a close approximation of an actual boundary of a continuously stiffened elastic panel.

In addition to the stiffened panel units, each aircraft sidewall contains three plexiglass windows. The port side pilot window is a single sheet curved panel while all the other windows are double wall constructions as shown in Fig. 6. Due to the very complex geometry of these windows, the natural frequencies and normal modes are estimated using more tractable analytical models. In this procedure, the double wall constructions are replaced with "equivalent" single sheet curved panels which are simply supported on all four edges. Furthermore, the irregular shape of window unit No. 8 is approximated by a rectangular panel. Then, the natural frequencies and normal modes are calculated using the expressions given in Ref. 30. However, to establish the equivalence criteria between the double wall and the single wall constructions, the natural frequencies and normal modes of the single sheet panels are modified utilizing the results from an analytical study of double wall windows [18]. Since the numerical results of Ref. 18 were available only for a few lower modes and frequencies, the equivalence criteria are established only in approximation.

### 3.4 Acoustic-Structural Model

The equations developed in previous sections can be combined to construct a noise transmission model. Then, from Eqs. 4 - 8 and 11 - 15, the acoustic pressure inside the cabin is

$$\bar{p}(x,y,z,\omega) = \frac{\rho\omega^2}{ab} \sum_{i=0}^{\infty} \sum_{j=0}^{\infty} Z_{ij}(z,\omega) X_{ij}(x,y) \sum_{m=1}^{\infty} \sum_{n=1}^{\infty} H_{mn}(\omega) L_{ijmn} P_{mn}^r(\omega) \quad (25)$$

The cross-spectral density of the interior acoustic pressure  $S_p(x_1, x_2; y_1, y_2; z_1, z_2; \omega)$  can be obtained by taking the mathematical expectation of Eq. 25 and using the procedures given in Ref. 17. By setting  $x_1 = x_2 = x$ ,  $y_1 = y_2 = y$ ,  $z_1 = z_2 = z$ , the spectral density of the interior acoustic pressure is

$$S_p(x, y, z, \omega) = (\rho\omega^2/ab)^2 \sum_{i,j,k,\ell=0}^{\infty} Z_{ij}(z, \omega) Z_{k\ell}^*(z, \omega) X_{ij}(x, y) X_{k\ell}(x, y) \cdot \sum_{m,n,r,s=1}^{\infty} H_{mn}(\omega) H_{rs}^*(\omega) L_{ijmn} L_{k\ell rs} S_{mnrs}(\omega) \quad (26)$$

where the cross-spectral density of the generalized random forces,  $S_{mnrs}$ , is given in Eq. 20. The sound pressure levels in the cabin are obtained from

$$SPL(x, y, z, \omega) = 10 \log \{S_p(x, y, z, \omega) \Delta\omega / p_0^2\} \quad (27)$$

where  $\Delta\omega$  is the selected bandwidth and  $p_0$  is the reference pressure ( $p_0 = 2.9 \times 10^{-9}$  psi,  $p_0 = 20 \mu\text{N/m}^2$ ).

Noise reduction is defined as the quantity which relates the interior acoustic pressure spectral density  $S_p$  to the exterior input pressure spectral density  $S_p^e(\omega)$ ,

$$NR(x, y, z, \omega) = 10 \log \{S_p^e(\omega) / S_p(x, y, z, \omega)\} \quad (28)$$

The interior noise levels given by Eq. 27 correspond to the noise transmitted by a single stiffened panel or window unit located at  $z = 0$ . The total noise transmitted by all the panel units composing the entire sidewall can be determined by superposition of the contributions from each panel unit. In this case, the inputs of each panel unit are taken to be uncorrelated and the motions of each panel unit are assumed to be independent. Then, the in-

terior sound pressure levels transmitted by the entire sidewall can be estimated from

$$\text{SPL}^T(x,y,z,\omega) = 10 \log \left\{ \sum_{i=1}^M S_p^i(x,y,z,\omega) \Delta\omega / p_0^2 \right\} \quad (29)$$

where M is the total number of selected panel units of which the aircraft sidewall is composed.

The solution for the spectral density of the interior noise pressure given in Eq. 26 can be separated into two parts. The first part contains direct terms for which  $i = k, j = \ell, m = r, n = s$ ; and the second part contains cross-modal terms for which  $i \neq k, j \neq \ell, m \neq r, n \neq s$ . A common practice in modal analysis is to neglect the cross-modal terms, since for low damping, well separated modal frequencies and slowly varying input spectral densities, the contribution from these terms to the total response is usually small. However, for rapidly varying inputs such as propeller noise (shown in Figs. 7 - 13) and the anticipated large damping values of the treated structures, the cross-modal terms can have a significant effect on noise reduction at certain frequencies. This is illustrated in Fig. 19 where noise reduction is plotted for a typical stiffened panel unit with and without cross-modal terms. Due to the significance of these results, cross-modal terms are included in the analytical model of the present study. Furthermore, utilizing the computer algorithms available for complex numbers, makes the additional computational time and costs needed to include these terms negligible.

The convection effects for the surface pressures due to propeller rotation are included in the formulation of the generalized random forces. The

A-weighted interior noise levels are shown in Fig. 20 for cases with and without convection. The transmitted noise levels are in general lower when the convection effects of the propeller noise are included. Furthermore, the convection velocities seem to have more effect at higher frequencies. These results correspond to non-decaying spatial correlation functions with a convection velocity of 700 ft/sec along the propeller rotation and sonic convection velocity normal to the propeller rotation plane.

### 3.5 Acoustic Absorption

When calculating the transmitted noise into the cabin, it is assumed that the interior surfaces are locally reacting such that the interior absorption at the boundary can be represented by a point impedance model  $Z_A(\omega)$ . To simplify the numerical calculations, it is further assumed that  $Z_A$  is uniformly distributed over the interior cabin sidewalls. The point impedance is modeled by

$$Z_A(\omega) = R(\omega) + i X(\omega) \quad (30)$$

where the resistance  $R$  and the reactance  $X$  are given by [19,31]

$$R(\omega) = \rho c [1 + .0571(2\pi R_1/\rho\omega)^{0.752}] \quad (31)$$

$$X(\omega) = \rho c [0.087(2\pi R_1/\rho\omega)^{0.722}] \quad (32)$$

where  $\rho c$  is the characteristic impedance of the air and  $R_1$  is the flow resistivity of the porous materials. In addition to the acoustic absorption at the sidewalls, the acoustic absorption due to the interior furnishings, carpeting, passengers, etc. need to be accounted for. In the present study, we assume that the acoustic power losses in the cabin due to these treatments

can be represented by a modal acoustic damping coefficient  $\xi_{ij} = \xi_0(\omega_{10}/\omega_{ij})$  where  $\xi_0$  is a prescribed damping coefficient of the lowest acoustic mode in the cabin and  $\omega_{ij}$  are the modal acoustic frequencies. Even though it is possible to obtain a relationship between  $\xi_{ij}$  and  $Z_A$  [6], it is difficult to prescribe proper values for  $Z_A$  to account for the energy losses due to the furnishings, passengers, etc. In the present study, noise transmission was estimated for  $\xi_0 = 0.03$  (baseline aircraft),  $\xi_0 = 0.09$  (medium acoustic damping) and  $\xi_0 = 0.18$  (large acoustic damping). The following values for flow resistivity were chosen:

$$\begin{aligned} R_1 &= 12.5 \text{ lb-sec/in}^4 & f < 125 \text{ Hz} \\ R_1 &= 25 \text{ lb-sec/in}^4 & 125 \text{ Hz} \leq f \leq 250 \text{ Hz} \\ R_1 &= 62.5 \text{ lb-sec/in}^4 & f > 250 \text{ Hz} \end{aligned}$$

### 3.6 External Pressure Field

The external pressure acting on the aircraft is propeller noise due to blade passage harmonics. The experimental information on surface pressures [21-23] for ground test conditions is used to select the input pressure levels for each panel unit shown in Fig. 4. These sound pressure levels, digitized at 2 Hz bands, are shown in Figs. 7-13 for the ten panel units of which the sidewall of the aircraft is composed. To include convection effects in the present analytical model, the cross-spectral density of the input pressure is assumed to be separable in the direction of propagation and that perpendicular to it and is given as

$$S_i^e(\bar{x}, \bar{y}, \omega) = S_i(\omega) e^{i\omega\bar{x}/V_x} e^{i\omega\bar{y}/V_y} \quad (33)$$

where  $S_i(\omega)$  is the input power spectral density for the  $i$ -th panel unit, and  $V_x$  and  $V_y$  are the trace velocities corresponding to the  $x$ - and  $y$ -directions, respectively. Utilizing the information available in Ref. 23, subsonic trace velocities corresponding to the vertical direction  $y$  (along the propeller rotation) and sonic trace velocities corresponding to the longitudinal direction  $x$  (normal to the propeller rotation plane) were chosen in this study. The values of  $V_y = 700$  ft/sec and  $V_x = 1120$  ft/sec were used for all the numerical computations.

The cross-spectral density of the generalized random forces due to propeller noise input can be evaluated from Eqs. 20 and 33. In this procedure, the pressure levels characterized by the spectral density  $S_i(\omega)$  are taken to be uniformly distributed over each panel surface, but varying in a step-wise fashion from one panel unit to another. For stiffened panels, the modes  $Y_{mn}(x,y)$  are prescribed numerically. Thus, numerical integration routines need to be utilized to calculate the generalized random forces defined in Eq. 20.

### 3.7 Total TL Including Add-On Treatment

The analytical model described in Sections 3.1 - 3.7 predicts noise transmission through a fuselage sidewall with or without treatments which are directly attached to the skin of the sidewall. These add-on treatments could include damping tape, honeycomb panels, non-load carrying mass, etc. In addition, the effect of acoustic absorption within the cabin is included according to the procedures described in Section 3.5. To estimate the noise losses due to acoustic blankets, septum barriers and trim panels, an analytical procedure based on the impedance transfer method is used [19,20]. A reasonable agreement between these analytical predictions and experimental measurements has been

achieved for a typical aircraft panel with add-on treatments [4,15]. Then, the interior noise levels in the treated aircraft are estimated by adding the noise losses calculated by the impedance transfer method (acoustic blankets, septum barriers, trim panels) to the noise levels obtained directly by modal analysis from Eqs. 27 and 29. Then, the interior noise transmitted through a panel with acoustic add-on treatments is calculated from

$$\text{SPL}(x,y,z,\omega)|_{\text{treated}} = \text{SPL}(x,y,z,\omega)|_{\text{untreated}} + \Delta\text{TL}(\omega) \quad (34)$$

where  $\Delta\text{TL}$  is the additional noise loss provided by the add-on acoustic treatments. It should be noted that the effect of treatments which are directly attached to the aircraft skin (damping tape, non-load carrying mass, honeycomb panels) is included in the term  $\text{SPL}(x,y,z,\omega)|_{\text{untreated}}$ . Since these treatments have a direct effect on the dynamic characteristics of the load bearing external skin, the  $\Delta\text{TL}$  term, derived from a simplistic impedance transfer method which assumes uniformly treated panels of infinite extent, will not account properly for the additional noise losses from the add-on treatments directly attached to the elastic skin of the sidewall.

The added transmission loss  $\Delta\text{TL}$  at an incident plane wave angle  $\theta_1$  (see Fig. 14) is obtained from

$$\Delta\text{TL}(\omega, \theta_1) = -10 \log \tau(\omega, \theta_1) \quad (35)$$

where  $\tau$  is the transmission coefficient of the add-on acoustic treatment defined as [5]

$$\tau(\omega, \theta_1) = \left| \frac{(p_1/p_2)_{\text{untreated}}}{(p_1/p_2) \dots (p_{n-1}/p_n)_{\text{treated}}} \right|^2 \quad (36)$$

where  $p_{n-1}/p_n$  are the pressure ratios across the boundaries between adjacent media and the pressure ratios across the media themselves as shown in Fig. 14. Acoustic plane waves are incident on the exterior of the structure with an angle  $\theta_1$  and reflected and transmitted according to the various impedances present at the different layers. The interior of the media is assumed to extend to infinity with an acoustic termination impedance  $\rho c$ . To obtain the pressure ratios  $p_{n-1}/p_n$ , the expressions for the characteristic impedances of the various media are utilized.

Following Refs. 5, 19 and 20, and using Fig. 14, the pressure ratio across the untreated elastic panel is

$$(p_1/p_2)_{\text{untreated}} = 1 + Z_p/Z_2 \quad (37)$$

where the impedance,  $Z_p$ , of an infinite stiffened panel can be written as [5]

$$Z_p = \omega \mu_1 [X\eta + i(1 - X)] \quad (38)$$

in which

$$X = \omega^2 \sin^4 \theta_2 \Delta / (\mu_1 c_2^4) \quad (39)$$

$$\theta_2 = \sin^{-1}(c_2 \sin \theta_1 / c_1) \quad (40)$$

$$\Delta = D_x \cos^4 \phi + 2H \cos^2 \phi \sin^2 \phi + D_y \sin^4 \phi \quad (41)$$

$D_x, D_y$  = bending rigidity of the stiffened panel in sections perpendicular to x-axis and y-axis, respectively

$H$  = cross-rigidity of the panel

$\phi$  = azimuthal angle relative to x-axis [5]

$\mu_1$  = surface density of the sidewall

$\eta$  = loss factor of the sidewall

The impedance for the interior acoustic medium is

$$Z_2 = \rho c / \cos \theta_2 \quad (42)$$

The pressure ratios across the different layers of the medium shown in Fig. 14 are estimated in the following fashion. The pressure ratio across the elastic panel bounded by porous acoustic blankets on the interior side (located in space 2) is

$$(p_1/p_2)_t = 1 + Z_p/Z_2' \quad (43)$$

where  $Z_p$  is the elastic panel impedance given in Eq. 38 and  $Z_2'$  is the impedance of the acoustic blankets

$$Z_2' = Z_{B2} \coth (b_2 d_2 \cos \theta_2 + \psi_2) / \cos \theta_2 \quad (44)$$

where

$$Z_{B2} = -i K_2 b_2 / \omega Y_2 \quad (45)$$

$$\theta_2 = \sin^{-1} (c_2 \sin \theta_1 / c_1) \quad (46)$$

$$\psi_2 = \coth^{-1} (Z_3 \cos \theta_2 / Z_{B2}) \quad (47)$$

$$c_2 = \omega / \beta_2; \text{ speed of sound in region 2} \quad (48)$$

$$b_2 = \alpha_2 + i\beta_2; \text{ propagation constant in region 2} \quad (49)$$

$$b_2 = i\omega(\bar{\rho}_2 Y_2 / K_2)^{1/2} (1 - i\bar{R}_2 / \bar{\rho}_2 \omega)^{1/2} \quad (50)$$

$$\bar{\rho}_2 = \rho_2 \left\{ \frac{(R_1/\rho_m \omega)^2 (Y_2 + \rho_m/\rho) + 1}{1 + (R_1/\rho_m \omega)^2} \right\} \quad (51)$$

$$\bar{R}_2 = R_1 / (1 + (R_1/\rho_m \omega)^2) \quad (52)$$

$$Y_2 = 1 - \rho_m/\rho_f; \text{ porosity} \quad (53)$$

$K_2$  = compressibility of gas in porous material  
(= atmospheric pressure)

$\rho_m$  = bulk density of sample

$\rho_f$  = density of fibers

$R_1$  = flow resistivity of acoustic blankets

The septum impedance,  $Z_3$ , is

$$Z_3 = i\omega\mu_3 + Z_4 \quad (54)$$

where  $\mu_3$  is the surface density of the septum material and  $Z_4$  is the impedance of the acoustic blankets in region 4. The pressure ratio across the acoustic blankets of region 2 is

$$\left(\frac{p_2}{p_3}\right)_t = \frac{\cosh(b_2 d_2 \cos\theta_2 + \psi_2)}{\cosh \psi_2} \quad (55)$$

The pressure ratio for the septum is

$$(p_3/p_4)_t = Z_3/Z_4 \quad (56)$$

where

$$Z_4 = Z_{B4} \coth(b_4 d_4 \cos \theta_4 + \psi_4) \quad (57)$$

$$\theta_4 = \sin^{-1}(c_4 \sin \theta_2 / c_2) \quad (58)$$

$$c_4 = \omega / \beta_4 \quad (59)$$

The pressure ratio across the acoustic blankets in region 4 is

$$(p_4/p_5)_t = \frac{\cosh(b_4 d_4 \cos \theta_4 + \psi_4)}{\cosh \psi_4} \quad (60)$$

where

$$\psi_4 = \coth^{-1}(Z_5 \cos \theta_4 / Z_{B4}) \quad (61)$$

The trim panel impedance,  $Z_5$ , is

$$Z_5 = i\omega\mu_5 + Z_6 \quad (62)$$

where  $\mu_5$  is the surface density of the trim panel and  $Z_6$  is the impedance of the receiving space

$$Z_6 = \rho_6 c_6 / \cos \theta_6 \quad (63)$$

in which

$$\theta_6 = \sin^{-1}(c_6 \sin \theta_4 / c_4) \quad (64)$$

$c_6$  = speed of sound in the receiving space

$\rho_6$  = air density of the receiving space

The pressure ratio across the trim panel is

$$(p_5/p_6)_t = Z_5/Z_6 \quad (65)$$

The acoustic properties of the porous blankets in region 4 can be evaluated from Eqs. 49-53 by substituting the parameters corresponding to those of region 4.

The added transmission loss given in Eq. 35 is calculated using the narrow band approach. It can be shown that the one-third octave transmission loss  $\Delta TL|_{1/3}$  can be estimated from

$$\Delta TL(\theta)|_{1/3}^i = 10 \log \frac{\Delta\omega|_{1/3}^i}{\int_{\omega_\ell^i}^{\omega_u^i} (10^{-0.1\Delta TL(\theta, \omega)}) d\omega} \quad (66)$$

where  $\Delta\omega|_{1/3}^i$  is the i-th bandwidth of the one-third octave frequency band and  $\omega_\ell^i$  and  $\omega_u^i$  are the lower and upper frequencies, respectively, of the corresponding one-third octave frequency band.

#### 4. Interior Noise Optimization

The analytical model described in previous sections is applied to optimize cabin noise to an average overall A-weighted level of about 85 dBA. The non-structural add-on treatments applied to the fuselage sidewalls of the aircraft were designed to have low surface density and high transmission loss. To achieve this goal, the following systematic procedure was undertaken.

An interior point in the propeller plane at about ear level and 8 inches from the sidewall was selected. Cabin noise was calculated at this point for all treatment conditions. Numerical computations were performed using a nar-

row band analysis for frequencies ranging from 0 - 1122 Hz and a bandwidth of  $\Delta f = 2$  Hz. The one-third octave levels and the overall levels were obtained from the narrow band results and numerical integration. The optimization procedure was based on the A-weighted one-third octave noise levels. Then, the noise transmitted by each panel unit (Fig. 4) was calculated for each add-on treatment and for various combinations of add-on treatments. The amount of treatment was increased until a pre-selected acceptable A-weighted interior noise level was reached. In the present study, a level of 78 dBA for all one-third octave frequencies was selected as the upper bound for the noise transmitted by each individual panel unit. If the selected optimization goal is not satisfied, this noise level might have to be changed. The treatment or combination of treatments which reduces the transmitted noise to this value for the least amount of added weight was taken as the best treatment for that panel unit. The procedure was repeated for all panel units and the results were superimposed (including noise transmitted through windows) to determine the total transmitted noise in the cabin. The add-on treatments include honeycomb panels, damping tapes, non-load carrying mass, porous acoustic blankets, septum barriers and trim panels. A simplified flow chart of the optimization procedure is shown in Fig. 15. The computing prediction system consisted of three basic computer programs. The first program calculated the natural frequencies and mode shapes of the stiffened panels using the transfer matrix approach (Section 3.3), the second program estimated pressure levels in the cabin by the modal approach (Section 3.4), while the third program calculated the additional noise losses  $\Delta TL$  (Section 3.7) due to add-on treatments not attached directly to the skin.

## 5.0 Numerical Results

### 5.1 Baseline Aircraft

The aircraft used in the present study is the Model 680 AeroCommander shown in Figs. 1 and 2. This aircraft has a take-off gross weight of about 7,000 lbs., cruises at an airspeed of 262 ft/sec at 10,000 ft altitude with each engine running at 70% power. Each engine has six cylinders, each engine is rated at 320 hp, and drives a 7.74 ft diameter three-bladed propeller through a gearing system that turns the propeller at about 64% of the engine rpm. The propeller tip clearance from the sidewall is about 5 inches and the propeller plane intersects the fuselage at approximately the middle of the cabin. The original cabin interior was finished in standard trim (acoustic blankets, trim panels) and provided seats for pilot, copilot and four passengers. The flight tests run at an altitude of 7,000 ft and 75% power (both engines running at equal power output) indicate that the A-weighted overall interior noise level varies with the position in the cabin and range from about 96 dBA to 103 dBA [9]. The ground tests under static operations [21 - 23] showed similar values for the interior noise in the cabin. The highest A-weighted noise levels occurred in the frequency range of about 100 - 600 Hz.

The baseline aircraft to which the analytical optimization models were applied was assumed to be an aircraft similar to the one described above, but with all the interior treatments (acoustic blankets, trim panels) and interior furnishings (carpeting, seats) removed. Furthermore, the mathematical model does not provide for noise transmission into the cabin through the rear bulkhead. The inputs to the baseline aircraft corresponding to ground tests under static operations were taken from Refs. 21 and 23.

## 5.2 Modes and Frequencies

The normal modes and natural frequencies of the stiffened elastic panels were obtained using the transfer matrix procedures described in Section 3.3. The modes and frequencies of the single and double window constructions were determined by the procedures given in Refs. 18 and 30. The panel and stringer geometries are shown in Figs. 4 and 16, respectively. The skin of all the aluminum panels has a thickness of 0.04 inches except for Panel No. 2 which has a thickness of 0.08 inches. The windows are made from 0.14 inch thickness plexiglass. The geometric and material properties of the stringers are given in Table 1 for each stiffened panel unit. Utilizing these data, the natural frequencies and normal modes were calculated for all the panels shown in Fig. 4 for a frequency range of 0 - 1122 Hz. The natural frequencies corresponding to the odd spanwise modes ( $n = 1,3,5,\dots$ ) are given in Table 2. Due to the very large number of natural frequencies for the selected frequency range, only those frequencies below 400 Hz are included in this table. The modal frequencies obtained by experimental measurements for the same aircraft are included for comparison [33]. The mode shapes and frequencies were measured for Panel Nos. 1, 2, 6 and 8, using experimental modal analysis techniques. For other panels, the modal frequencies were extracted from the frequency response functions. The agreement between theory and experiment for estimating the modal frequencies of the aircraft panels, in general, is satisfactory in view of the fact that some stringers contained cut-outs and various attachments which are difficult to include in a structural model. The experimental frequencies given for Panel No. 2 correspond to a skin thickness of 0.04 inches while the theoretical results are for a panel with a thickness of 0.08 inches. The theoretical sidewall model corresponds to the starboard side

where the thickness of Panel No. 2 is 0.08 inches. Honeycomb panels were attached to this panel. Thus, the frequencies and modes were measured for Panel No. 2 located on the port side which has a thickness of 0.04 inches. The experimental results include those frequencies corresponding to even and odd modes. However, due to the complexity of the modal shape of the stiffened panels and double wall windows, the separation of experimental data into even and odd modes is a difficult task. Several typical measured and calculated modes corresponding to the first frequency band are plotted in Fig. 17 for Panel No. 6.

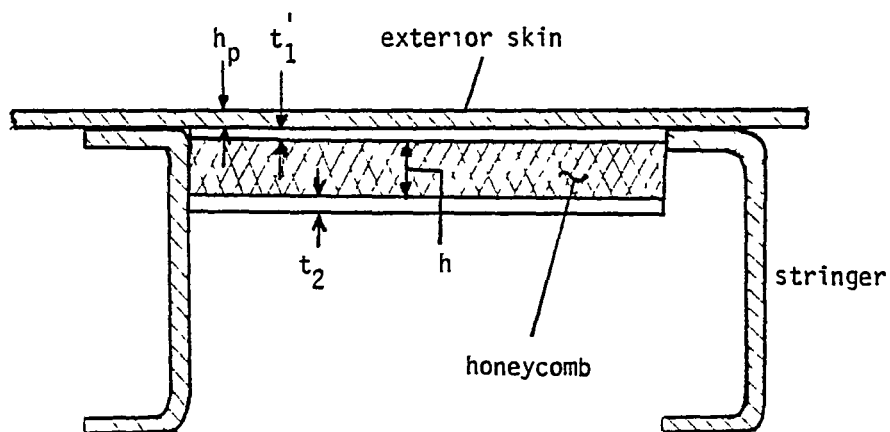
### 5.3 Noise Levels in Baseline Aircraft

The interior noise levels in the aircraft due to propeller noise inputs taken from static ground tests were calculated utilizing the analytical models presented in this study. The narrow band ( $\Delta f = 2$  Hz) interior sound pressure levels calculated at  $x = 50$  in,  $y = 40$  in, and  $z = 8$  in, are shown in Fig. 18. In order to have a valid comparison between theory and experiment, analytical calculations were performed for interior conditions similar to those of the experimental aircraft. The sidewalls and ceiling of the experimental aircraft were treated with one-inch acoustic blankets and cloth-type interior trim. Furthermore, carpeting and all seats were left intact during the test. The interior noise levels were estimated for the baseline aircraft using modal analysis. (The baseline aircraft is a bare fuselage without treatments or furnishings.) Then, the additional noise losses due to sidewall treatments were added to these levels to arrive at the results shown in Fig. 18. In view of the complexity of the sidewall construction and the uncertainty of the treatment conditions, the agreement between theory and experiment is reasonable. Theory seems to predict higher noise levels

by about 5 - 8 dB for the first four blade passage harmonics. The limitations of the analytical model with regard to uniform propeller noise pressure distributions and to the independent responses of each panel unit mean that it tends to overestimate the transmitted noise levels. Furthermore, due to uncertainty of the effectiveness of the original add-on treatments (acoustic blankets, carpeting, cloth trim), the additional noise losses  $\Delta TL$  calculated by the impedance transfer method might be underestimated in the low frequency range. It should be noted that theory was in very good agreement with the laboratory tests where all the parameters could be carefully controlled or measured [9, 12, 15].

#### 5.4 Sidewall Treatment With Honeycomb Panels

The effect of the stiffening of the sidewall panels on noise transmission is investigated. Additional stiffening is achieved by attaching honeycomb panels to the interior walls of the aircraft as shown in the sketch below:



The transverse stiffness per unit width of the treated panel (elastic skin + honeycomb) is obtained from

$$D_t = \frac{E_1 \cdot E_2 t_1 t_2 h^2}{(E_1 t_1 + E_2 t_2)(1 - \nu^2)} \quad (67)$$

where  $E_1, E_2$  are the effective moduli of the facings,  $\nu$  is Poisson's ratio of the facings ( $\nu_1 = \nu_2 = \nu$ ),  $h$  is the distance between the facing centroids and  $t_1, t_2$  are the thicknesses of the facings. In the present study, we take  $t_1 = t_1' + h_p$  where  $t_1'$  is the thickness of the facing of the honeycomb panel. Numerical results were obtained for  $E_1 = E_2 = 10.0 \times 10^6$  psi,  $\nu = 0.3$ ,  $t_1' = 0.0$ ,  $t_2 = 0.016$ ,  $h = 0.288$ , surface density of the honeycomb panel =  $0.37$  lb/ft<sup>2</sup> and  $t_1' = 0.032$  in,  $t_2 = 0.032$  in,  $h = 0.429$  in, surface density of the honeycomb panel =  $1.4$  lb/ft<sup>2</sup>. The natural frequencies and normal modes of the skin-stringer panels stiffened with the honeycomb construction were calculated using the transfer matrix procedures given in Section 3.3. The natural frequencies corresponding to the first frequency band of both the treated and untreated skin-stringer panels are presented in Table 3. Due to a significant increase in the total panel stiffness (aluminum panel + honeycomb panel), the modal frequencies shift to higher frequency values. The panels with light honeycomb treatment ( $h = 0.286$  in) were assumed to be simply supported at the boundaries perpendicular to the stiffeners and elastically supported at the boundaries parallel to the stiffeners. The panels with heavy honeycomb treatment ( $h = 0.429$  in) were taken to be simply supported on all four edges.

To estimate the effect of sidewall stiffening on noise transmission, the interior noise was calculated for several add-on treatments with honeycomb panels. The one-third octave A-weighted interior noise levels transmitted

by the baseline panels and panels with light honeycomb treatment are given in Figs. 21-26. (Due to the large stiffness of baseline Panel No. 9, no add-on treatment is attached to this panel). The overall noise levels for both treated and untreated panels are also given in these figures. The structural and acoustic damping is taken to be the same for both cases. As can be observed from these results, the effect on the noise transmission due to stiffening the sidewall panels varies from one panel unit to another. This kind of variation can be attributed to structural differences among the stiffened panel units, nonuniformity of surface noise pressure and input spectra composed of sharp peaks at the propeller blade passage harmonics. More noise is transmitted by Panel Nos. 1 and 4 when the stiffness of these panels is increased. However, for Panel Nos. 2, 3 and 6, a significant amount of noise reduction is achieved with the stiffening add-on treatment. The noise reduction achieved for Panel No. 2 with this treatment might not be realistic. Experiments [3] indicate a very strong coupling between the vibrations of Panel Nos. 1 and 2 when honeycomb panels are added. For a relatively stiff baseline panel (skin thickness = 0.08 in) stiffened with honeycomb panels, only a few modes are accounted for in the selected frequency range 0 - 1122 Hz. A better structural model would be achieved if Panel Nos. 1 and 2 were combined into a single stiffened panel. Such an approach was used in obtaining the results shown in Fig. 28. For Panel No. 10 only, a small amount of noise reduction is obtained with the honeycomb panel treatment. The one-third octave and overall noise levels for the entire sidewall are shown in Fig. 27. With honeycomb treatment, the overall additional noise reduction for the entire sidewall is about 3 dBA when  $h = 0.286$  in. The total added weight to one sidewall is about 7 lbs.

The effect on noise transmission due to heavy honeycomb treatment ( $h = 0.429$  in) is illustrated in Figs. 28-31 for Panel Nos. 1, 2, 3, 4 and 6 and for the entire sidewall in Fig. 32. Since strong coupling was observed between Panel Nos. 1 and 2 [33], for heavy honeycomb treatment, Panel Nos. 1 and 2 were combined into one panel unit. Furthermore, no heavy honeycomb treatment was added to Panel Nos. 9 and 10 and window units Nos. 5, 7 and 8. The results indicate that about 13 dBA noise reduction for the sidewall can be achieved with this honeycomb treatment. Heavy honeycomb treatment was observed to be most effective for Panel Nos. 3 and 6.

#### 5.5 Damping Tape and Mass Addition

The damping tapes chosen in this study are commercially available tapes composed of aluminum foil, synthetic rubber adhesive (or foam adhesive) and liner. These damping tapes show good damping characteristics for frequencies in the range of 100 - 200 Hz and temperatures from (- 65°F) - (+ 250°F). By applying several layers of these damping tapes to the panel surface, an average loss factor on the order of 0.2 (10% of the critical damping) can be achieved. The theoretical loss factor of the aluminum panels with damping tape added is estimated using the procedures of constrained layer damping presented in Ref. 31. It is calculated that with heavy damping tape treatment, the structural damping corresponding to the fundamental panel mode would increase from  $\zeta_0 = 0.03$  (baseline aircraft) to  $\zeta_0 = 0.075$  (baseline + damping tape). The other modal coefficients are calculated from  $\zeta_{mn} = \zeta_0 (\omega_{11}/\omega_{mn})$  where  $\omega_{mn}$  are the natural frequencies of the stiffened panel units.

When damping tape with a thin constraining layer (aluminum foil) is added to the panel surface, the mass of the panel increases, without an

appreciable increase in the panel stiffness. Thus, the modal frequencies of the stiffened panels tend to shift to the lower frequency values. For propeller noise input, such a frequency shift could result in a resonance condition. However, with the large damping provided by the damping tape action, these panel resonances will be suppressed. The increase in panel modal damping due to the addition of damping tape is accounted for by the increase in the structural damping coefficient  $\zeta_0$  [14]. Thus, the resonance peaks in Eqs. 12 and 13 are reduced. In Table 4, the fundamental frequencies of the stiffened panels are given for several conditions of damping tape treatment.

The A-weighted interior sound pressure levels transmitted by each panel unit are shown in Figs. 33-38 for a damping tape treatment with a surface density of  $0.38 \text{ lb/ft}^2$ . The noise transmitted by the entire sidewall (including windows) is plotted in Fig. 39. From these results, it can be seen that approximately 1 - 10 dBA noise reduction can be achieved for different panel units. The amount of noise reduction for each panel unit is influenced by the value of the ratio added mass/panel mass (mass law action) and the location of the panel resonance frequencies (after treatment) with respect to the frequencies of the propeller blade passage harmonics. The overall noise reduction for the entire sidewall is about 6 dBA and the total added weight to the sidewall is 7.05 lbs. For the baseline aircraft, the interior noise is dominated by the first and second blade passage harmonics, while the treated aircraft is dominated by the second, third and fourth blade passage harmonics. This difference is believed to be caused mainly by the shift of the modal frequencies to lower values.

To illustrate the effect of mass and damping tape addition, the noise

transmitted by Panel Nos. 1, 2, 4 and 6 is shown in Figs. 40-45 for several combinations of damping tape and non-load carrying mass add-on treatments. It can be observed that when the surface densities of the added mass (non-load carrying mass + damping tape) reach about  $2.3 \text{ lbs/ft}^2$ , the noise levels for Panel Nos. 1 and 2 are close to or below the selected sound pressure level of 78 dBA. A similar condition is observed for Panel No. 4 when the added surface density reaches  $1.59 \text{ lbs/ft}^2$ . However, for Panel No. 6, this level is exceeded even when the surface density of the add-on treatment reaches  $3.28 \text{ lbs/ft}^2$ . The baseline construction of Panel No. 6 is relatively stiff when compared to that of the other panel units. The fundamental frequency of this panel is 169 Hz. With added mass, the modal frequencies shift toward the lower frequency values and the number of modes in the selected frequency range 0 - 1122 Hz increase significantly. Thus, some blade passage harmonics could induce resonances which are not observable for the untreated (baseline) case.

As can be observed from these results, noise reduction does not follow a universal rule for the uniform mass/unit area treatment of different panel units. Furthermore, adding mass might even have a negative effect on the interior noise at some frequencies. The results presented indicate a relative sensitivity of the various panels to mass and damping tape treatments. From the results shown in Figs. 37 and 38, it can be observed that for a treated sidewall, the interior noise is mainly controlled by Panel No. 6. Panel No. 6 is located in the propeller plane and in the vicinity of where the interior noise is calculated.

#### 5.6 Honeycomb and Damping Tape Treatment

The results presented indicate that treating the aircraft sidewall with

honeycomb panels or damping tape could have a positive effect on noise reduction. However, in some cases, a large amount of stiffening or heavy mass needs to be added to reduce the transmitted noise to acceptable levels. It was found that better noise reduction can be achieved for less added weight when both of these add-on treatments are combined together. Panel stiffening is achieved by attaching honeycomb panels to the elastic skin and then adding damping tape to the honeycomb construction.

The one-third octave A-weighted interior noise levels for honeycomb-damping tape treatment are given in Figs. 46-52. From these results, it can be seen that the interior noise is dominated by the second blade passage harmonic due to the noise transmitted by Panel No. 3. Even though a significant amount of noise reduction is achieved at most frequencies with honeycomb-damping tape treatment, the noise levels at the second blade passage harmonic are about 10 dBA above the selected optimization level. However, by adding a very stiff honeycomb panel (surface density = 1.4 lb/ft<sup>2</sup>) to Panel No. 3 and then applying damping tape, a desirable amount of noise reduction can be achieved as shown in Fig. 53.

#### 5.7 Additional Noise Losses Due to Acoustic Blankets, Septum and Trim Panel

The additional noise losses  $\Delta TL$  are calculated for various combinations of acoustic blankets, septum and trim panels using the procedures given in Section 3.7. Numerical results were obtained for the following data:  $\eta = 0.04$  (no damping tape),  $\eta = 0.08$  (with damping tape),  $c_1 = c_6 = 1128$  ft/sec,  $D_x = 88$  lb<sub>m</sub>-ft<sup>2</sup>/sec<sup>2</sup>,  $D_y = 149,133$  lb<sub>m</sub>-ft<sup>2</sup>/sec<sup>2</sup>,  $H = 3731$  lb<sub>m</sub>-ft<sup>2</sup>/sec<sup>2</sup>,  $\rho_1 = 0.07657$  lb/ft<sup>3</sup>,  $\rho_1 = \rho_2 = \rho_4 = \rho_6$ ,  $\rho_m = 0.864$  lb<sub>m</sub>/ft<sup>3</sup>,  $\rho_f = 21.55$  lb<sub>m</sub>/ft<sup>3</sup>,  $K_2 = K_4 = 14.7$  psi,  $R_1 = 64$  lbs-sec/in<sup>4</sup>.

The additional transmission losses across a sidewall are given in Figs. 54-58 for acoustic blankets and for semi-rigid materials. A semi-rigid material would correspond to a material which does not have loose fibers and is heavier than an acoustic blanket. The propagation constants of semi-rigid materials were taken from Refs. 5 and 31. The results in Figs. 54-58 show that the general trends of  $\Delta TL$  are similar for both of these models. However, for large surface densities of trim panel, a stronger double wall resonance condition is observed when the space between the two walls is filled with porous acoustic blankets. Furthermore, with increasing cavity depth, semi-rigid materials show an increasingly larger amount of  $\Delta TL$  when compared to the results obtained for acoustic blankets. Thus, for distances between the exterior skin and the trim panel on the order of 4 in or more, semi-rigid materials would provide significantly greater noise transmission losses than noise losses from acoustic blankets.

The effect on  $\Delta TL$  due to variations in the surface density of the trim panel and septum is illustrated in Figs. 59 and 60, respectively. These results indicate that with increasing surface density of the trim panel, a stronger double wall resonance condition is observed. However, the frequency bandwidth of the double wall resonance region decreases with an increasing surface density of the trim panel. For larger values of  $\mu_5$  (above  $0.3 \text{ lb/ft}^2$ ) and for frequencies above 250 Hz,  $\Delta TL$  seems to double for each doubling of the frequency. These results tend to indicate that a heavy trim panel might have a negative effect on noise reduction for this aircraft in the frequency range of about 80 Hz - 200 Hz. The first two propeller blade passage harmonics are within this frequency range. For a septum with a surface density above  $0.1 \text{ lb/ft}^2$ , a strong double wall resonance is observed

between the elastic panel and the septum. The double wall frequency can be calculated using the formulas given in [5]. The frequency of this resonance is higher than that of the double wall resonance of the elastic panel-trim panel configuration. This is due to the fact that the distance between the elastic panel and septum is one-half the distance between the elastic panel and the trim panel. A heavy septum ( $0.1 - 1.0 \text{ lb/ft}^2$ ) might have a negative effect on  $\Delta TL$  in the frequency range 125 - 250 Hz. The second and third blade passage harmonics are in this frequency range. For frequencies above 300 Hz, a significant amount of  $\Delta TL$  can be achieved with a heavy septum. From Fig. 63, it can be seen that when the surface densities of both the septum and trim panel are large, two double wall resonance conditions are observed in the frequency range 100 - 300 Hz. Thus, a heavy septum and heavy trim panel might have a negative effect on noise reduction in this frequency range even though a large  $\Delta TL$  can be achieved for higher frequencies (above 300 Hz).

The additional noise losses corresponding to different cavity depths and a very light septum are shown in Fig. 61. A significant amount of noise loss can be realized for deep cavities and for frequencies above the double wall resonance frequency. In fact, as the distance between the elastic panel and the trim panel increases, the double wall resonance frequency decreases. The effect on  $\Delta TL$  due to the location of the septum is shown in Figs. 62 and 63 for a light and heavy septum, respectively. For a heavy septum, significant differences in  $\Delta TL$  were observed for the different distances between the elastic panel and the septum. Two double wall resonance conditions were obtained in the frequency range 100 - 300 Hz. In this frequency range, some advantage in  $\Delta TL$  can be gained by locating a heavy septum near the trim panel.

### 5.8 Noise Transmission Through Windows

The noise transmitted through window units (Panel Nos. 5, 7 and 8) is shown in Figs. 64-66. These results are based on simply supported "equivalent" single sheet plexiglass panels as described in Sections 3.3 and 5.1. As can be seen from those results, the noise transmitted by Panel Nos. 5 and 7 satisfy the selected upper noise limit for all frequencies. However, treatments needed to be added to Panel No. 8 in order to meet the upper limit criterion. This was achieved by reducing the window area and adding damping tape to the interior side of the window.

### 5.9 Noise Optimization in the Aircraft

The interior noise in the cabin was optimized utilizing the computation procedure shown in Fig. 15. In this approach, the noise transmitted by each panel unit was calculated for each add-on treatment and then for a combination of several treatments. The amount of treatment was increased until a selected target noise level at a critical point in the cabin was reached. An interior point in the propeller plane at about ear level and 8 inches from the sidewall was selected as the critical point in the cabin. A level of 78 dBA for all one-third octave frequencies was taken as the upper bound for the noise transmitted by each individual panel unit. The treatment or combination of treatments which reduces the transmitted noise to this value for the least amount of added weight was assumed to be the best treatment for that panel unit. Then, the one-third octave and the overall noise levels were calculated for the entire sidewall for the same add-on treatments considered for individual panel units. An 88 dBA overall noise level was selected as the optimization target for the noise transmitted by the entire sidewall. The one-third octave 78 dBA and the overall 88 dBA levels were

selected as typical optimization goals for the present aircraft. Depending on the required comfort criteria for a particular aircraft, these levels could be adjusted to meet the prescribed conditions of interior noise. The non-structural add-on treatments applied to the fuselage sidewalls were evaluated for low surface density and high transmission loss. The add-on treatments included honeycomb panels, damping tapes, non-load carrying mass, porous acoustic blankets, septum barriers and trim panels. Acoustic blankets were added to all the panels except the windows.

The results of the optimization study are given in Figs. 67-73 for the individual panels and Fig. 74 for the entire sidewall. Since the amount of add-on treatments varies from one panel unit to another, the surface densities given in Fig. 73 for the sidewall are average values. The added weight was calculated by multiplying the total surface density by the panel area and then adding 5% of the total weight. The optimized interior noise in the cabin at the selected point is 88 dBA. The measured average noise levels in the cabin are typically 3 - 5 dBA less than the highest noise level at the selected critical point [9]. Thus, the optimized average noise level in the cabin would be about 85 dBA. Furthermore, experimental data for this aircraft suggest that no significant increase in interior noise is observed when both engines are running as compared to only one engine running [21]. Therefore, the noise transmitted by one sidewall is taken as the total interior noise in the cabin.

To reach the 85 dBA (average) noise level in the cabin, 30 lbs. of add-on treatments were added to one sidewall (a total of 60 lbs. for both sidewalls). In addition, light treatments (damping tape and acoustic blankets) need to be added to the ceiling area of the aircraft. For a ceiling area

of about 47 ft<sup>2</sup> and surface density of damping tape equal to 0.25 lb/ft<sup>2</sup>, the weight of this treatment is about 15 lbs. Interior furnishings such as carpeting and seats are not included with the add-on treatments.

From the results shown in Figs. 67-74, it can be observed that the most critical noise path is through Panel No. 6. The input noise levels prescribed for the sidewall were highest over the region where Panel No. 6 is located. Other panels which seem to transmit high noise levels are Panel Nos. 1, 2 and 3. These panels are also located in the vicinity of the propeller plane where the input noise levels are high. By stiffening these panels, damping out the resonance vibrations and using absorptive materials, it is possible to reduce transmitted noise to acceptable levels. To isolate the vibrations of the skin-stringer panels from those of the limp-mass trim panel, damping tape with a thickness ranging from 0.25 in - 0.5 in is attached to the stringer as shown in Fig. 74. In addition to the vibration isolation, such a construction would increase the distance between the elastic skin and the trim panel, allowing for greater additional noise losses.

The overall A-weighted sound pressure levels are plotted versus the ratio of treated/untreated weight for the sidewall in Fig. 75. The points corresponding to baseline and optimized conditions are connected by a straight line. These noise levels are assumed to be the average sound pressure levels in the cabin. Several points are included in this diagram to illustrate the effect of uniform treatment on all the panel units (except windows). For a light treatment with damping tape, honeycomb panels and honeycomb-damping tape, the points are located near the straight line. However, for a very heavy add-on treatment with damping tape and non-load carrying mass, significant deviations from the straight line relation are observed. These

results tend to suggest that a linear relationship might be established between the noise reduction and added weight, if the add-on treatments are selected according to the optimization procedure used in this study. The final configuration of the aircraft sidewall with add-on treatments is shown in Fig. 76. There are basically three types of add-on treatments used for noise reduction: honeycomb-damping-tape-acoustic-blankets-trim, damping tape-acoustic blankets-trim and damping tape (windows). However, the surface densities of these treatments could vary from one panel unit to another. The distribution of the surface densities (baseline + treated, treated) for the optimized sidewall are given in Fig. 77. These results indicate the relative amount of treatment used for different panel units. The greatest amount of add-on treatment was applied to Panel Nos. 3 and 6.

## 6.0 Conclusions

An analytical model has been developed to predict the noise transmission into a twin engine G/A aircraft. The model has been used to identify the airborne noise transmission paths and to optimize the interior sound levels due to propeller noise inputs. The average cabin noise levels in the baseline aircraft reach a maximum of about 105 dBA and these levels are about 20 dBA higher than the optimization goal of 85 dBA. The results indicate that the required noise reduction has to be achieved mainly in the low frequency range of 70 - 350 Hz. For the type of aircraft considered, the first four propeller blade passage harmonics are within this frequency range.

The required noise attenuation has been obtained by add-on treatments which do not involve changes in the fuselage primary structure. These add-

on treatments include lightweight aluminum honeycomb panels, constrained layer damping tape, porous acoustic blankets and limp trim panels. Due to the non-uniform input pressure distribution and different structural dynamic characteristics of the sidewall panels, the amount and type of treatment applied to achieve the required noise reduction varies from one panel unit to another. The study indicates that the heaviest amount of treatment needs to be applied to those panels located in the vicinity of the propeller plane. Of the techniques investigated, the combination of honeycomb panels and constrained layer damping tape applied to the aircraft skin seems to promise the required reductions in noise transmission in the low frequency region (70 - 350 Hz). Noise attenuation for higher frequencies can be achieved with a double wall system composed of porous acoustic blankets and limp trim panels which are isolated from the fuselage vibrations. However, a heavy trim panel might not always be beneficial for noise control since double wall resonances might coincide with one of the low frequency propeller blade passage harmonics. The optimization study indicates that to reduce cabin noise to a satisfactory level for the least amount of added weight, a combination of different add-on treatments needs to be used. The total added weight to the aircraft is about 75 lbs which is about 1.1% of the take-off gross weight. It should be noted that in achieving these values the effect of potential flanking paths and noise entering through the front and rear bulkheads have not been included in the analytical model.

The analytical prediction method has been validated experimentally with laboratory tests wherein all parameters could be carefully controlled or measured. A relatively good agreement between theoretical predictions and experimental observations in the field under static operating conditions

has been achieved for the baseline aircraft. Further experimental validation of the predicted noise reduction for the optimized aircraft is needed, however.

## REFERENCES

1. Cockburn, J.A. and Jolly, A.C., "Structural Acoustic Response, Noise Transmission Losses, and Interior Noise Levels of an Aircraft Fuselage Excited by Random Pressure Fields," AFFDC-TR-68-2, August 1968, Air Force Flight Dynamics Laboratory Technical Report.
2. Koval, L.R., "Effect of Air Flow, Panel Curvature and Internal Pressurization on Field Incidence Transmission Loss," Journal of the Acoustical Society of America, 59, No. 6, 1976.
3. Koval, L.R., "On Sound Transmission into a Thin Cylindrical Shell under Flight Conditions," Journal of Sound and Vibration, 48, No. 2, 1976.
4. Revell, J.D., Balena, F.J. and Koval, L.R., "Analytical Study of Interior Noise Control by Fuselage Design Techniques on High-Speed, Propeller-Driven Aircraft," NASA Contract Report 159222, July 1978.
5. Rennison, D.C., Wilby, J.F., March, A.M. and Wilby, E.G., "Interior Noise Control Prediction Study for High-Speed, Propeller-Driven Aircraft," NASA Contract Report 159200, September 1979. (Also AIAA-80-0998, presented at the AIAA 6th Aeroacoustics Conference, June 4-6, 1980, Hartford, Conn.).
6. Dowell, E.H., Gorman, III, G.F. and Smith, D.A., "Acoustoelasticity: General Theory Acoustic Natural Modes and Forced Response to Sinusoidal Excitation, Including Comparisons with Experiment," Journal of Sound and Vibration, 52, 4, 1977, pp. 519-592.
7. Sen Gupta, G., "Reduction of Cabin Noise During Cruise Conditions by Stringer and Frame Damping," AIAA Journal, Vol. 17, No. 3, March 1979.
8. Unruh, J.F., "A Finite Element Subvolume Technique for Structural-Borne Interior Noise Prediction," AIAA 5th Aeroacoustics Conference, Paper No. 79-0585, Seattle, Washington, March 1979.
9. Mixson, J.S., Barton, C.K. and Vaicaitis, R., "Investigation of Interior Noise in a Twin Engine Light Aircraft," Journal of Aircraft, AIAA, Vol. 15, No. 4, April 1978, pp. 227-233.
10. Vaicaitis, R., Slazak, M. and Chang, M.T., "Noise Transmission - Turbo-prop Problem," AIAA 5th Aeroacoustics Conference, Paper No. 79-0645, Seattle, Washington, March 1979.
11. Vaicaitis, R., Slazak, M. and Chang, M.T., "Noise Transmission and Attenuation by Stiffened Panels," AIAA 6th Aeroacoustics Conference, Paper No. 80-1034, Hartford, Conn., June 4-6, 1980.
12. Vaicaitis, R. and Slazak, M., "Noise Transmission Through Stiffened Panels," Journal of Sound and Vibration, 70, 3, 1980, pp. 413-426.
13. Vaicaitis, R. and Chang, M.T., "Noise Transmission into Semicylindrical Enclosures," ASME/ASCE Engineering Mechanics Conference, Boulder, Colo., June 1981.

14. Vaicaitis, R., "Noise Transmission into a Light Aircraft," Journal of Aircraft, AIAA, Vol. 17, No. 2, February 1980.
15. Mixson, J.S. et al., "Laboratory Study of Efficient Add-on Treatments for Interior Noise Control in Light Aircraft," AIAA 7th Aeroacoustics Conference, AIAA Paper 81-1969, Los Angeles, Ca., October 1981.
16. Lin, Y.K. and Donaldson, B.K., "A Brief Survey of Transfer Matrix Techniques with Special References to the Analysis of Aircraft Panels," Journal of Sound and Vibration, Vol. 10, 1969, pp. 103-143.
17. Lin, Y.K., Probabilistic Theory of Structural Dynamics, New York: McGraw-Hill, 1967.
18. Chao, Chen-Fu, "Modal Analysis of Interior Noise Fields," MAE Technical Report 1499-T, Princeton University, December 1980.
19. Beranek, L.L., "Acoustic Properties of Homogeneous, Isotropic Rigid Tiles and Flexible Blankets," Journal of the Acoustical Society of America, Vol. 19, No. 4, 1947.
20. Mulholland, K.A., Price, A.J. and Parbrook, H.D., "Transmission Loss of Multiple Panels in a Random Incidence Field," Journal of the Acoustical Society of America, Vol. 43, No. 6, 1968.
21. Piersol, A.G., Wilby, E.G., Wilby, J.F., "Evaluation of Aerocommander Propeller Acoustic Data: Static Operations," NASA Contractor Report 158919, May 1978.
22. Piersol, A.G., Wilby, E.G., Wilby, J.F., "Evaluation of Aero Commander Propeller Acoustic Data: Taxi Operations," NASA Contractor Report 159124, July 1979.
23. Piersol, A.G., Wilby, E.G., Wilby, J.F., "Evaluation of Aero Commander Sidewall Vibration and Interior Acoustic Data: Static Operations," NASA Contractor Report 159290, October 1980.
24. Lyon, R., "Noise Reduction of Rectangular Enclosures with One Flexible Wall," Journal of the Acoustical Society of America, Vol. 35, 1963, pp. 1791-1797.
25. Kihlman, T., "Sound Radiation into a Rectangular Room: Application to Airborne Sound Transmission into Buildings," Acustica, Vol. 18, pp. 11-20.
26. Strawderman, W.A., "The Acoustic Field in a Closed Space Behind a Rectangular Simply-Supported Plate Excited by Boundary Layer Turbulence," Underwater Sound Laboratory Report No. 827, 1967.
27. Bhattacharya, M.C. and Crocker, M.J., "Forced Vibration of a Panel and Radiation of Sound Into a Room," Acustica, Vol. 22, 1969/70, pp. 273-294.

28. Guy, R.W. and Bhattacharya, M.C., "The Transmission of Sound Through a Cavity-Backed Finite Plate," Journal of Sound and Vibration, Vol. 27, 1973, pp. 207-223.
29. Dowell, E.H. and Voss, H.M., "The Effect of Cavity on Panel Vibrations," AIAA Journal, Vol. 1, 1963, pp. 476-477.
30. Leissa, A., "Vibration of Plates," NASA Sp-160, 1969.
31. Beranek, L.L., Ed., Noise and Vibration Control, New York: McGraw-Hill, 1971.
32. Slazak, M., "Noise Transmission Through Stiffened Panels," Ph.D. Thesis, Department of Civil Engineering and Engineering Mechanics, Columbia University, New York, June 1979.
33. Geisler, D.L., "Experimental Modal Analysis of an AeroCommander Aircraft," NASA Contractor Report 165750, September 1981.

Table 1 Material and Geometric Properties of Stiffeners

Panel Unit	$E_s \times 10^{-6}$ psi	$I_z \times 10^2$ in <sup>4</sup>	$I_y \times 10^2$ in <sup>4</sup>	$s_z$ in	$c_z$ in	$c_y$ in	$J_s$ in <sup>4</sup>	$C \times 10^4$ in <sup>4</sup>	$C_{ws} \times 10^2$ in <sup>6</sup>	A in <sup>2</sup>	$\ell$ in
1	10.5	.347	.736	1.0	0.0	.323	.169	.189	.903	.038	26.4
2	10.5	.810	1.370	1.0	0.0	.319	.369	2.92	2.12	.203	26.4
3	10.5	.651	1.440	1.0	0.0	.320	.328	1.46	1.70	.161	26.4
4	10.5	.651	1.440	1.0	0.0	.320	.328	1.46	1.70	.161	23.5
6	10.5	.483	.926	1.0	0.0	.321	.227	5.42	1.26	.118	19.1
9	10.5	.810	1.370	1.0	0.0	.319	.369	2.92	2.12	.203	5.25
10	10.5	.651	1.160	1.0	0.0	.320	.300	1.46	1.70	.161	23.5

Table 2 Natural Frequencies of Sidewall Panels (n = 1, 2, 3)

Panel Unit	Frequencies, Hz	
	Theoretical	Experimental
1	72,84,111,149,172,178,181,189,224,228,245,254,259,276,338,345,359	71*,86*,137,146,(157),166,172,(177),183,189,234,(241),261,(269),282',288',310',336'
2	104,205,240,247,271,333,390,399	(94),114*,(161),217,224,241,(269),276,282',288',310',336',352
3	62,77,122,127,140,159,194,198,201,248,285,292,299,348,357,371,392,414	No data below 100 Hz 152,201,228,270 (Crude data)
4	68,80,95,130,138,155,160,173,196,223,230,237,256,264,285,300,310,340,375,384,406	Insufficient data
5	58	58,70,108,117,143,230,322
6	169,188,239,258,260,344,384,403	170(174),219,232,240,252,264,(278),305
7	122,284 <sup>+</sup>	323,406 Exterior window only
8	72,223 <sup>+</sup>	72*,97,112,(120),(129),146,158,167,185,194,209,223+,243+,264,273,283+,321
9	276,296,338,377	No data
10	147,206,324,348,434	No data

<sup>+</sup> window dilatational mode  
\* global modes participating

( ) two frequencies for similar mode coupling, between panels 1 and 2  
○ even modes with n (n = 2, 4, ...)

Table 3 Natural Frequencies of Stiffened Panels for Aero-  
Commander Sidewall with Honeycomb Add-On Treatment

(First Frequency Band)

Panel Unit	Baseline-Untreated Hz	Honeycomb h = 0.286 in Hz	Honeycomb h = 0.429 in Hz
1	72, 84, 111	161, 194, 262	{ 199*, 232*, 307*
2	104, 205	124, 192	
3	62, 77	184, 233	405, 510
4	68, 80, 96	229, 250, 300	292, 336, 403
6	169, 188, 259	347, 413, 512	519, 617, 765
9	276	379	x
10	147	327	x

Panel Units 5, 7 and 8 are windows  
 \* Panels 1 and 2 combined into one unit  
 x Frequency above 1000 Hz

Table 4 Fundamental Frequencies of the Stiffened Panel Units with Different Damping Tape Add-On Treatment

Panel Unit	Baseline-Untreated Hz	Damping Tape S.D. = .38 lb/ft <sup>2</sup> Hz	Damping Tape S.D. = .78 lb/ft <sup>2</sup> Hz	Damping Tape S.D. = 2.42 lb/ft <sup>2</sup> Hz
1	72	57	51	33
2	104	92	84	57
3	62	50	45	30
4	68	54	48	32
6	169	131	116	75
9	276	214	189	127
10	147	131	121	84

S.D. = Surface Density

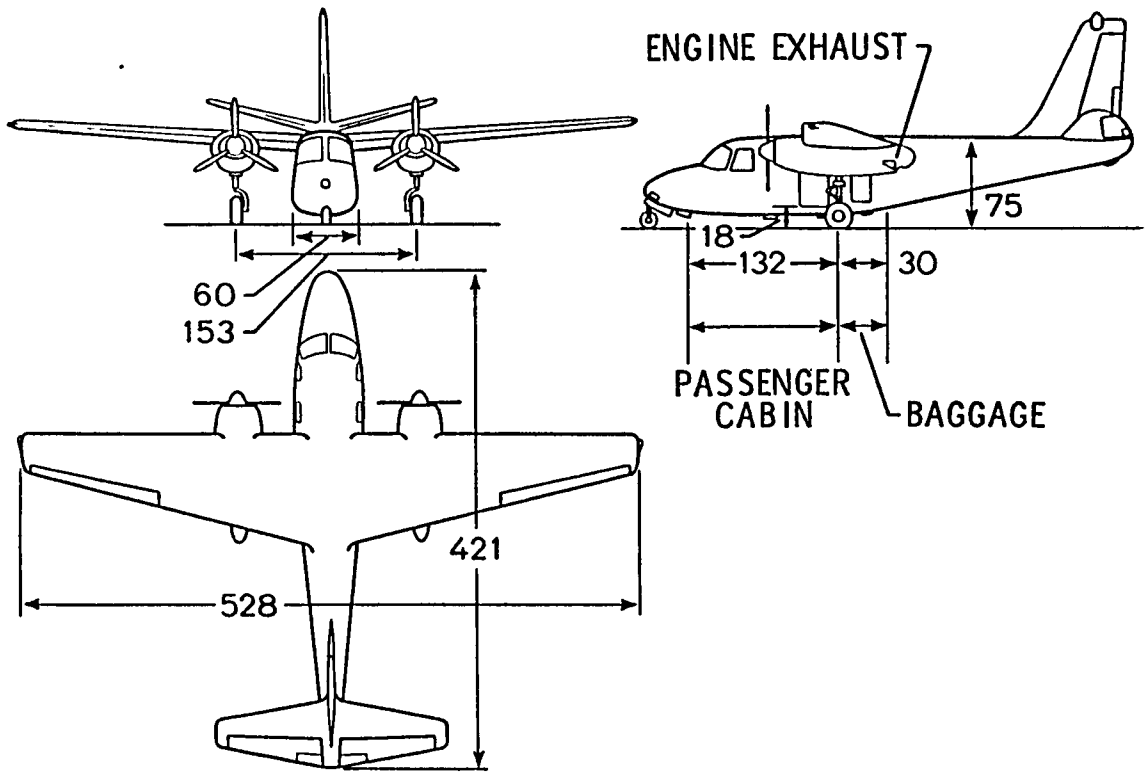


Fig. 1 Twin-engine aircraft used in the noise optimization study

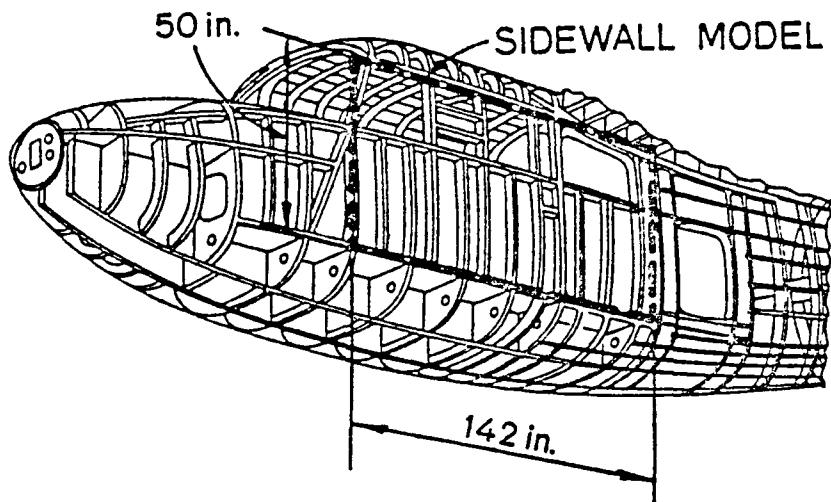


Fig. 2 Structural features of a twin-engine light aircraft

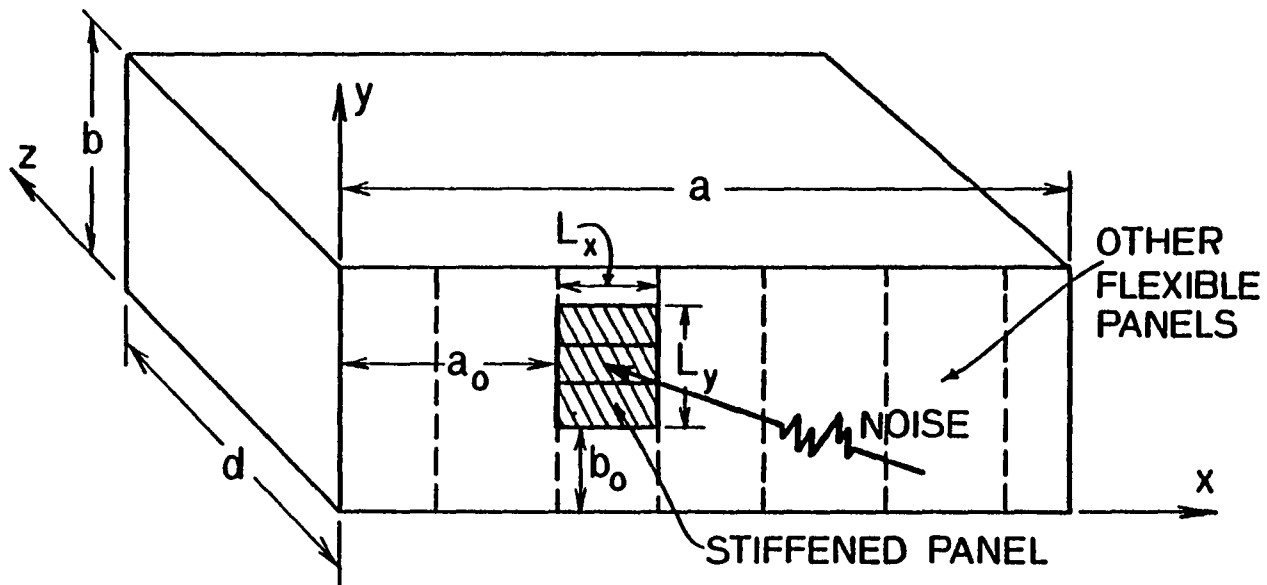


Fig. 3 Simplified geometry of aircraft cabin model

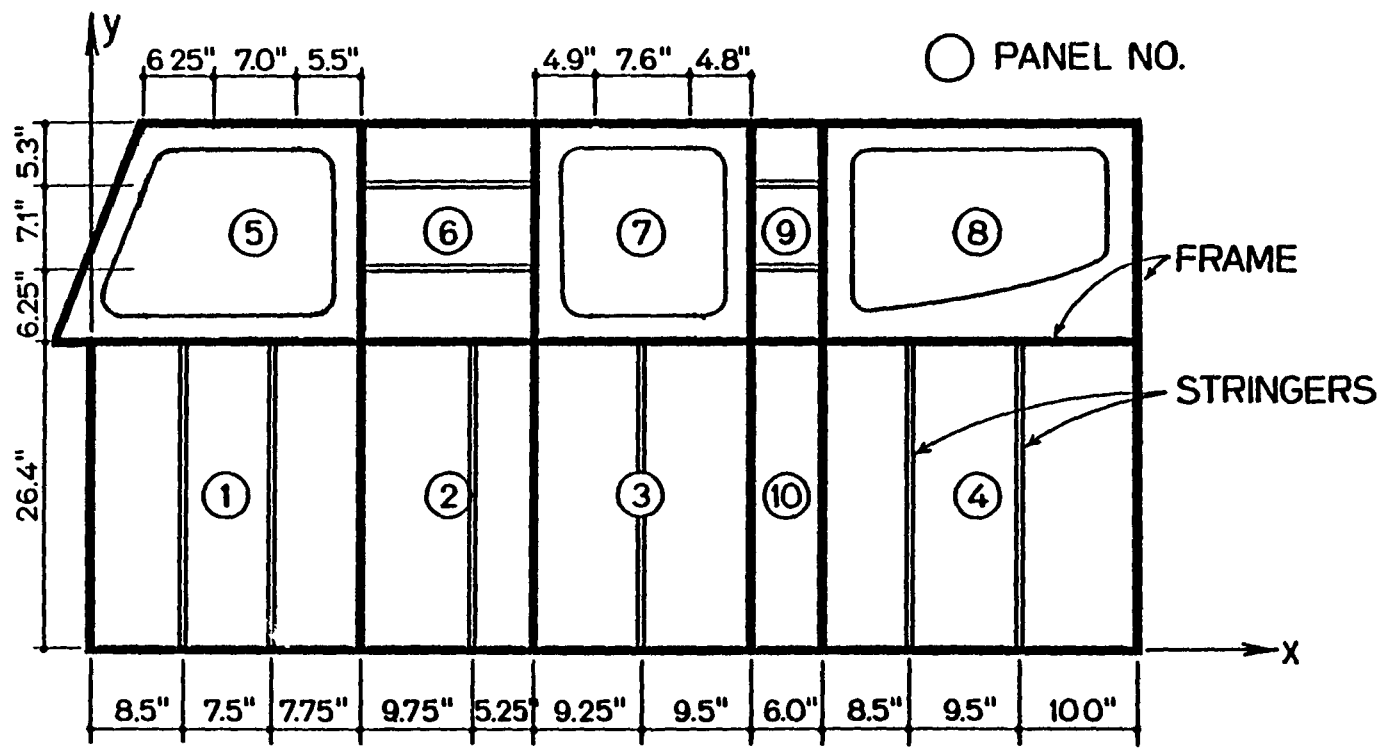


Fig. 4 Aircraft sidewall used for noise transmission study

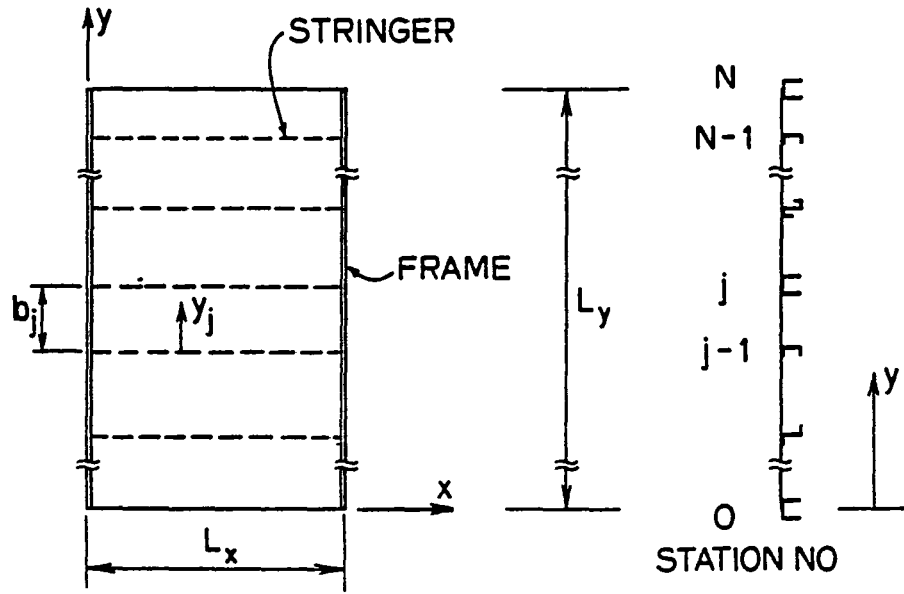


Fig. 5 A multispanned skin-stringer system

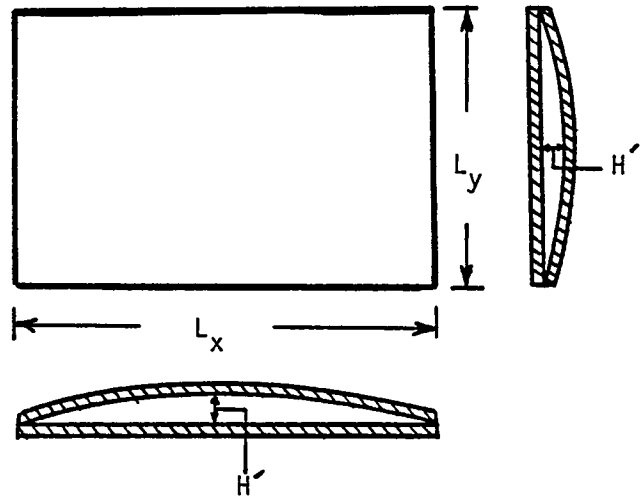


Fig. 6 Geometry of a double wall window construction

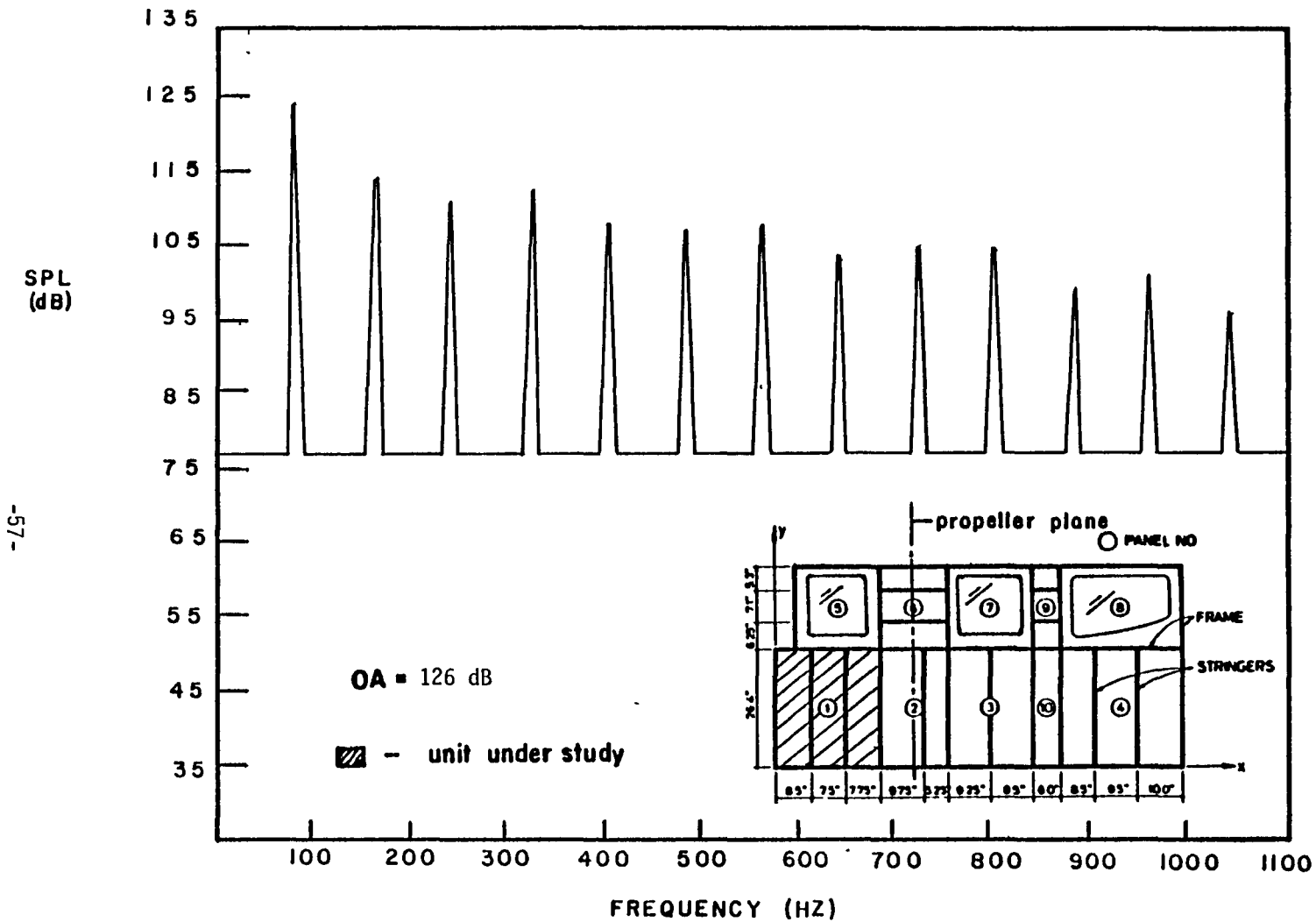


Fig. 7 PROPELLER NOISE INPUT (PANEL UNIT No. 1 )

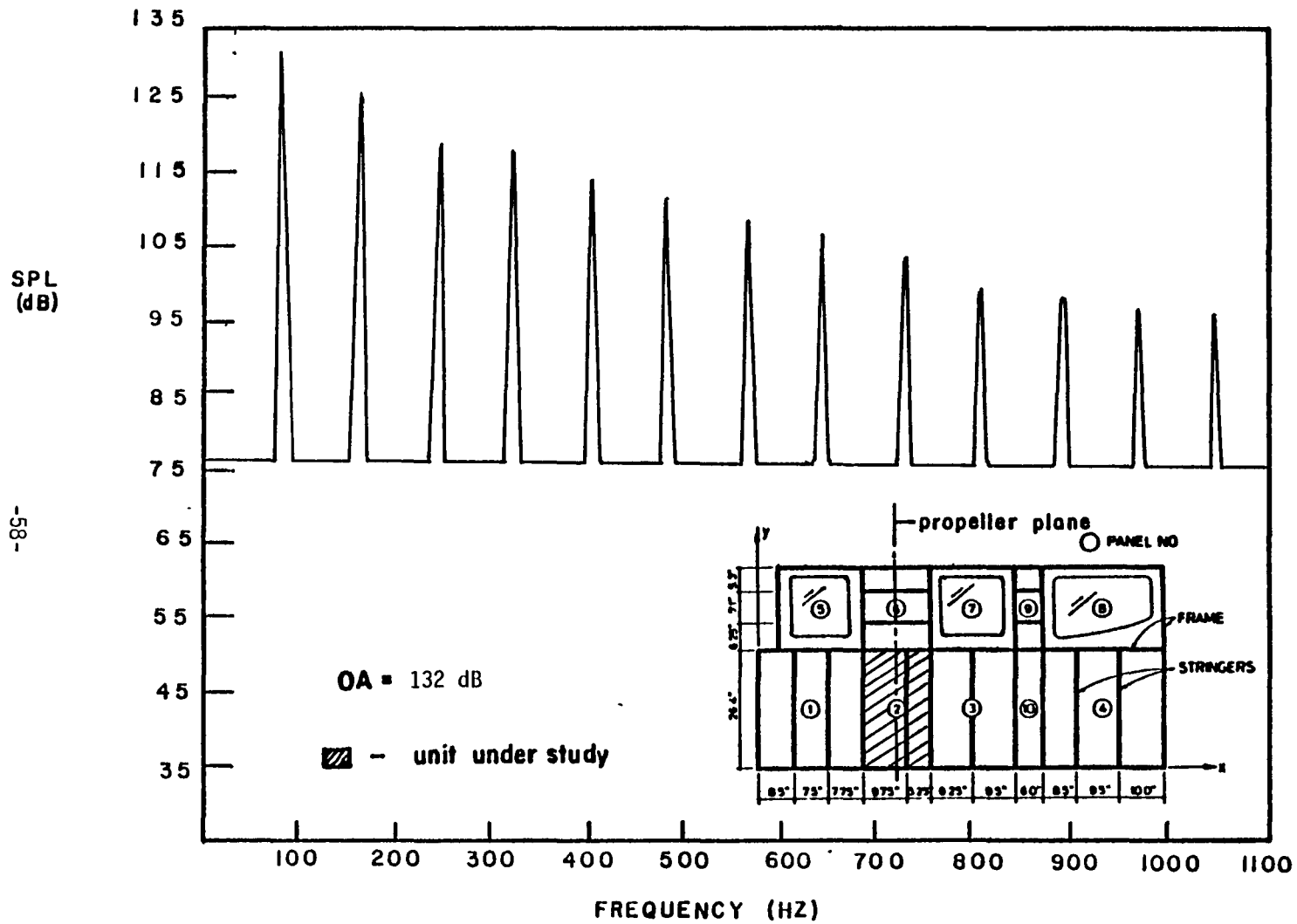


Fig. 8 PROPELLER NOISE INPUT (PANEL UNIT No. 2 )

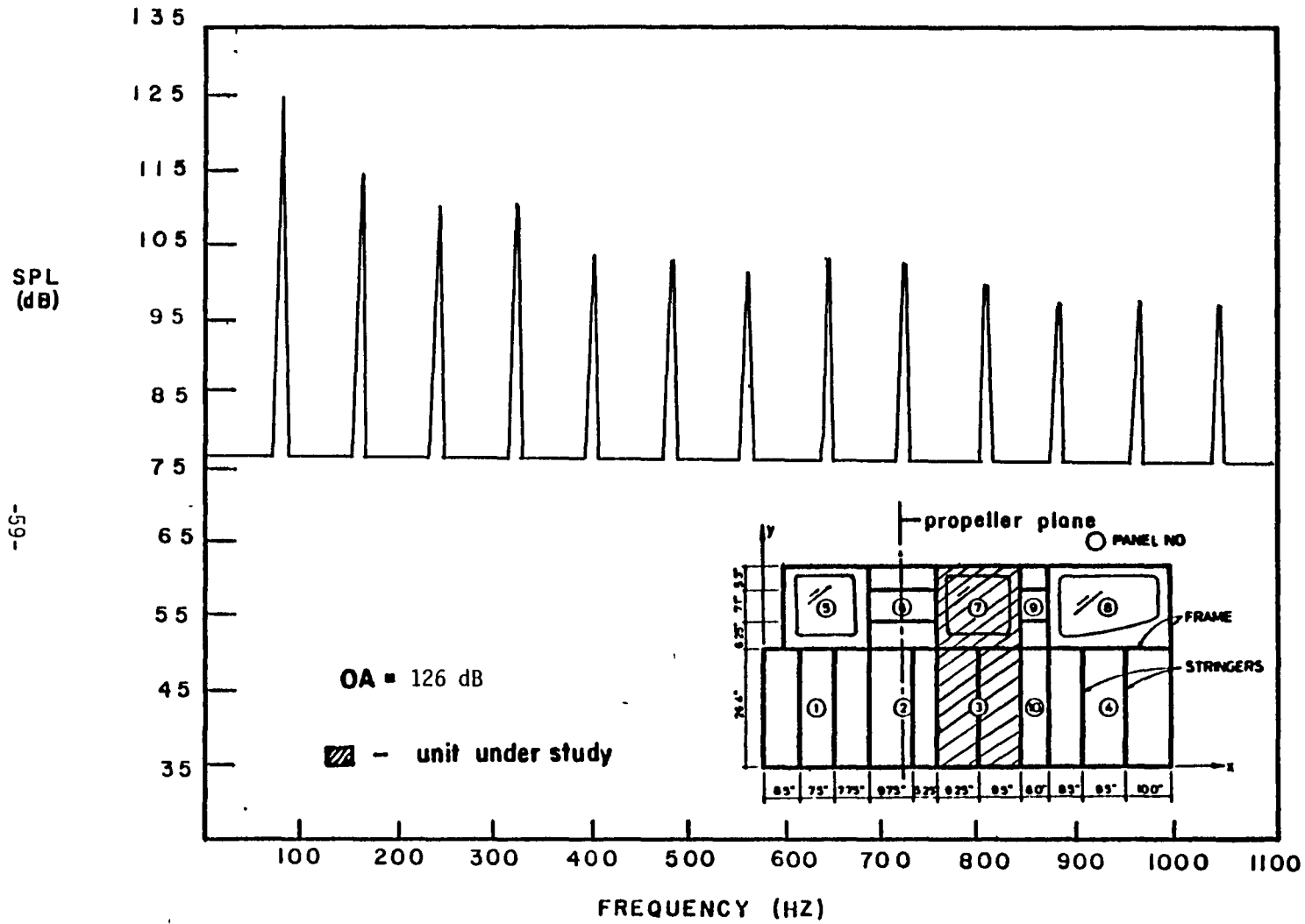


Fig. 9 PROPELLER NOISE INPUT (PANEL UNIT No. 3,7)

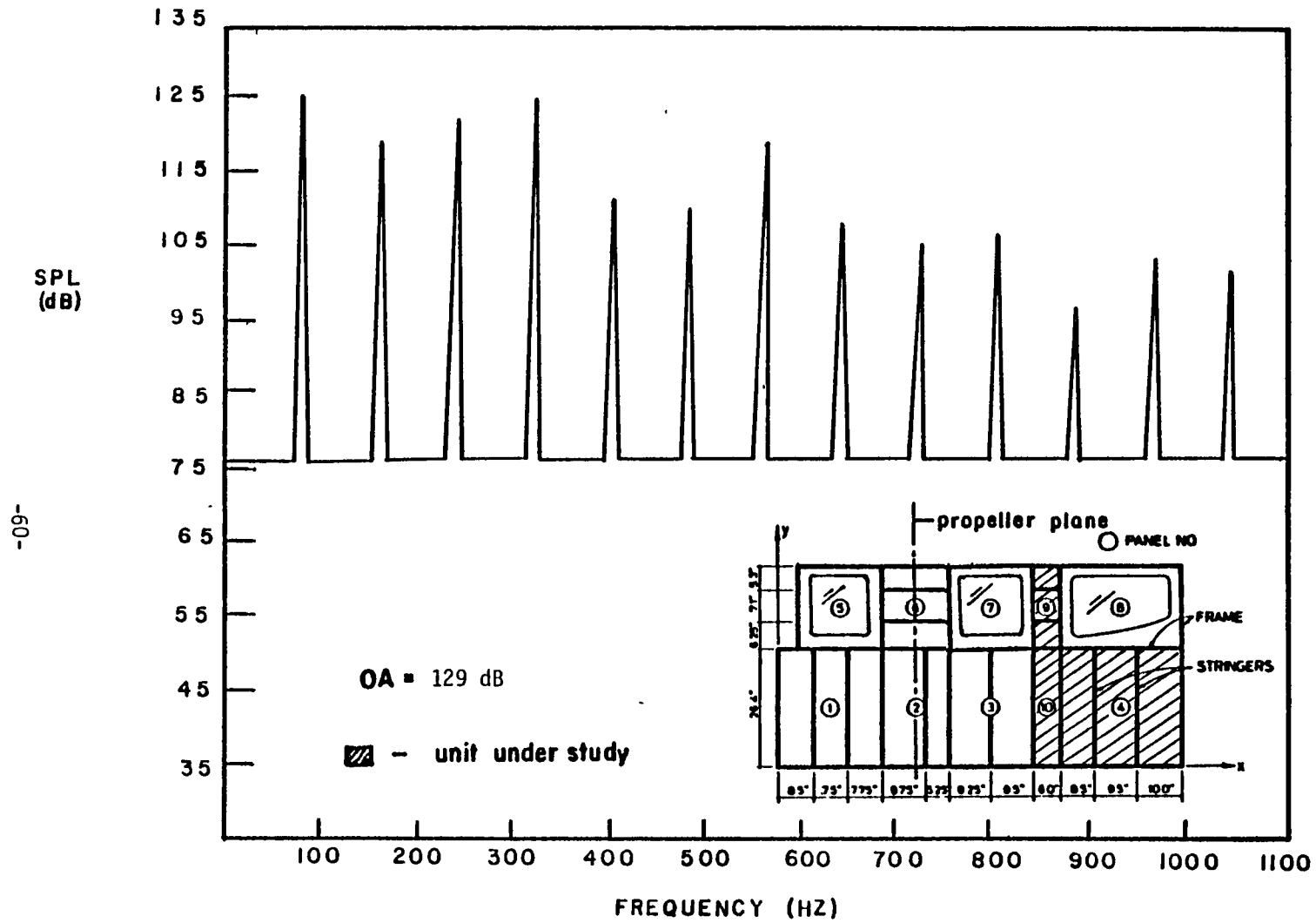


Fig. 10 PROPELLER NOISE INPUT (PANEL UNIT No. 4, 9, 10)

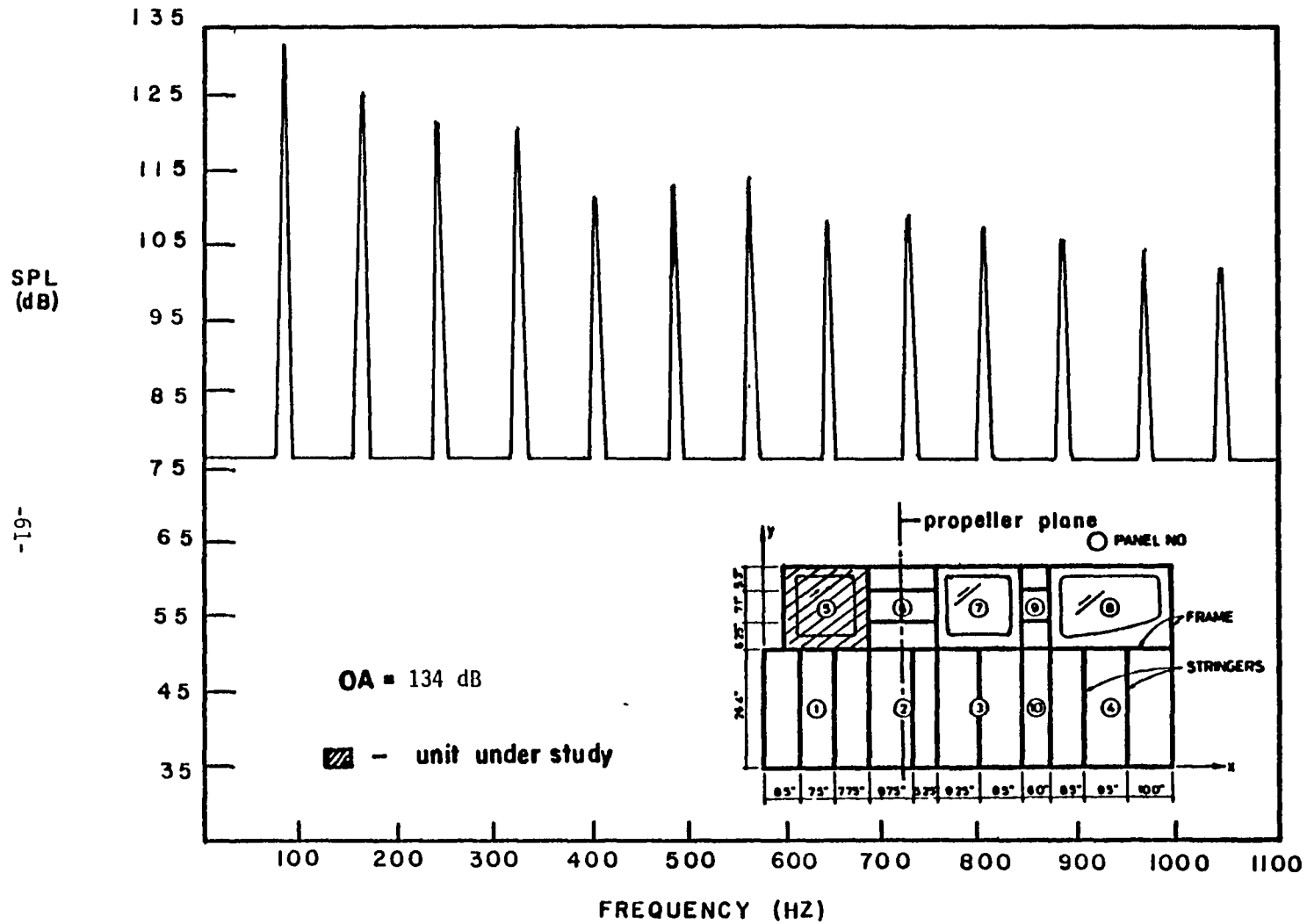


Fig. 11 PROPELLER NOISE INPUT (PANEL UNIT No. 5 )

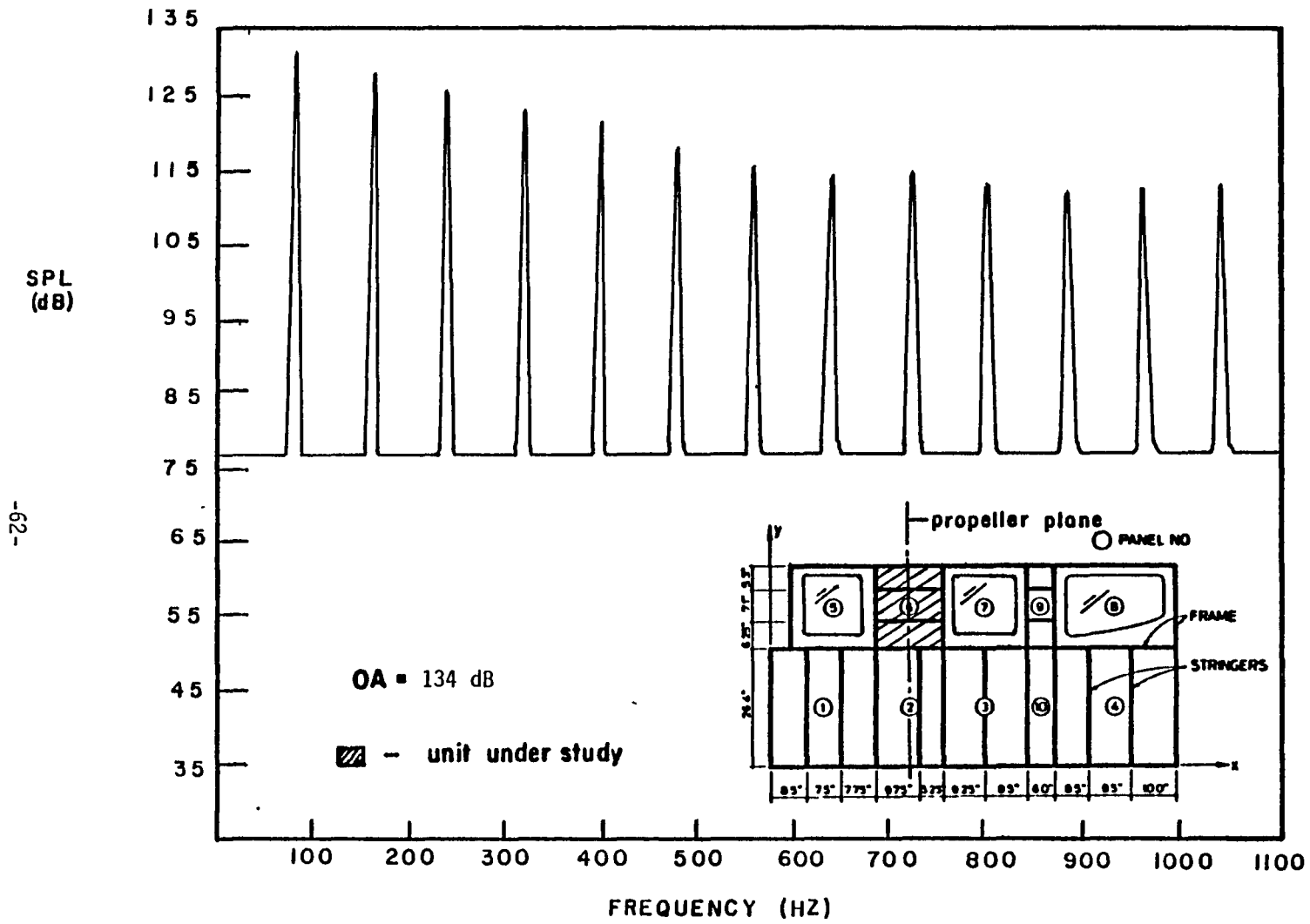


Fig. 12 PROPELLER NOISE INPUT (PANEL UNIT No. 6 )

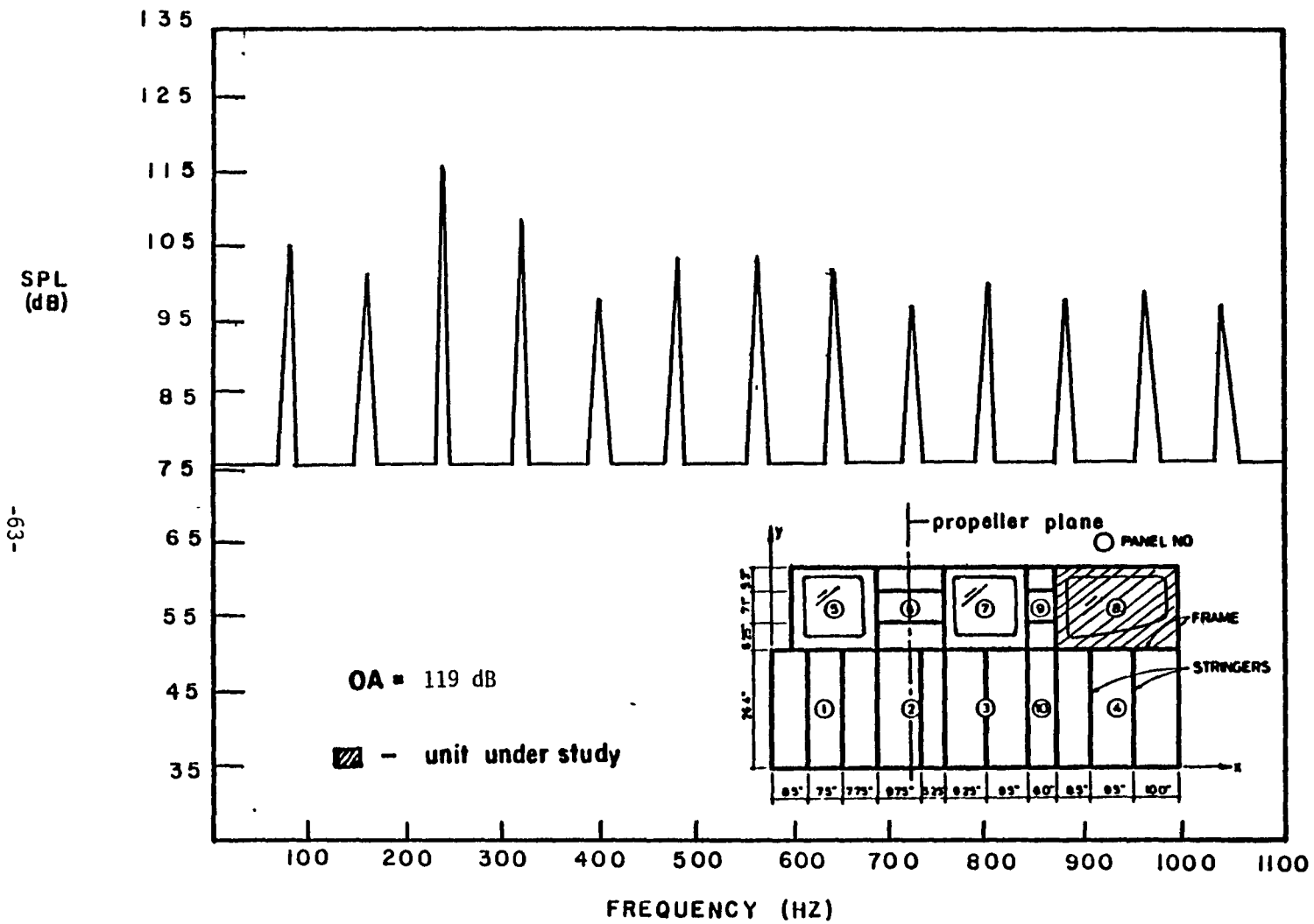


Fig. 13 PROPELLER NOISE INPUT (PANEL UNIT No. 8 )

### ACOUSTIC BLANKETS

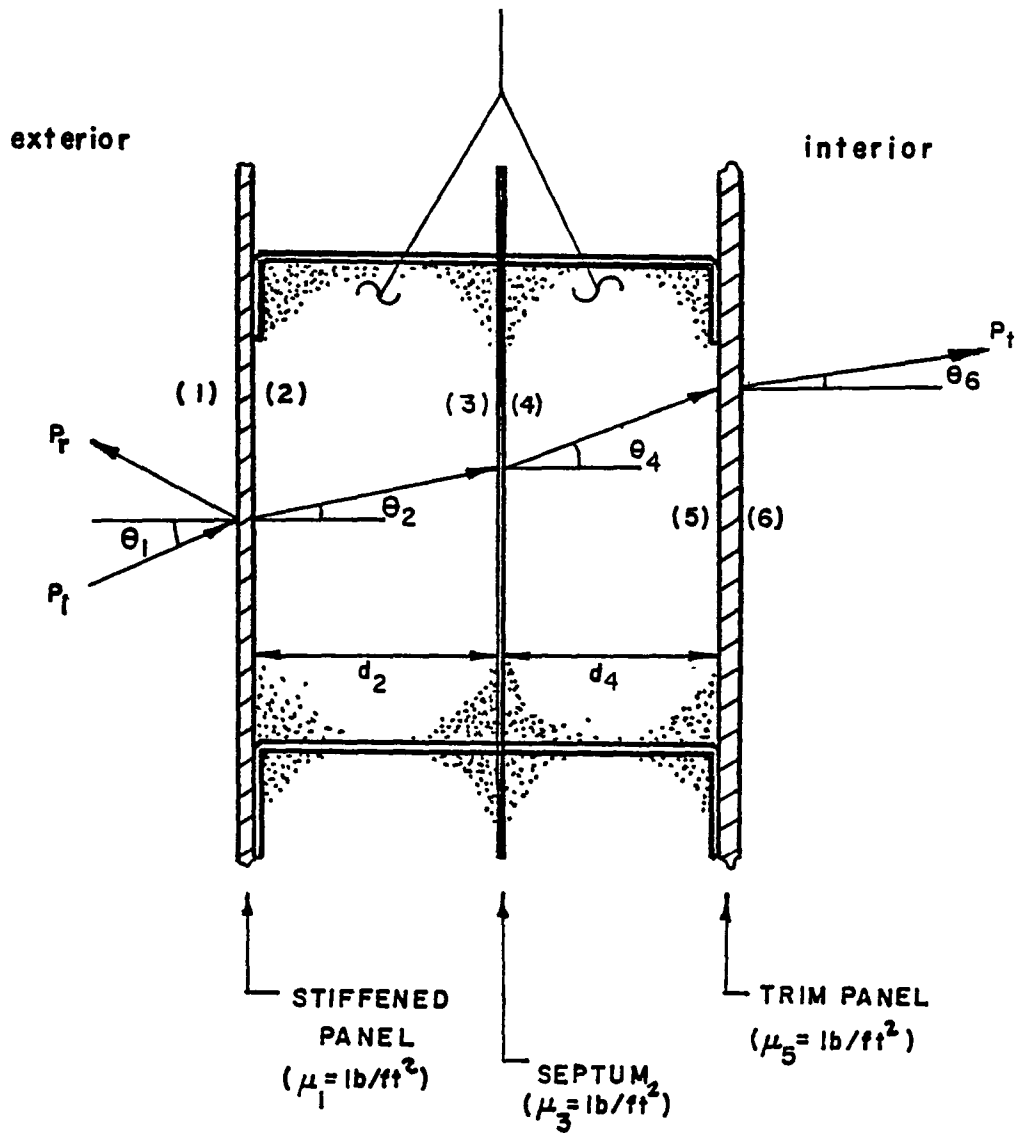


Fig. 14 Geometry of sidewall treatment

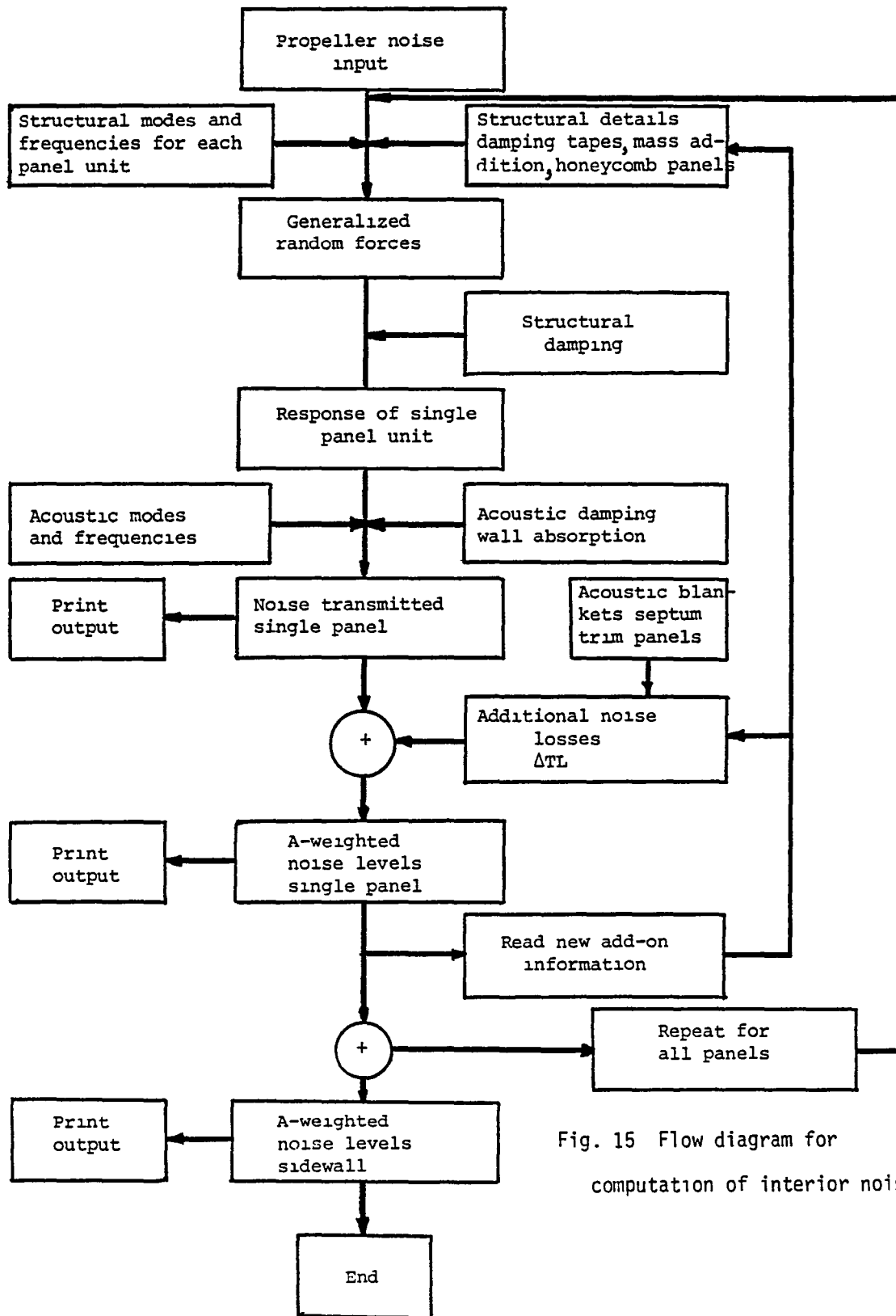


Fig. 15 Flow diagram for computation of interior noise

O - shear center

C' - centroid

S - point of stringer attachment to the skin

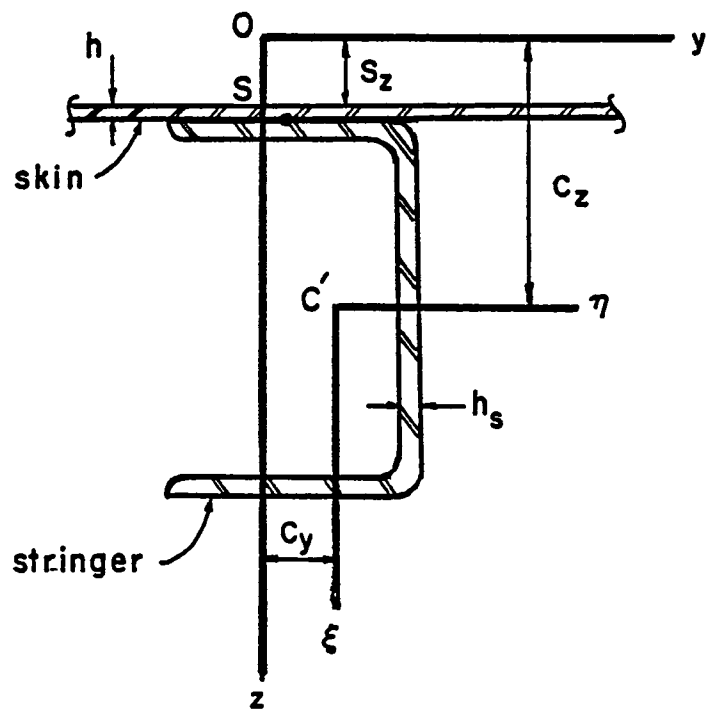


Fig. 16 Details of skin-stringer construction

$$f_{11} = 169 \text{ Hz}$$

$$f_{21} = 188 \text{ Hz}$$

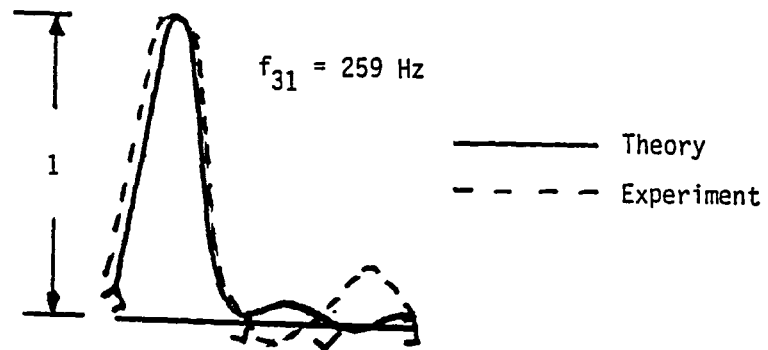
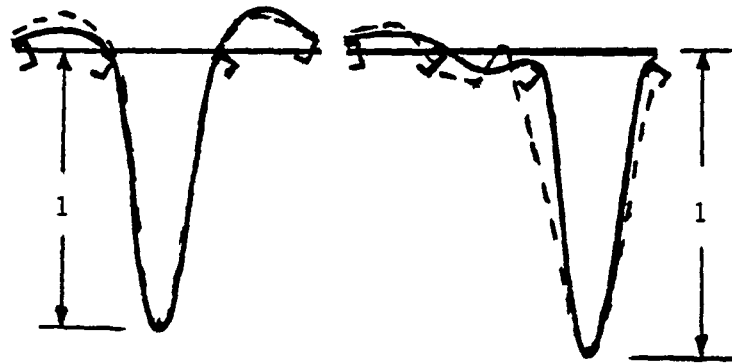


Fig. 17 Mode shapes of a stiffened panel for the first frequency band (panel No. 6)

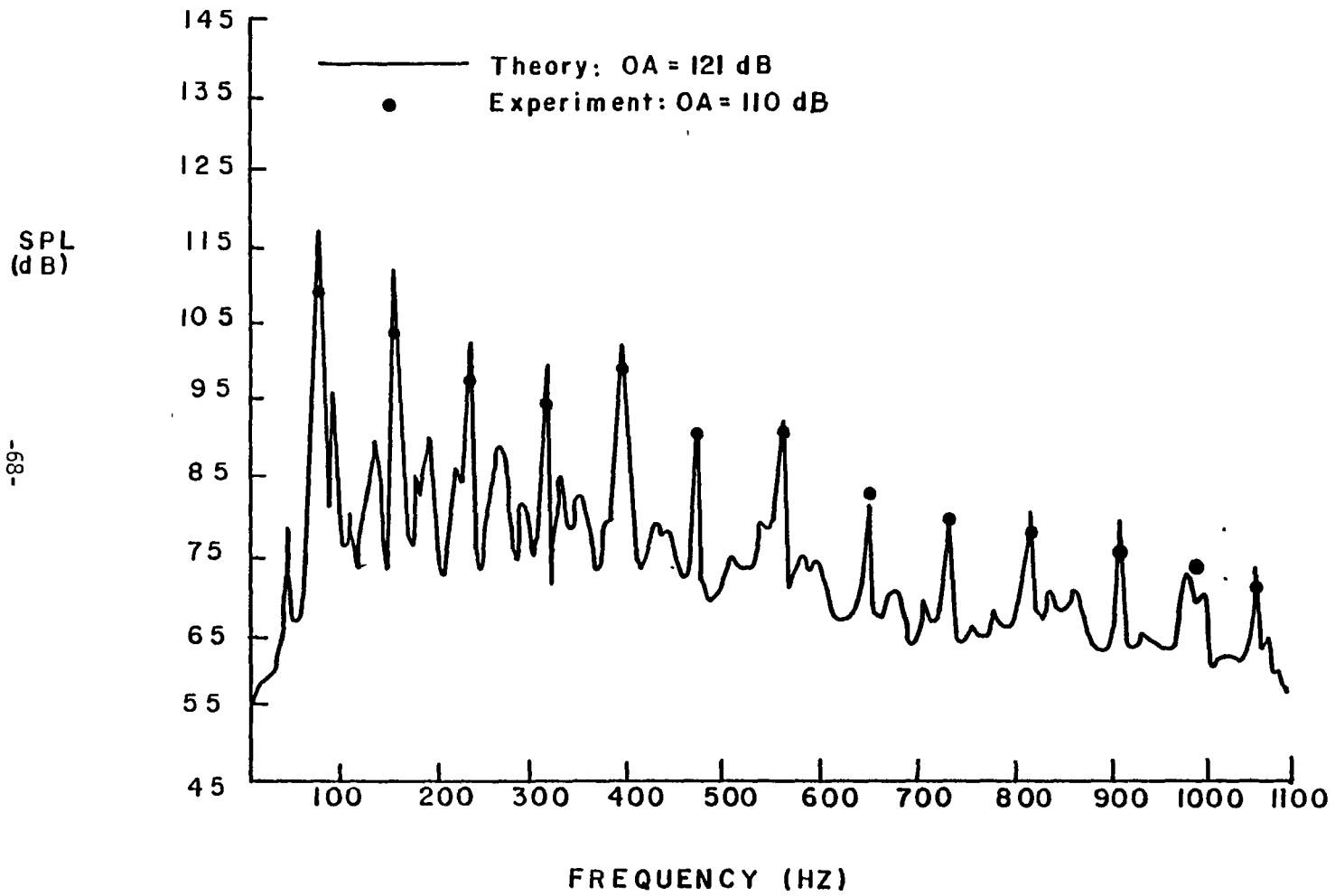


Fig. 18 Sound levels in the aircraft cabin

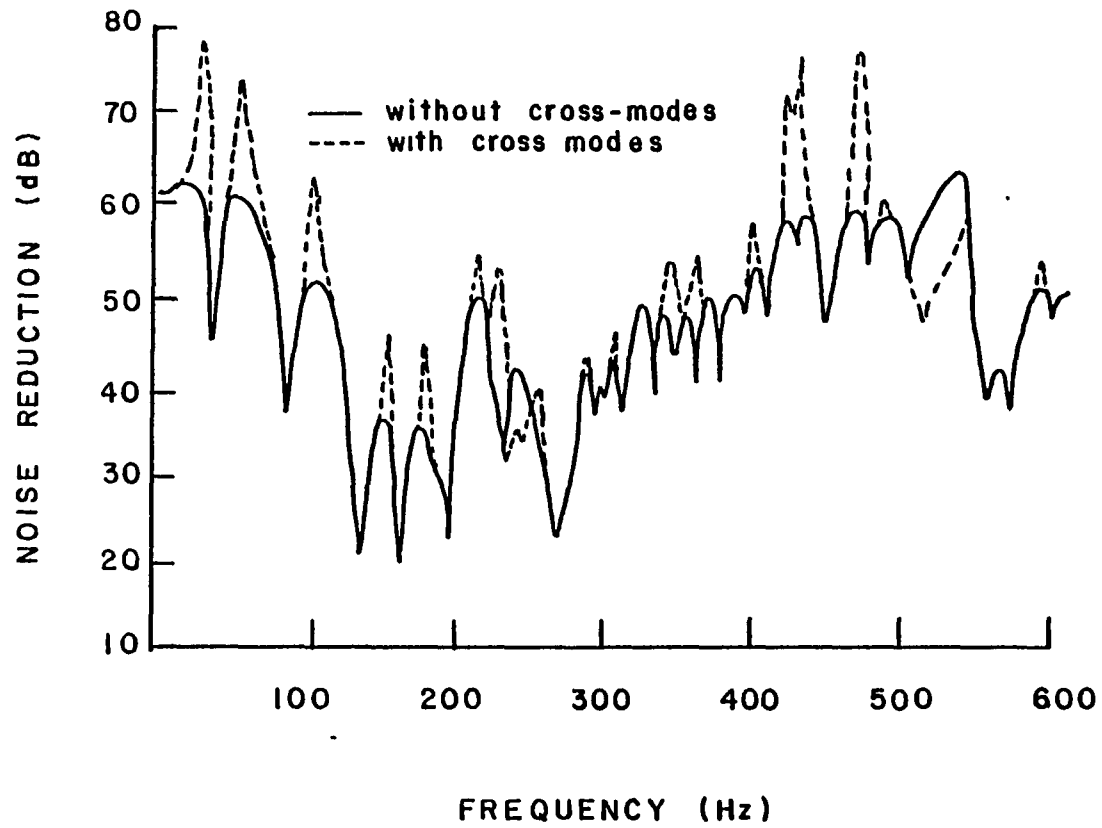


Fig. 19 Noise reduction for a stiffened panel with and without cross-modal terms

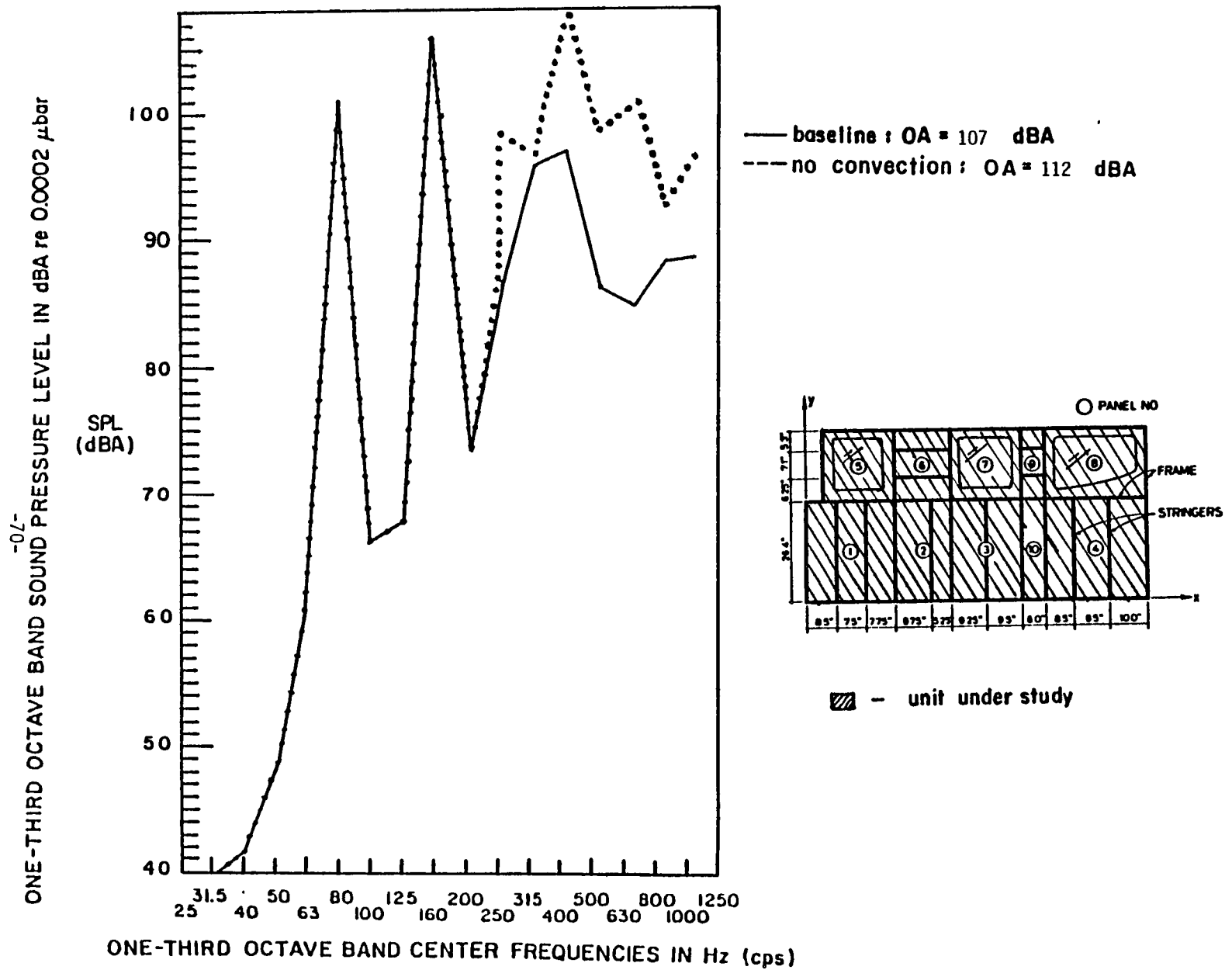
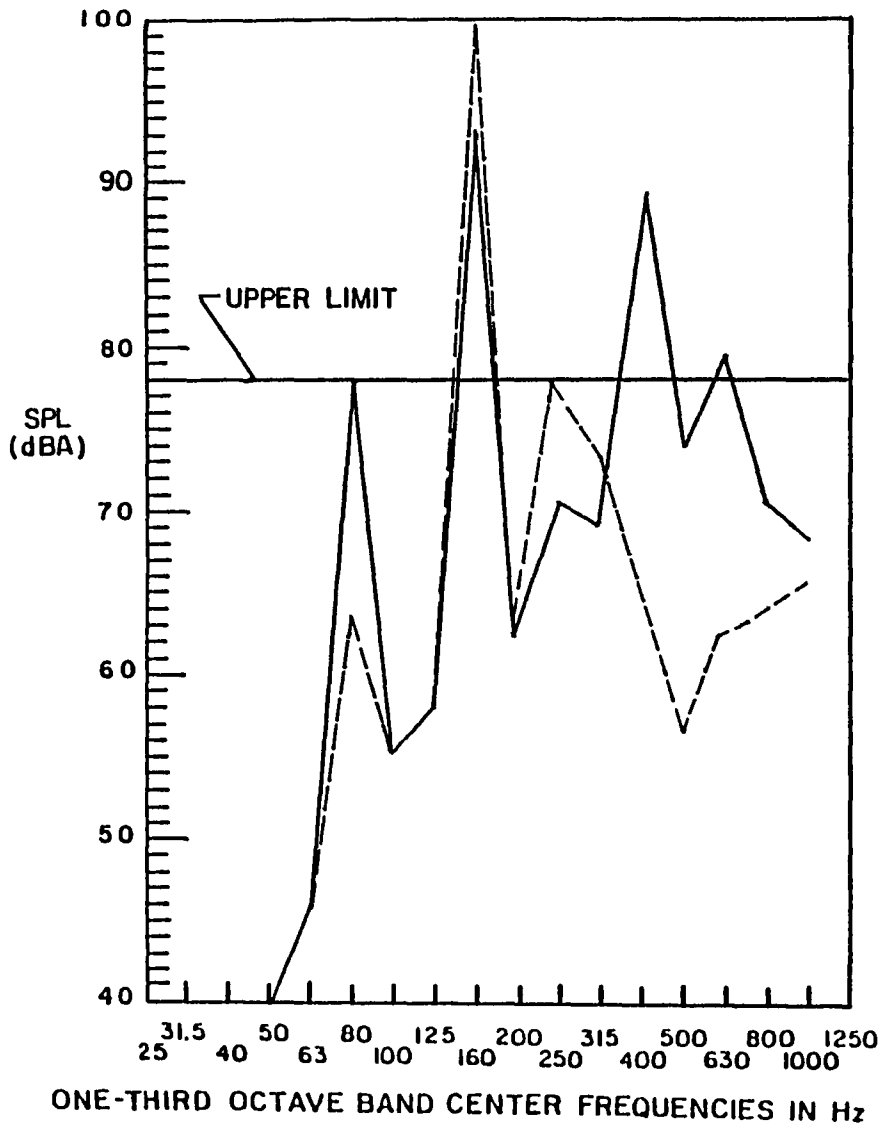


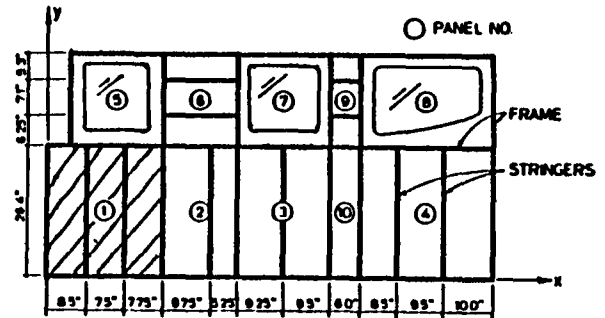
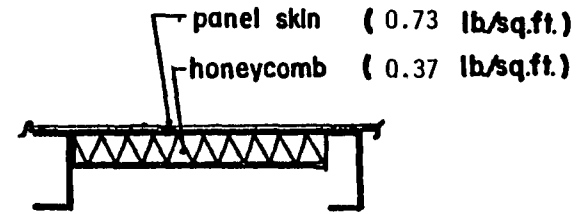
Fig. 20 Interior noise levels with and without convection

ONE-THIRD OCTAVE BAND SOUND PRESSURE LEVEL IN dBA re 0.0002  $\mu$ bar



— baseline : OA = 94 dBA  
 --- honeycomb : OA = 102 dBA

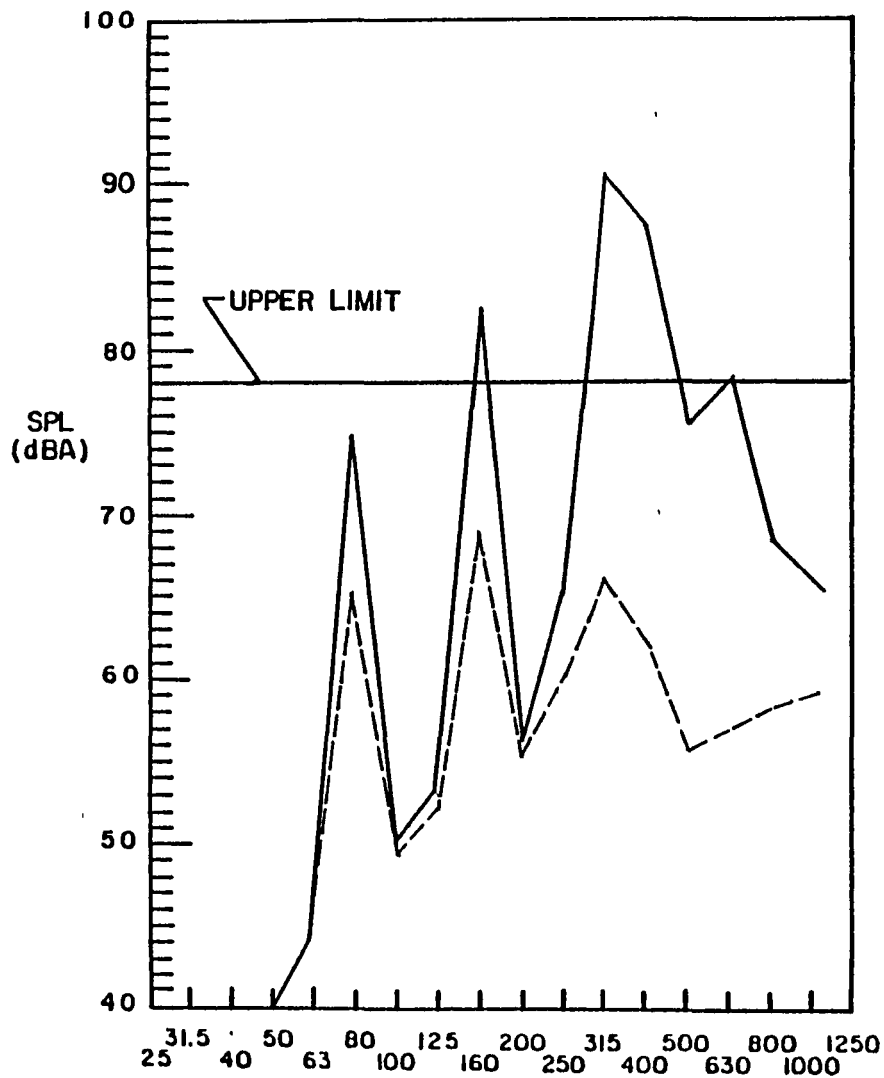
added weight = 1.63 lbs.  
 panel area = 4.4 sq.ft.



▨ - unit under study

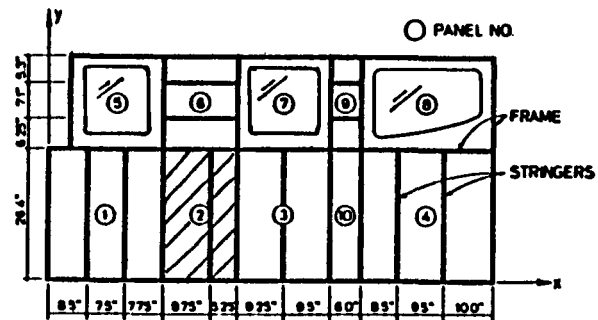
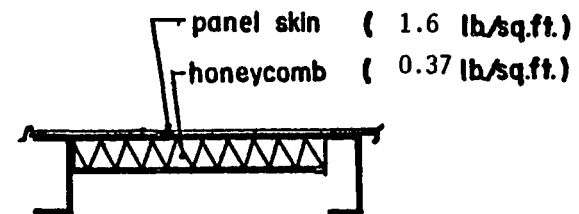
Fig. 21 Interior noise levels with honeycomb treatment (Panel No. 1)

ONE-THIRD OCTAVE BAND SOUND PRESSURE LEVEL IN dBA re 0.0002  $\mu$ bar



— baseline : OA = 92 dBA  
 --- honeycomb : OA = 72 dBA

added weight = 1.02 lbs.  
 panel area = 2.75 sq.ft.

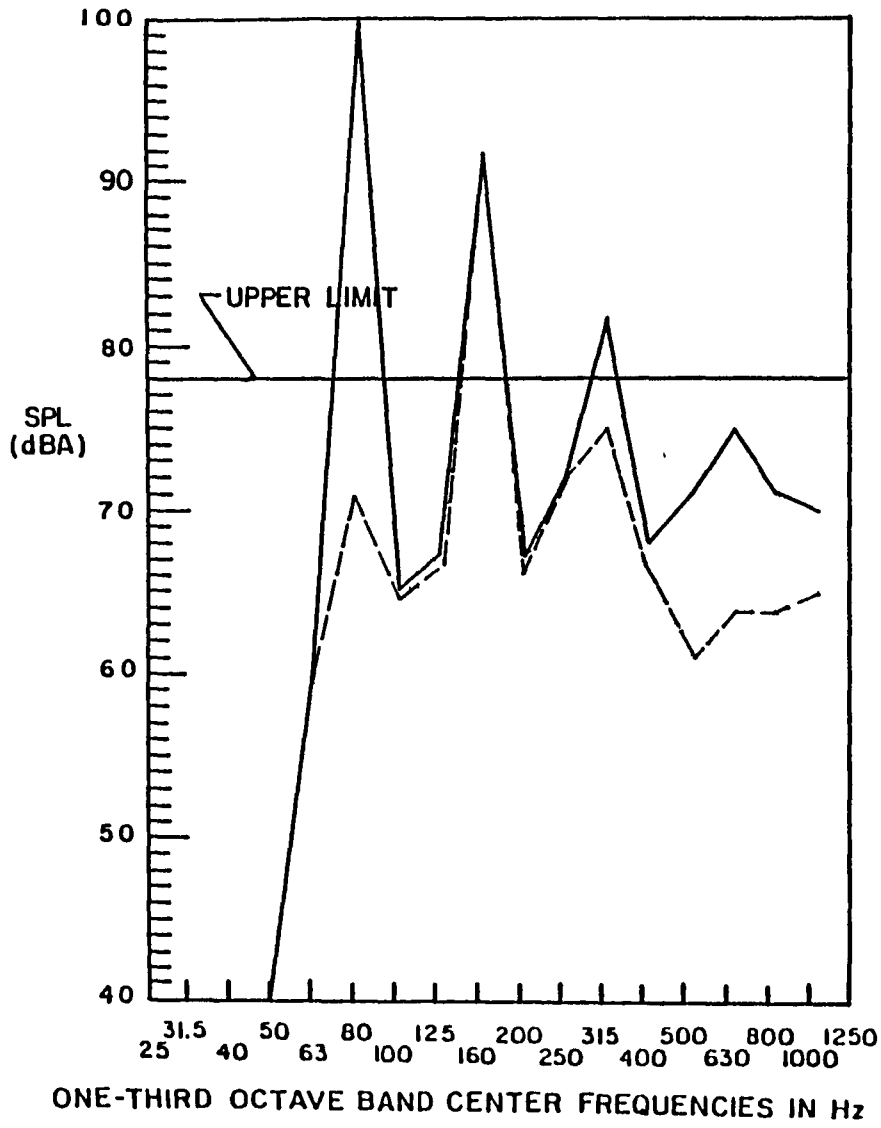


▨ - unit under study

ONE-THIRD OCTAVE BAND CENTER FREQUENCIES IN Hz (cps)

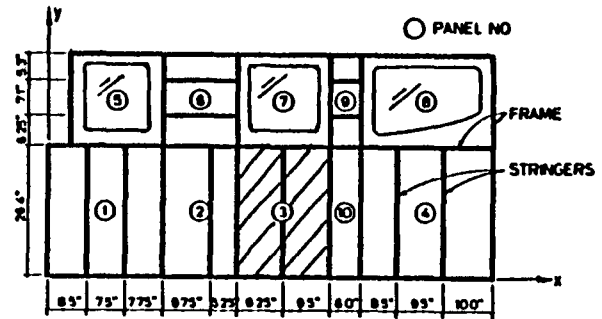
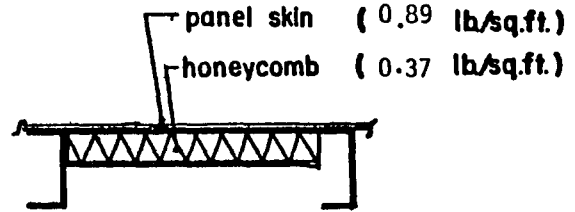
Fig. 22 Interior noise levels with honeycomb treatment (panel No. 2)

ONE-THIRD OCTAVE BAND SOUND PRESSURE LEVEL IN dBA re 0.0002  $\mu$ bar



— baseline ; OA = 102 dBA  
 --- honeycomb ; OA = 94 dBA

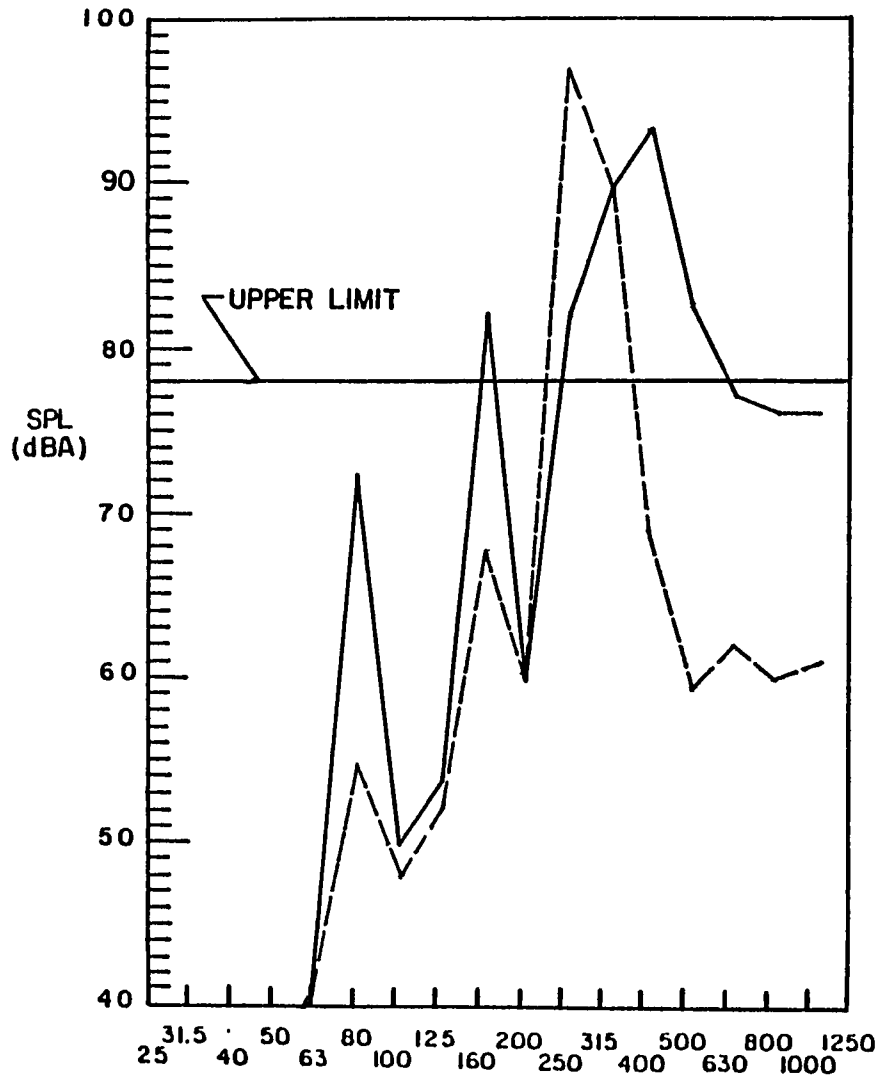
added weight = 1.27 lbs  
 panel area = 3.44 sq.ft.



▨ - unit under study

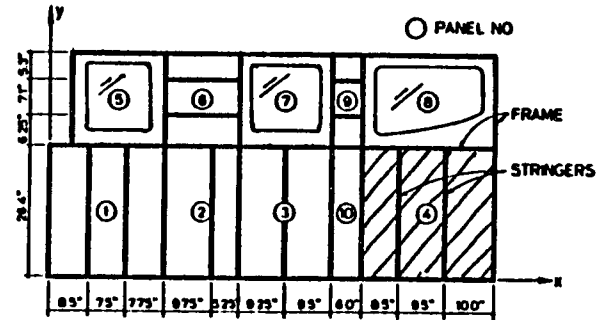
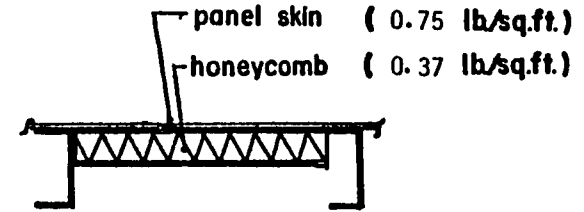
Fig. 23 Interior noise levels with honeycomb treatment (Panel No. 3)

ONE-THIRD OCTAVE BAND SOUND PRESSURE LEVEL IN dBA re 0.0002  $\mu$ bar



— baseline : OA = 95 dBA  
 --- honeycomb : OA = 99 dBA

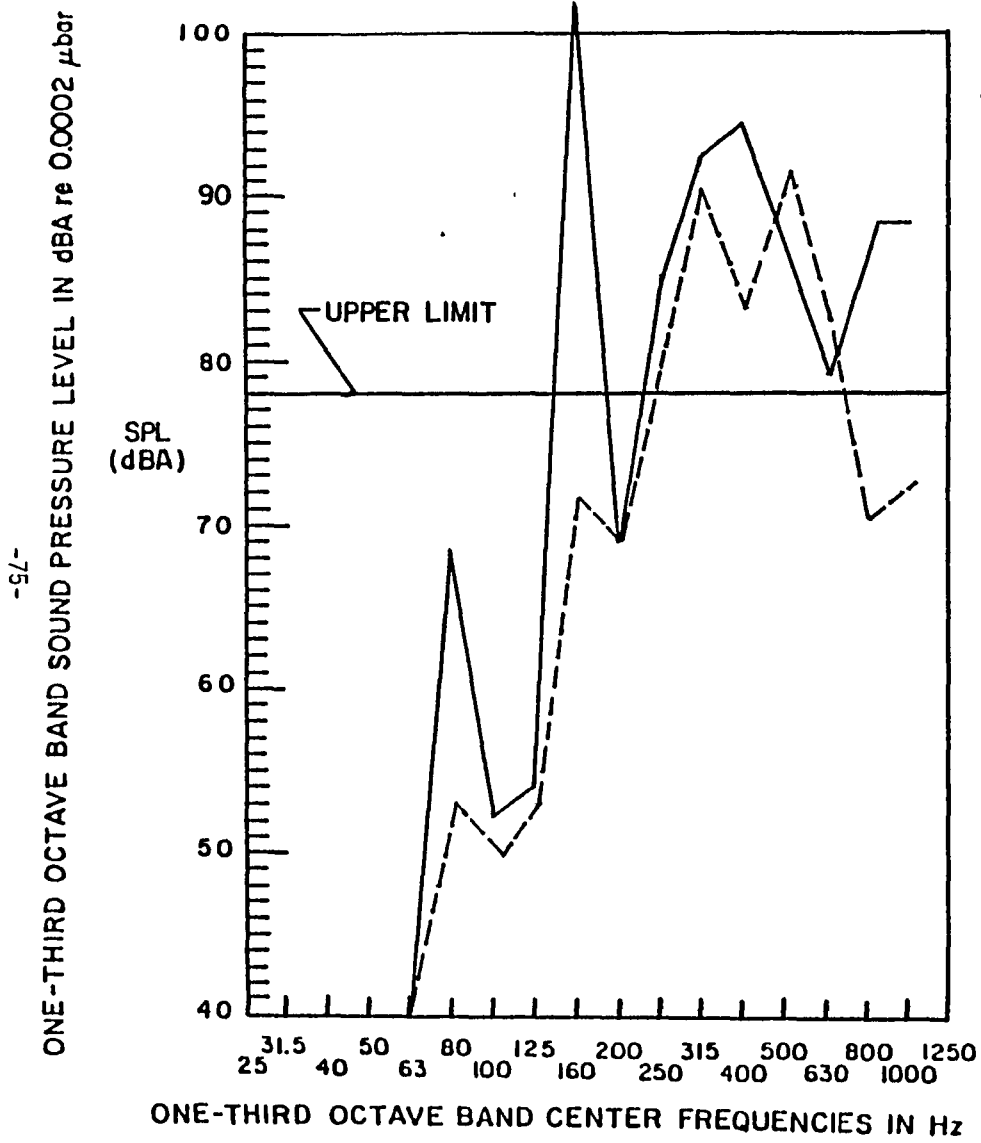
added weight = 1.90 lbs.  
 panel area = 5.13 sq.ft.



▨ - unit under study

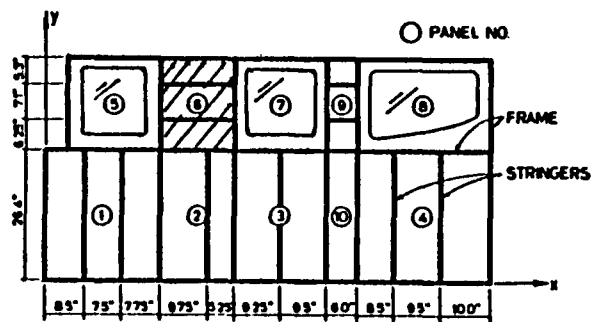
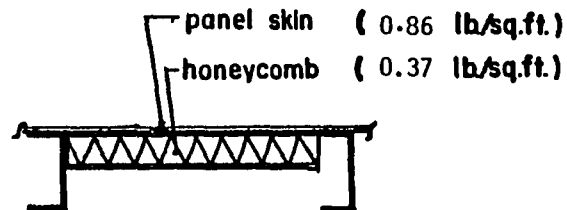
ONE-THIRD OCTAVE BAND CENTER FREQUENCIES IN Hz (cps)

Fig. 24 Interior noise levels with honeycomb treatment (Panel No. 4)



— baseline ; OA = 106 dBA  
 --- honeycomb ; OA = 95 dBA

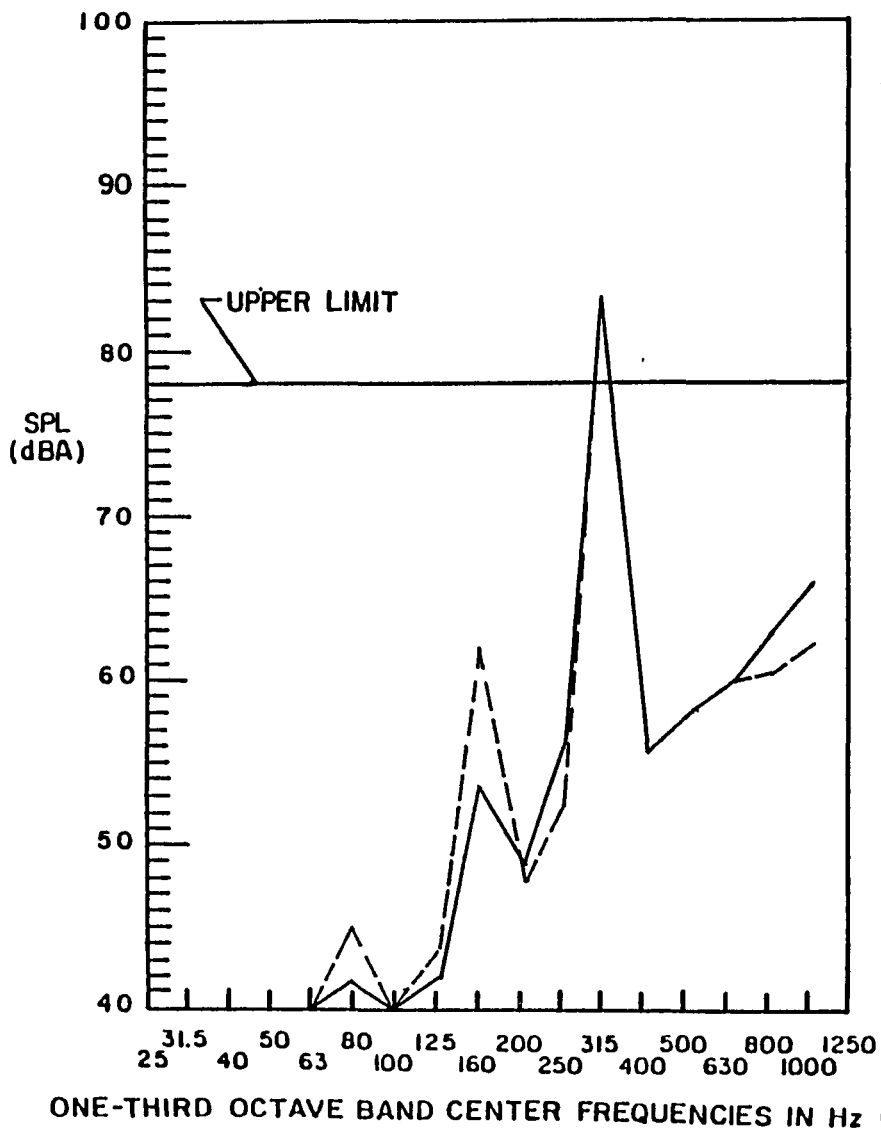
added weight = 0.72 lbs  
 panel area = 1.94 sq.ft.



▨ - unit under study

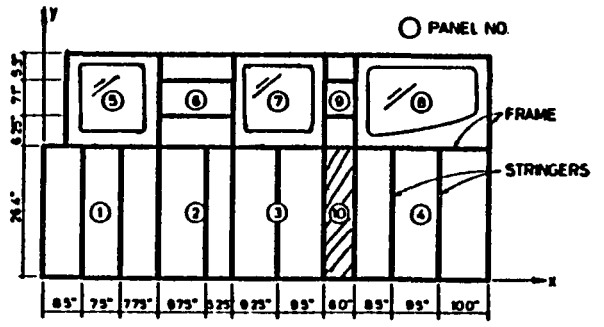
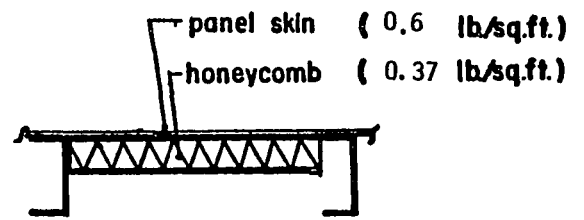
Fig. 25 Interior noise levels with honeycomb treatment (Panel No. 6)

ONE-THIRD OCTAVE BAND SOUND PRESSURE LEVEL IN dBA  $\mu$ bar



— baseline : OA = 86 dBA  
 --- honeycomb : OA = 85 dBA

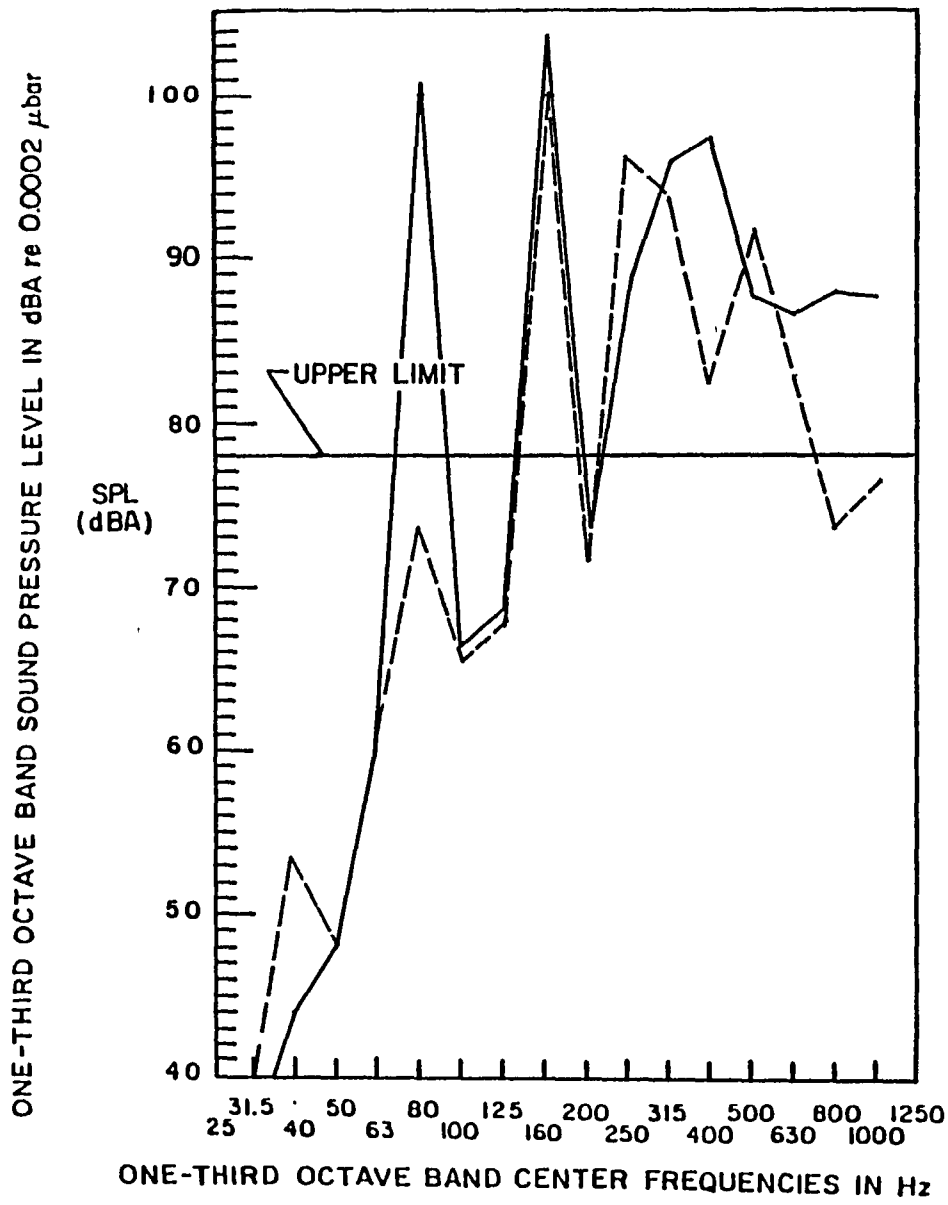
added weight = 0.42 lbs.  
 panel area = 1.1 sq.ft.



▨ - unit under study

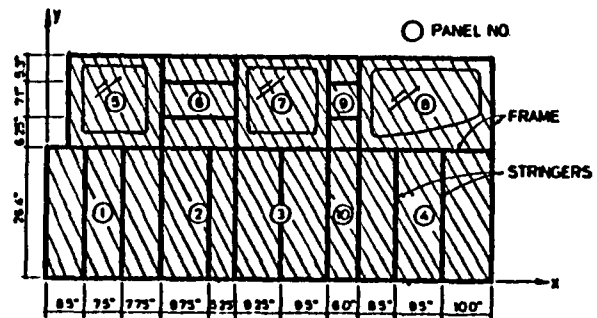
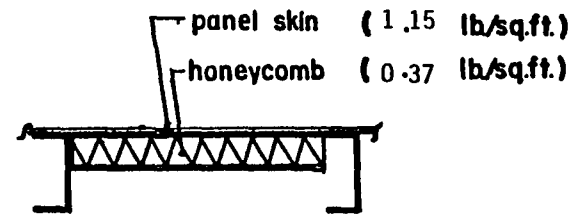
ONE-THIRD OCTAVE BAND CENTER FREQUENCIES IN Hz (cps)

Fig. 26 Interior noise levels with honeycomb treatment (Panel No. 10)



— baseline : OA = 107 dBA  
 --- honeycomb : OA = 104 dBA

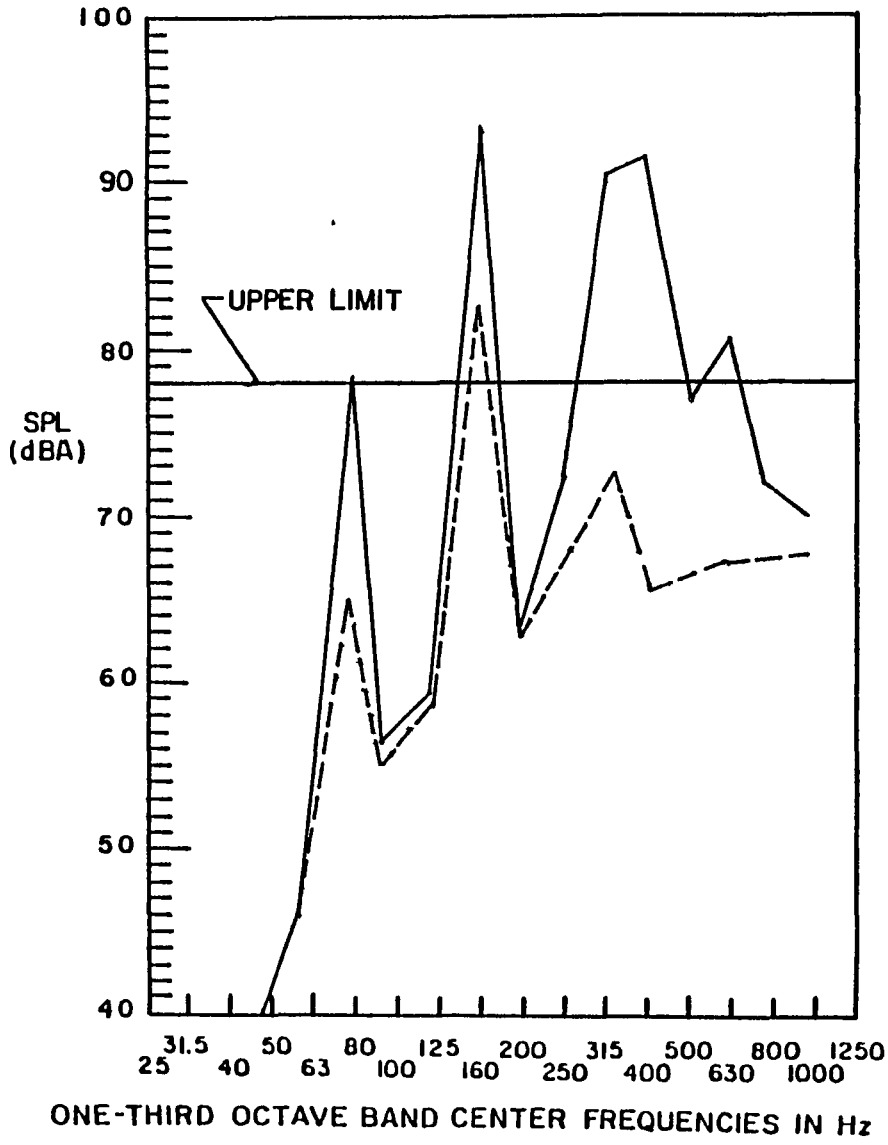
added weight = 7.0 lbs.  
 panel area = 29 sq.ft.



▨ - unit under study

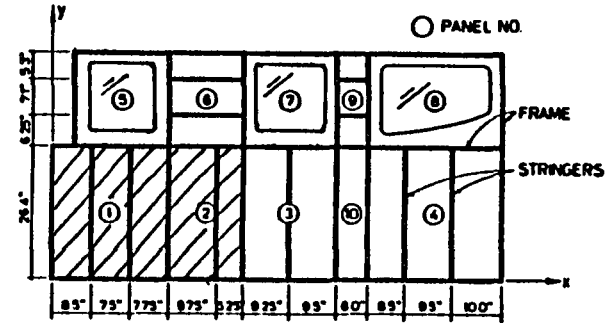
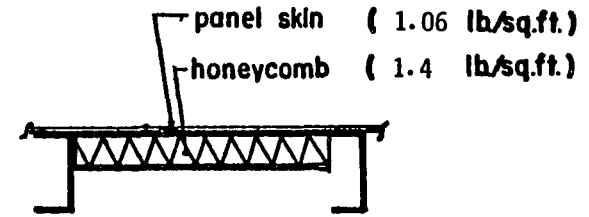
Fig. 27 Interior noise levels with honeycomb treatment (Sidewall)

ONE-THIRD OCTAVE BAND SOUND PRESSURE LEVEL IN dBA re 0.0002  $\mu$ bar



— baseline : OA = 97 dBA  
 --- honeycomb : OA = 85 dBA

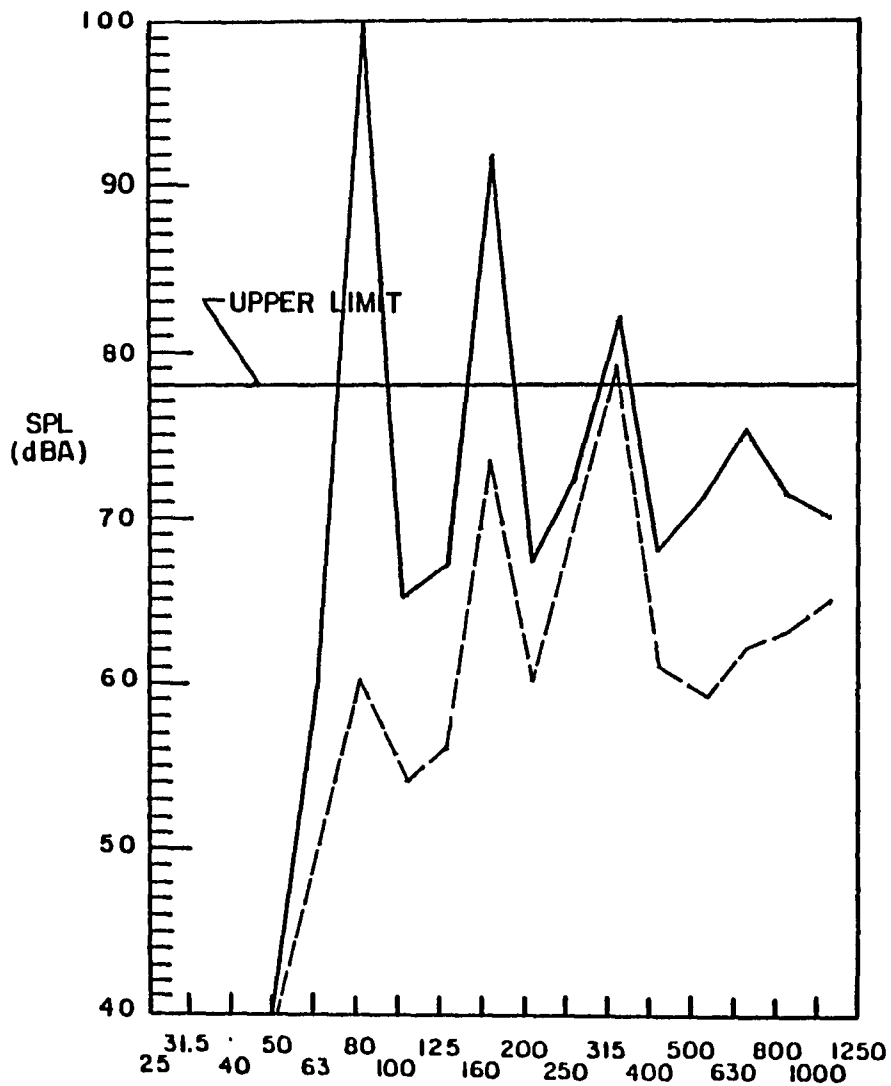
added weight = 10.01 lbs.  
 panel area = 7.15 sq.ft.



▨ - unit under study

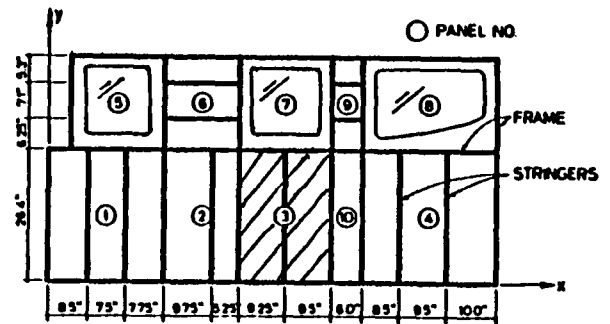
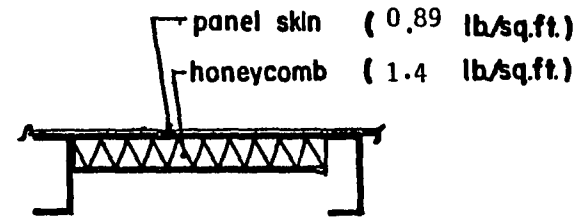
Fig. 28 Interior noise levels with heavy honeycomb treatment (Panels 1 and 2)

ONE-THIRD OCTAVE BAND SOUND PRESSURE LEVEL IN dBA re 0.0002  $\mu$ bar



— baseline : OA = 102 dBA  
 --- honeycomb : OA = 80 dBA

added weight = 4.76 lbs.  
 panel area = 3.44 sq.ft.

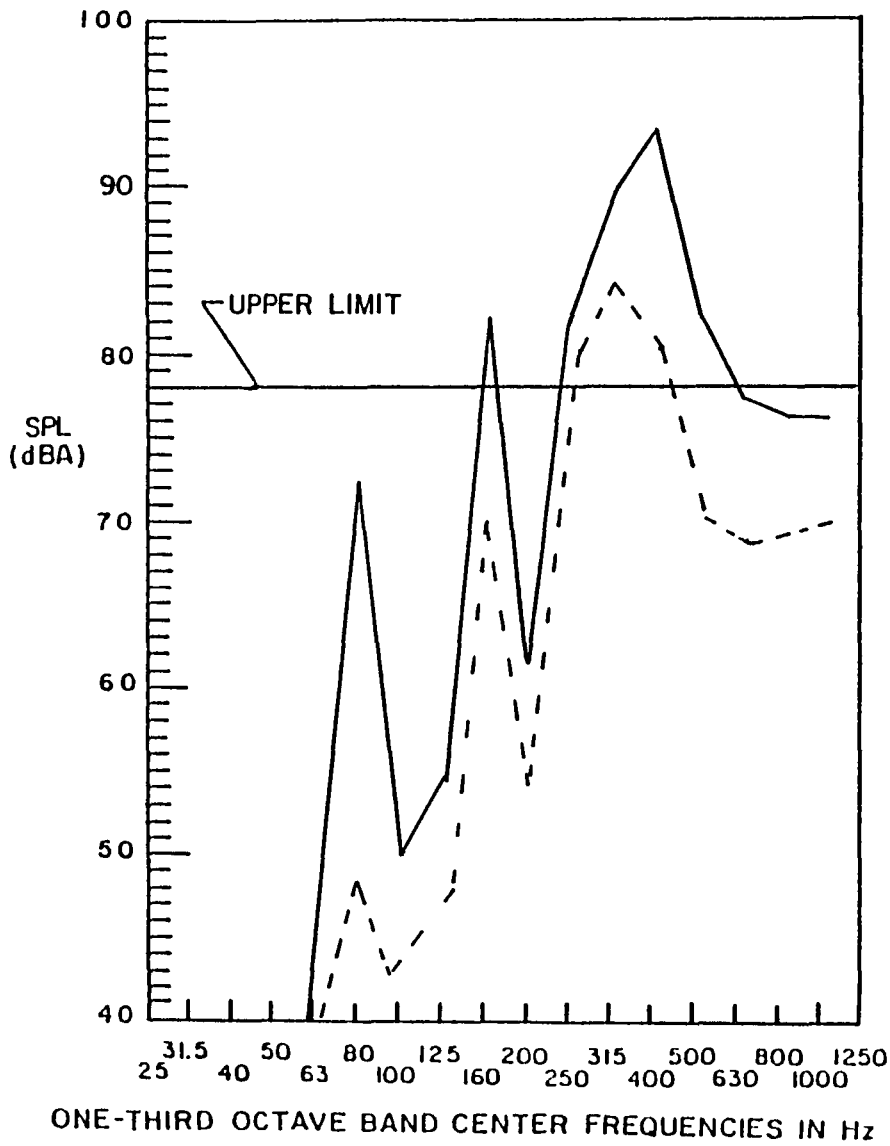


▨ - unit under study

ONE-THIRD OCTAVE BAND CENTER FREQUENCIES IN Hz (cps)

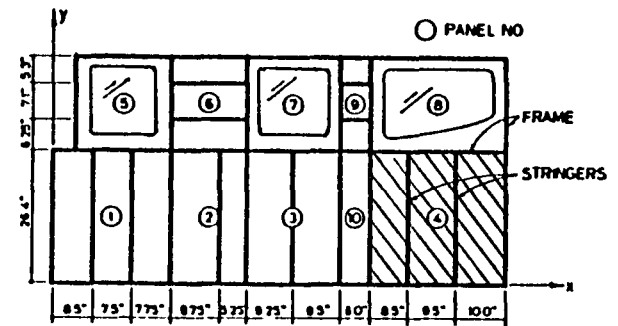
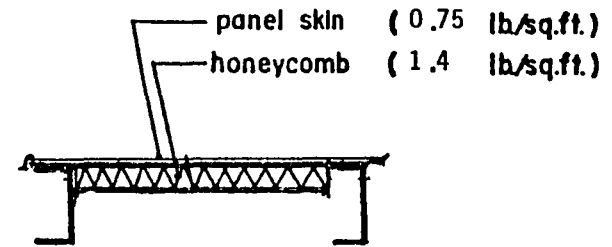
Fig. 29 Interior noise levels with heavy honeycomb treatment (Panel No. 3)

ONE-THIRD OCTAVE BAND SOUND PRESSURE LEVEL IN dBA re 00002  $\mu$ bar



— baseline ; OA = 95 dBA  
 - - - honeycomb ; OA = 87 dBA

added weight = 7.21 lbs.  
 panel area = 5.15 sq.ft.

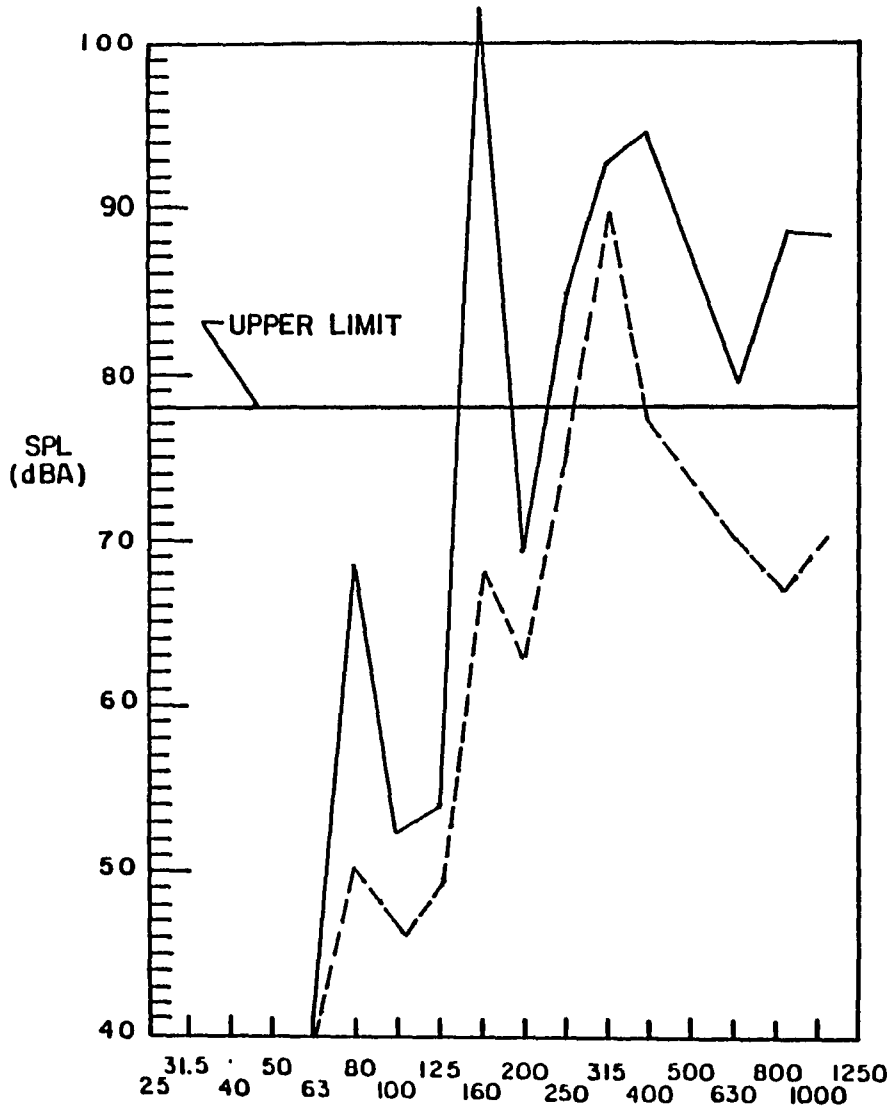


▨ - unit under study

ONE-THIRD OCTAVE BAND CENTER FREQUENCIES IN Hz (cps)

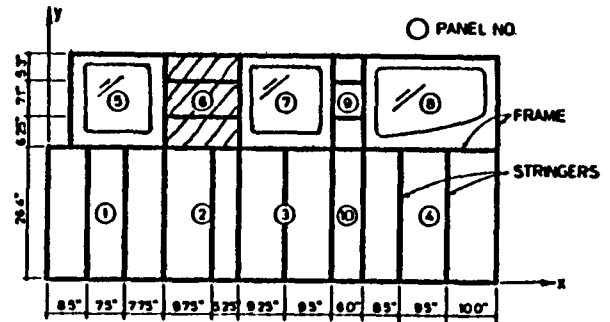
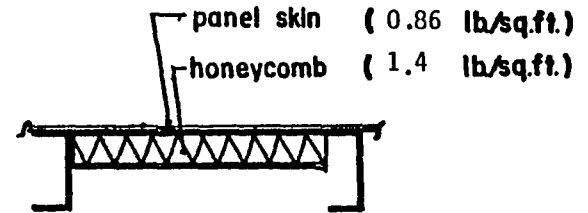
Fig. 30 Interior noise levels with heavy honeycomb treatment (Panel No. 4)

ONE-THIRD OCTAVE BAND SOUND PRESSURE LEVEL IN dBA re 0.0002  $\mu$ bar



— baseline : OA = 106 dBA  
 - - - honeycomb : OA = 90 dBA

added weight = 2.72 lbs.  
 panel area = 1.94 sq.ft.

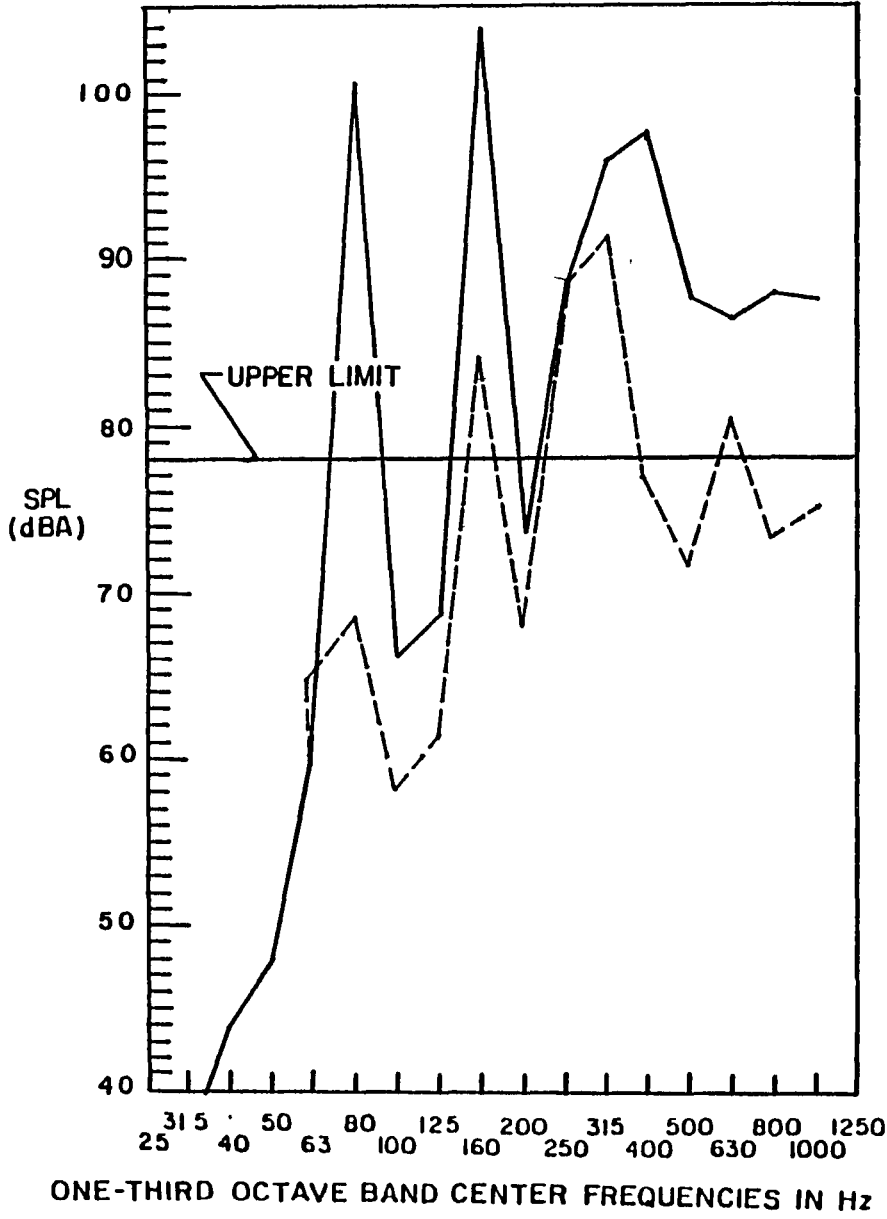


▨ - unit under study

ONE-THIRD OCTAVE BAND CENTER FREQUENCIES IN Hz (cps)

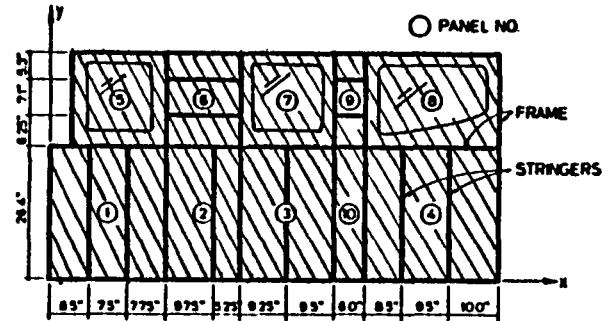
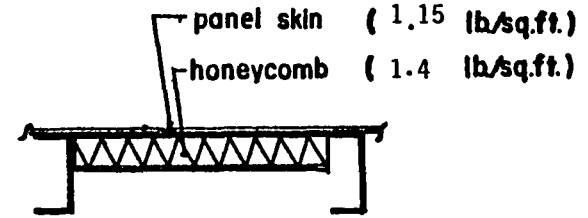
Fig. 31 Interior noise levels with heavy honeycomb treatment (Panel No. 6)

ONE-THIRD OCTAVE BAND SOUND PRESSURE LEVEL IN dBA re 0.0002  $\mu$ bar



— baseline : OA = 107 dBA  
 --- honeycomb : OA = 94 dBA

added weight = 25 lbs.  
 panel area = 29 sq.ft.

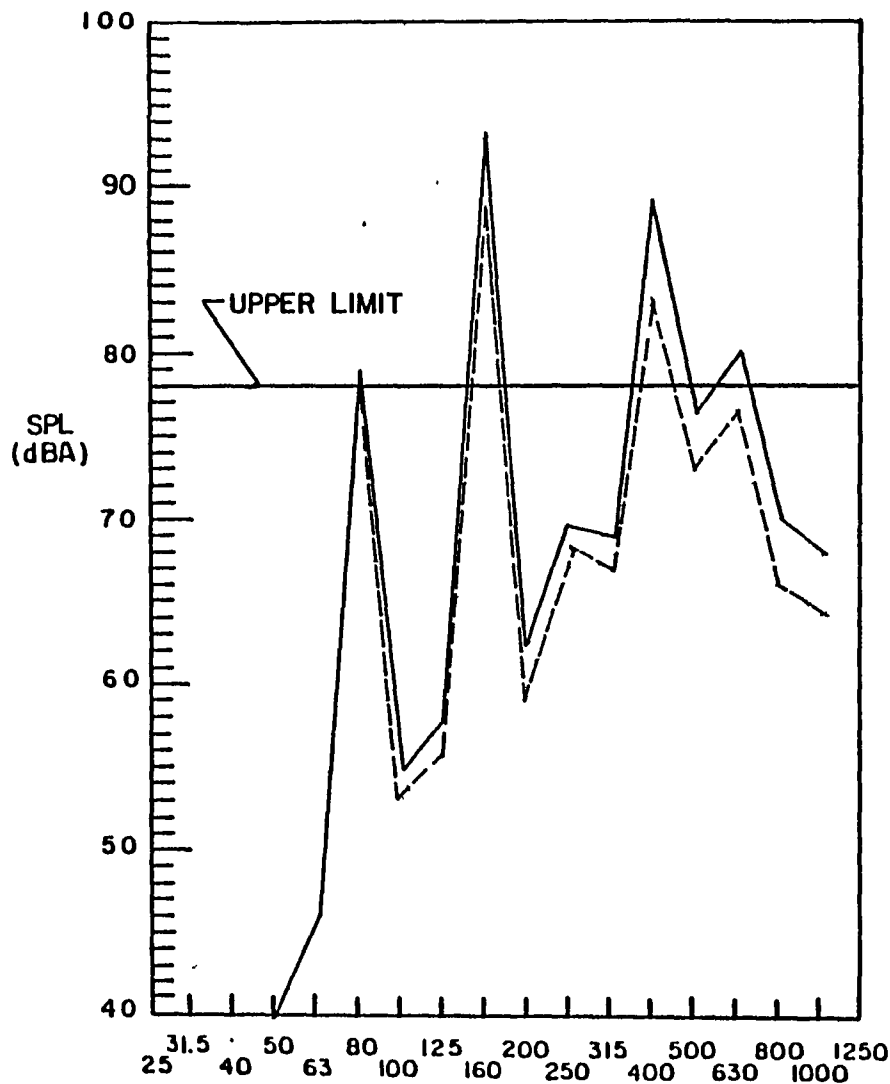


▨ - unit under study

ONE-THIRD OCTAVE BAND CENTER FREQUENCIES IN Hz (cps)

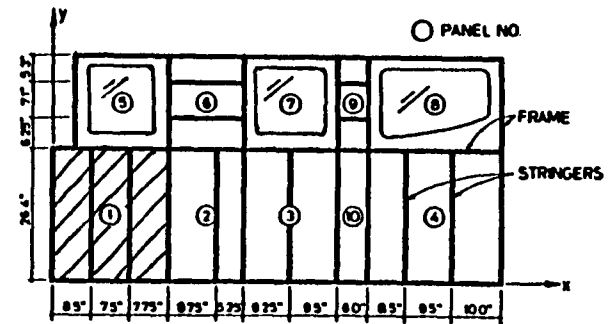
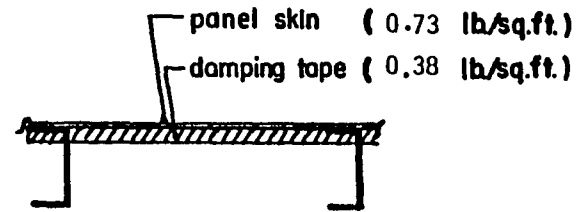
Fig. 32 Interior noise levels with heavy honeycomb treatment (Sidewall)

ONE-THIRD OCTAVE BAND SOUND PRESSURE LEVEL IN dBA re 0.0002  $\mu$ bar



— baseline : OA = 94 dBA  
 --- damping tape : OA = 89 dBA

added weight = 1.67 lbs.  
 panel area = 4.4 sq.ft.

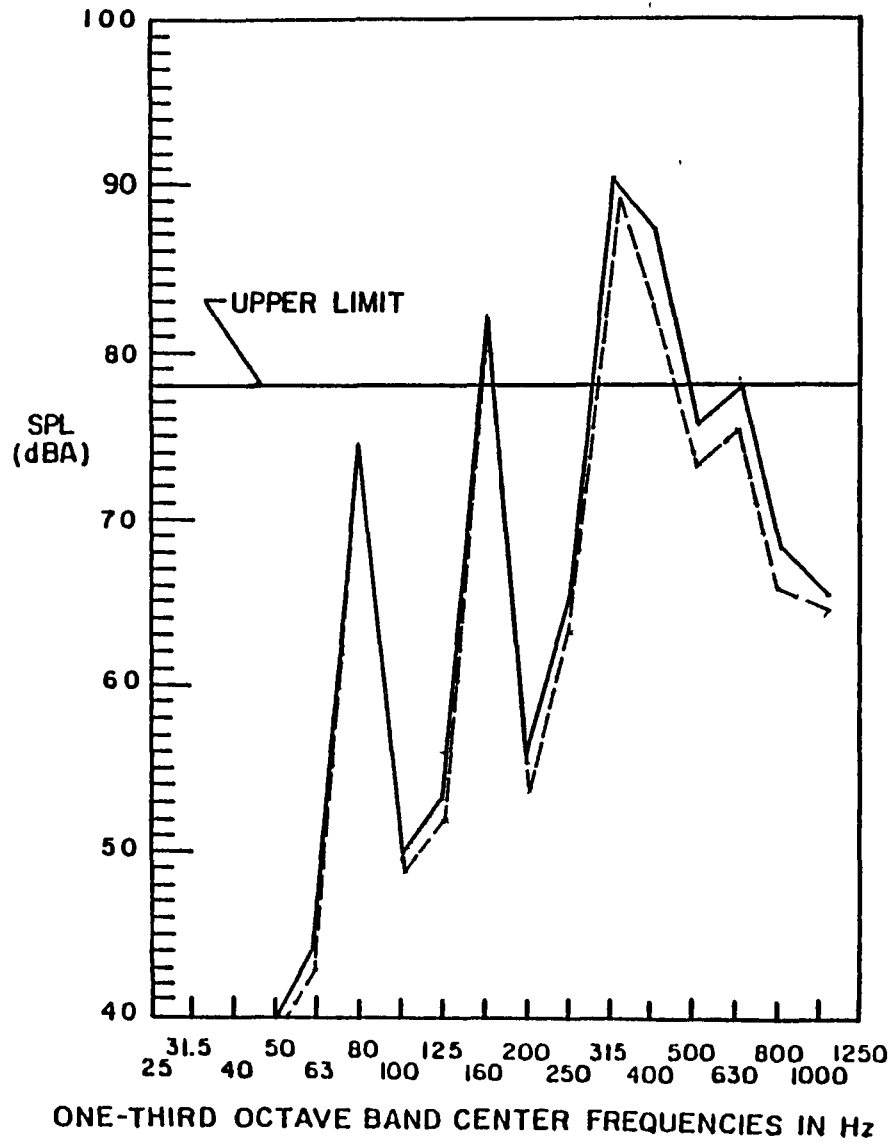


▨ - unit under study

ONE-THIRD OCTAVE BAND CENTER FREQUENCIES IN Hz (cps)

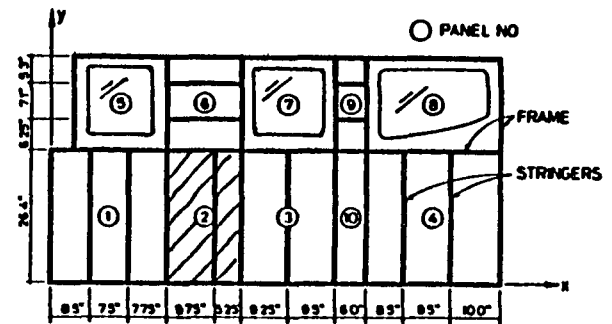
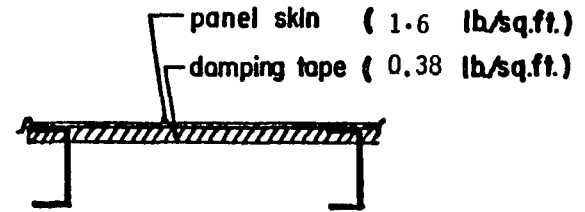
Fig. 33 Interior noise with damping tape treatment (Panel No. 1)

ONE-THIRD OCTAVE BAND SOUND PRESSURE LEVEL IN dBA re 0.0002  $\mu$ bar



— baseline : OA = 92 dBA  
 --- damping tape : OA = 91 dBA

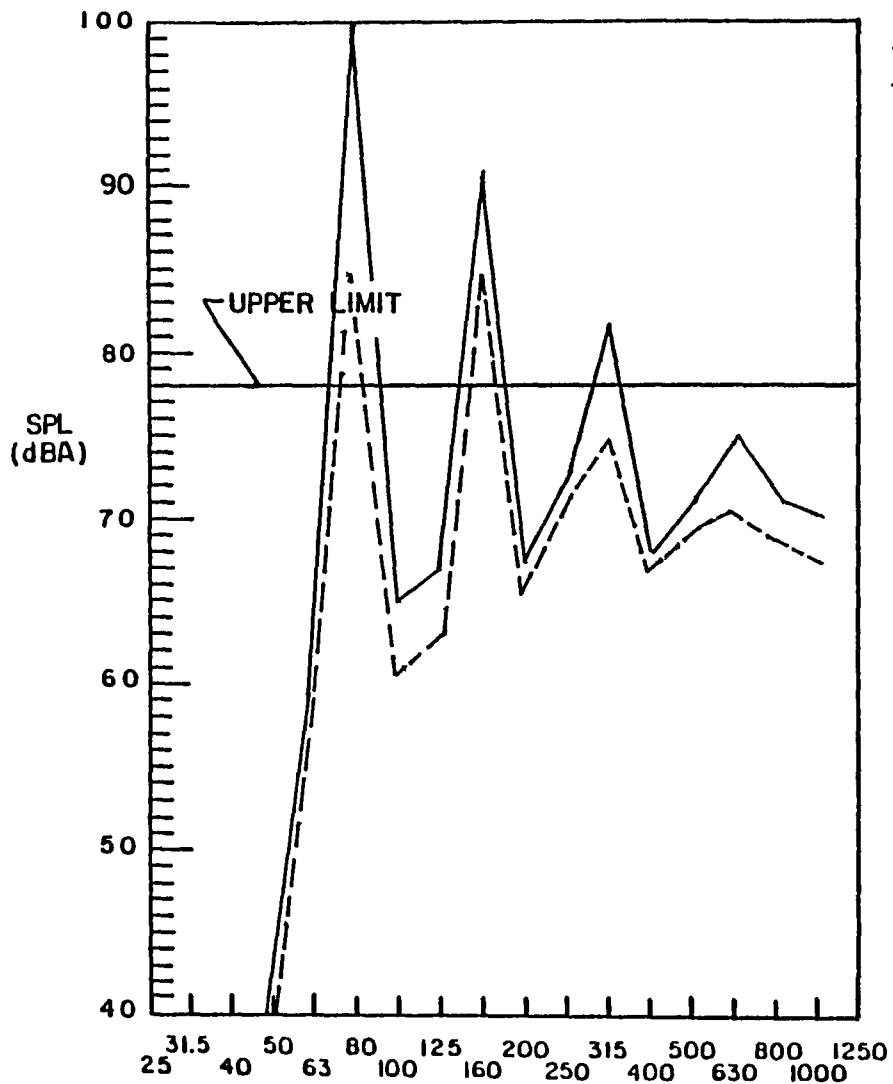
added weight = 1.10 lbs.  
 panel area = 2.75 sq.ft.



▨ - unit under study

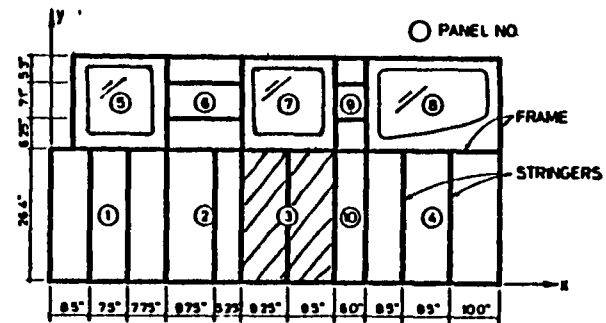
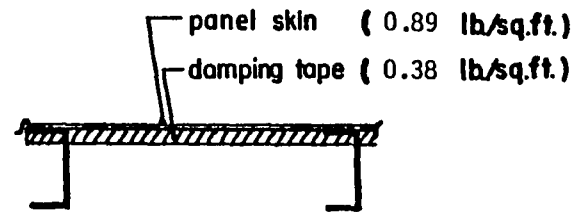
Fig. 34 Interior noise with damping tape treatment (Panel No. 2)

ONE-THIRD OCTAVE BAND SOUND PRESSURE LEVEL IN dBA re 0.0002  $\mu$ bar



— baseline ; OA = 102 dBA  
 --- damping tape ; OA = 92 dBA

added weight = 1.31 lbs.  
 panel area = 3.44 sq.ft.

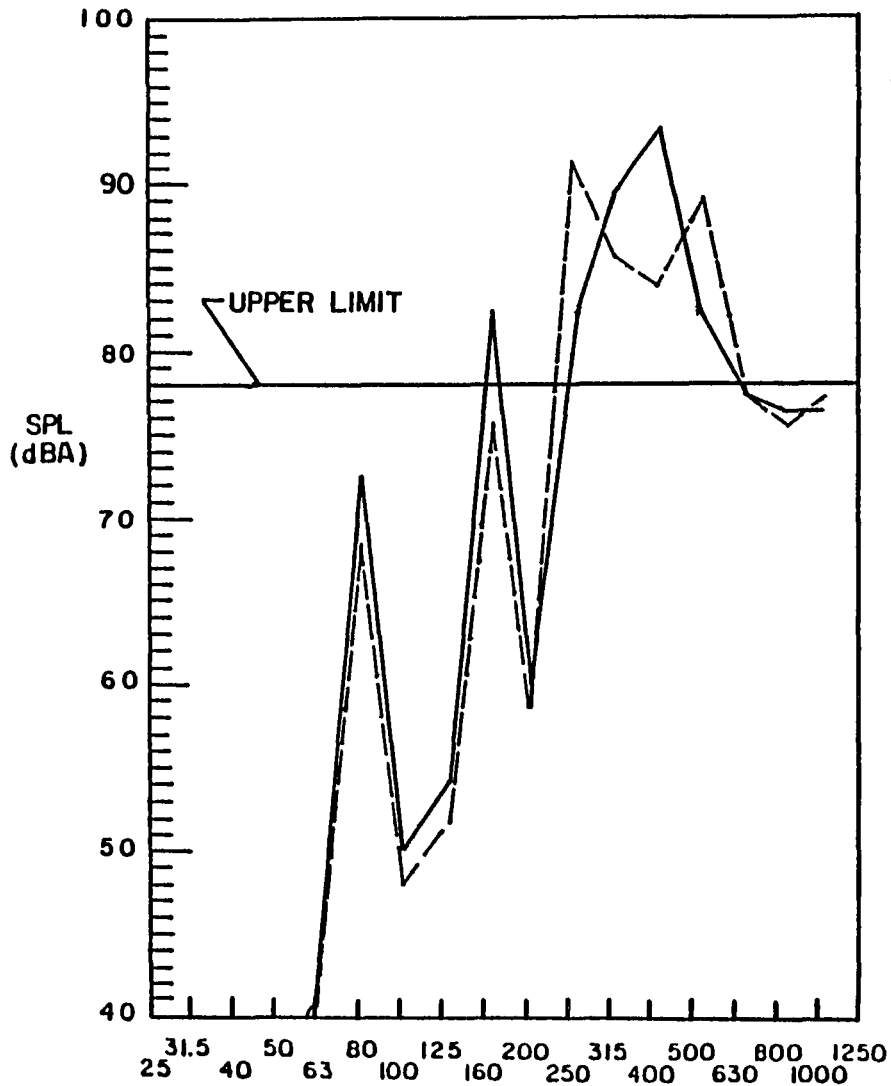


▨ - unit under study

ONE-THIRD OCTAVE BAND CENTER FREQUENCIES IN Hz (cps)

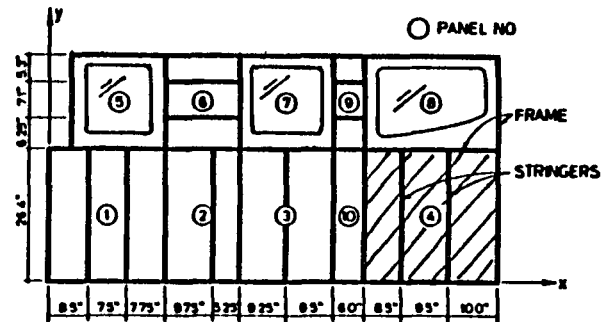
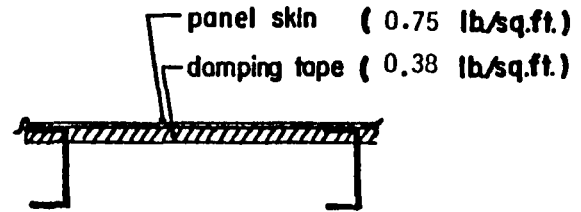
Fig. 35 Interior noise with damping tape treatment (Panel No. 3)

ONE-THIRD OCTAVE BAND SOUND PRESSURE LEVEL IN dBA re 0.0002  $\mu$ bar



— baseline : OA = 95 dBA  
 - - - damping tape : OA = 93 dBA

added weight = 1.95 lbs.  
 panel area = 5.13 sq.ft.

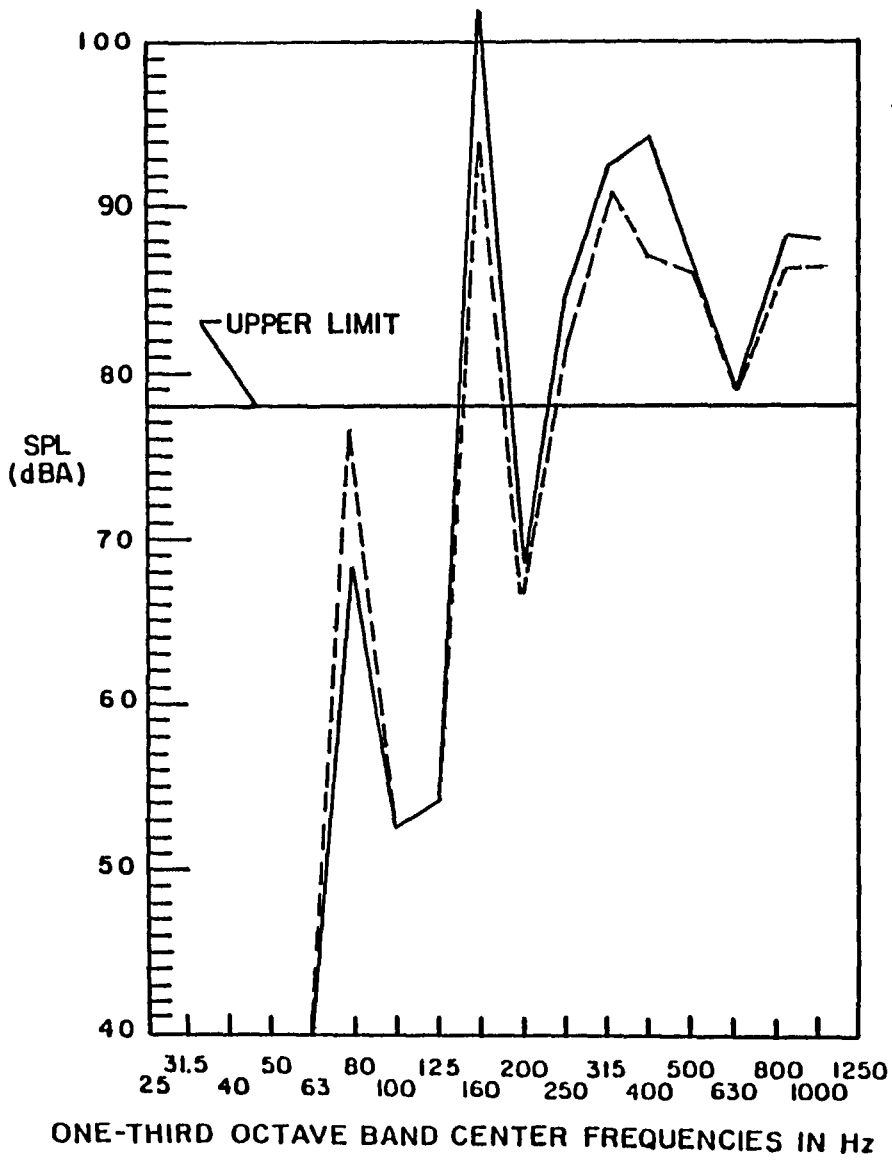


▨ - unit under study

ONE-THIRD OCTAVE BAND CENTER FREQUENCIES IN Hz (cps)

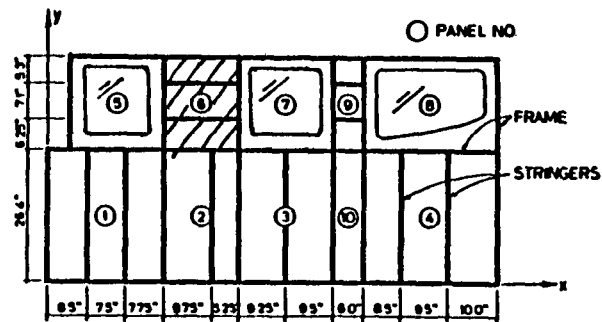
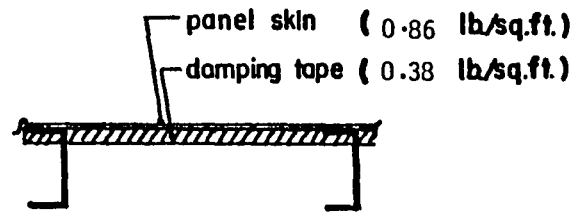
Fig. 36 Interior noise with damping tape treatment (Panel No. 4)

ONE-THIRD OCTAVE BAND SOUND PRESSURE LEVEL IN dBA re 0.0002  $\mu$ bar



— baseline : OA = 106 dBA  
 --- damping tape : OA = 96 dBA

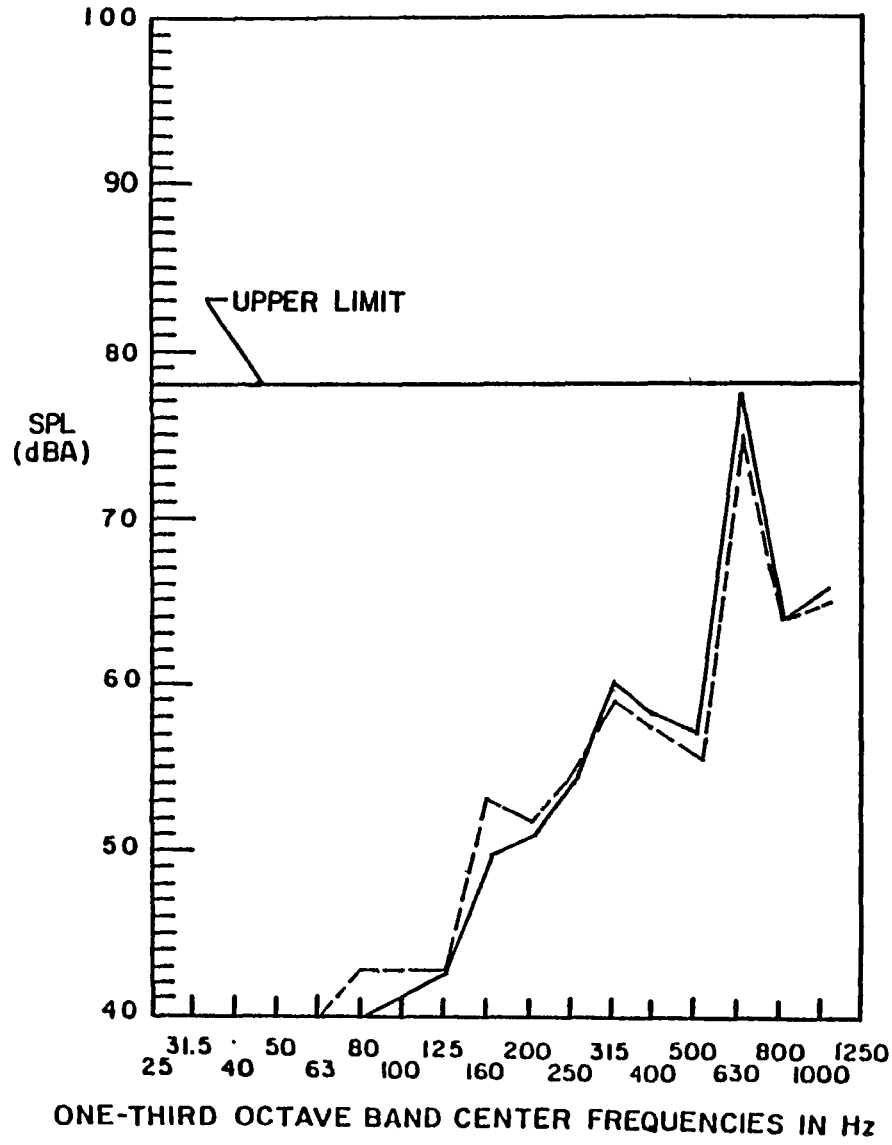
added weight = 0.74 lbs.  
 panel area = 1.94 sq.ft.



▨ - unit under study

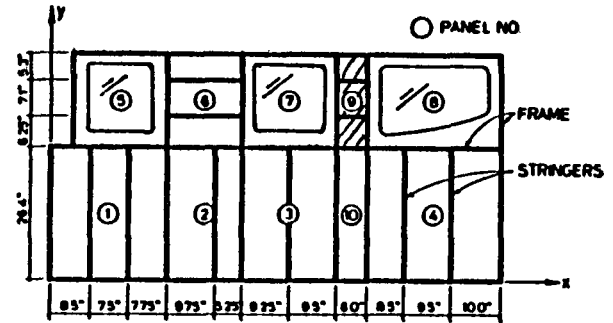
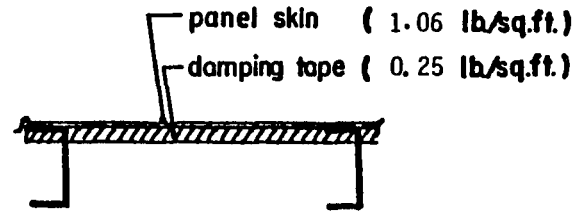
Fig. 37 Interior noise with damping tape treatment (Panel No. 6)

-88-  
ONE-THIRD OCTAVE BAND SOUND PRESSURE LEVEL IN dBA re 0.0002  $\mu$ bar



— baseline : OA = 78 dBA  
 --- damping tape : OA = 75 dBA

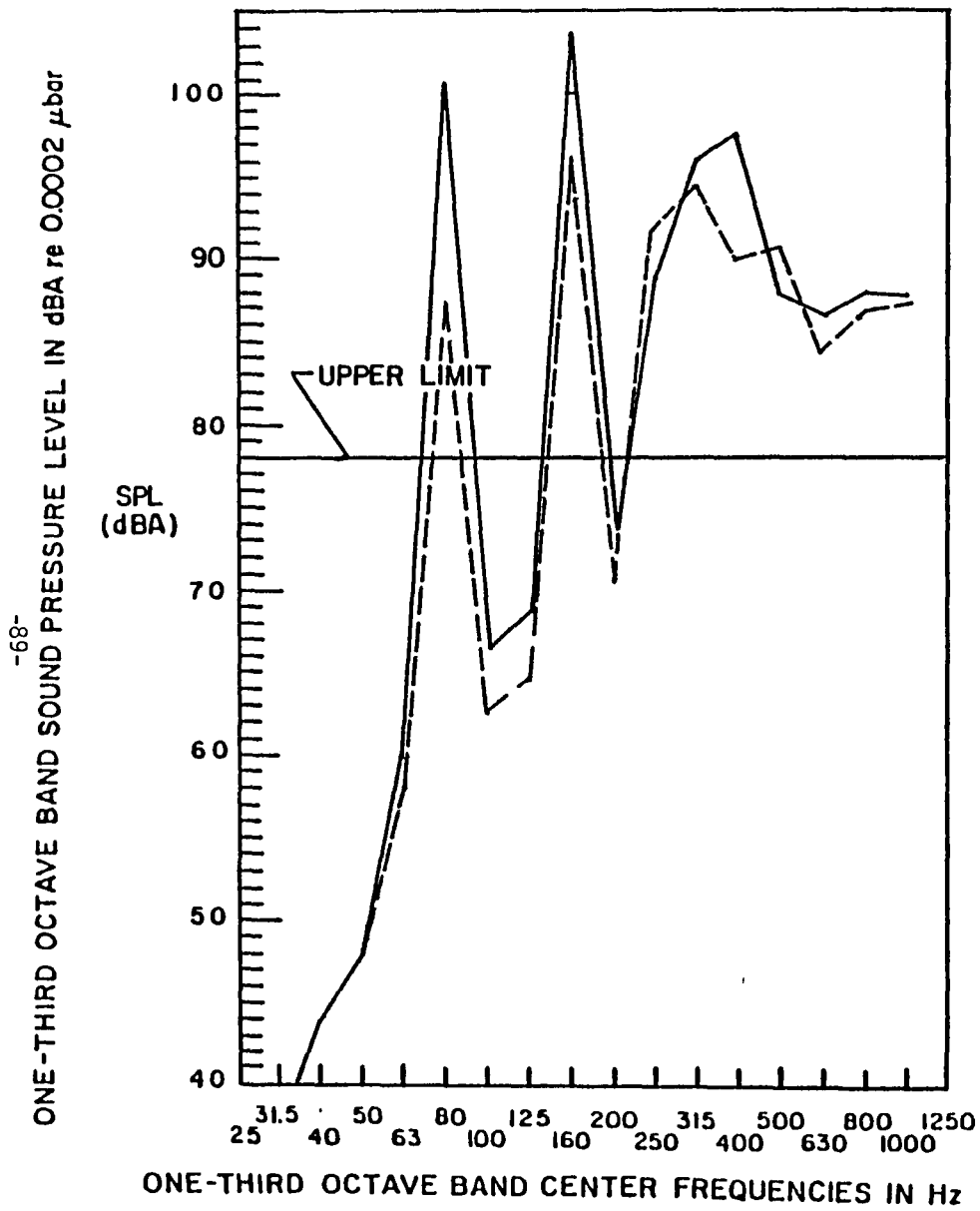
added weight = 0.19 lbs.  
 panel area = 0.77 sq.ft.



▨ - unit under study

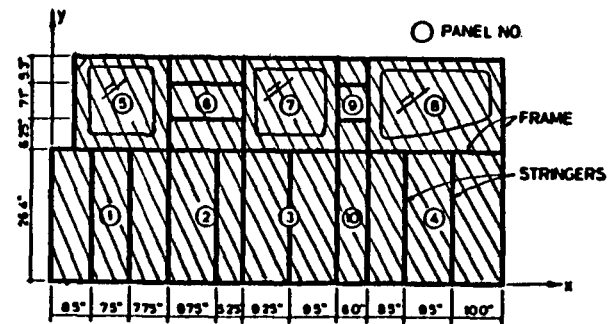
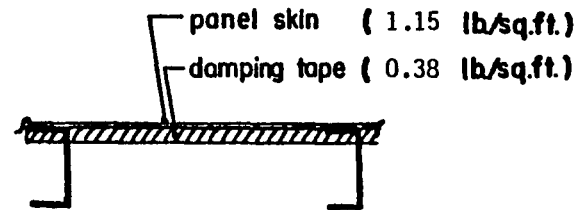
ONE-THIRD OCTAVE BAND CENTER FREQUENCIES IN Hz (cps)

Fig. 38 Interior noise with damping tape treatment (Panel 9)



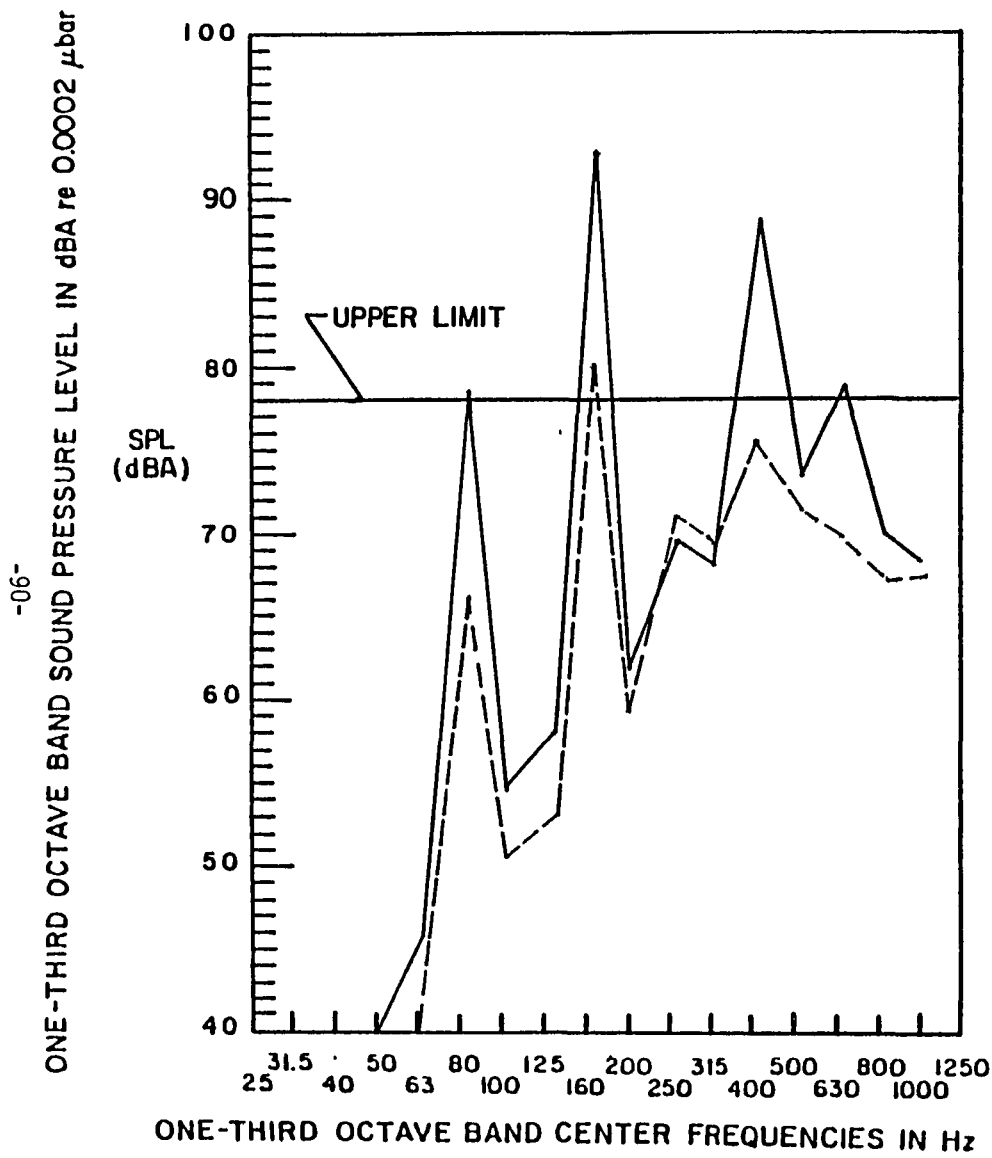
— baseline : OA = 107 dBA  
 - - - damping tape : OA = 101 dBA

added weight = 7.05 lbs.  
 panel area = 29 sq.ft.



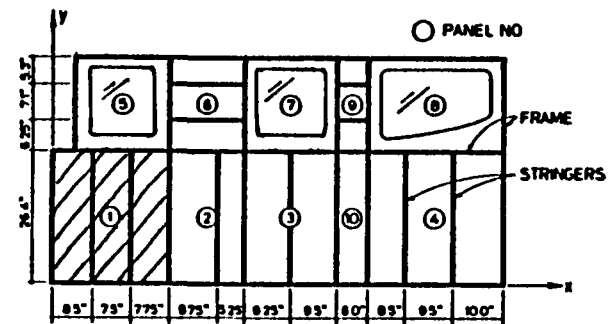
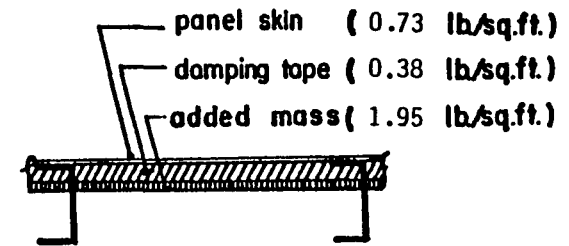
▨ - unit under study

Fig. 39 Interior noise with damping tape treatment (Sidewall)



— baseline ; OA = 94 dBA  
 --- damping tape ; OA = 82 dBA  
 + added mass

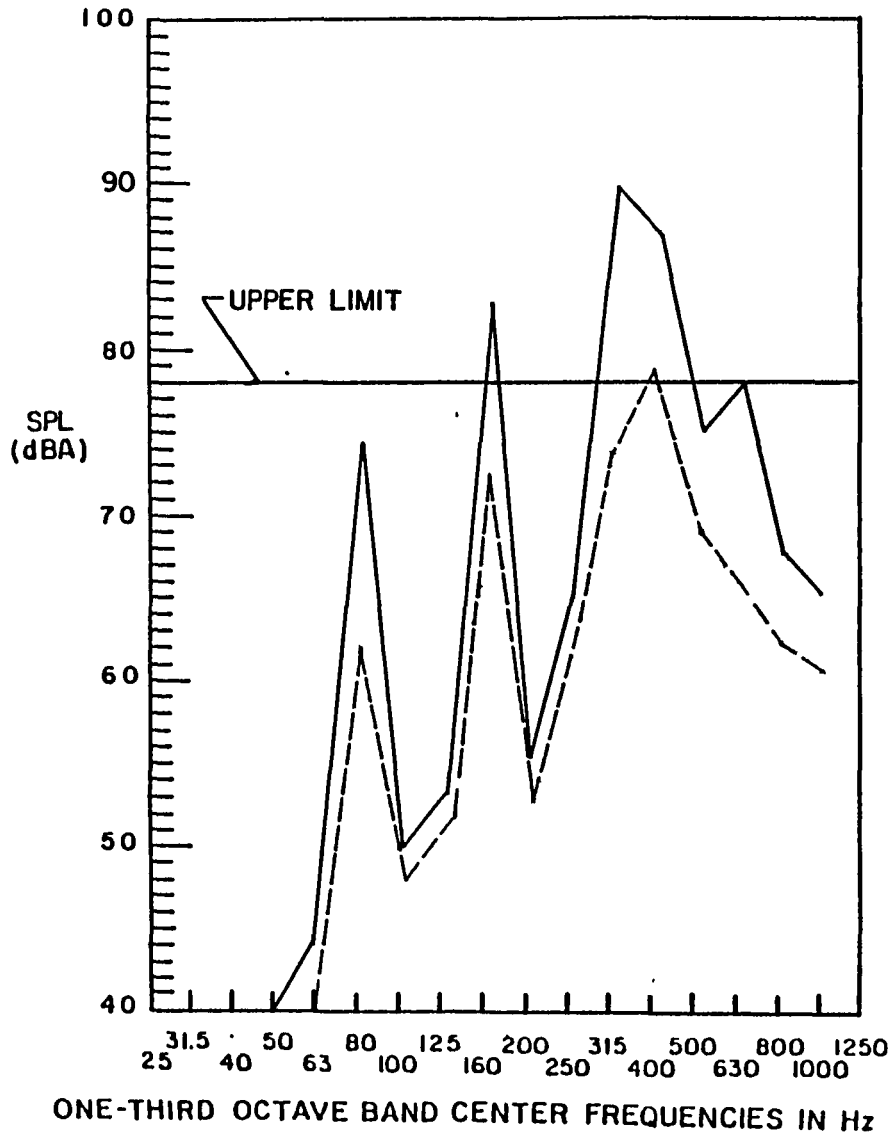
added weight = 10.25 lbs.  
 panel area = 4.4 sq.ft.



▨ - unit under study

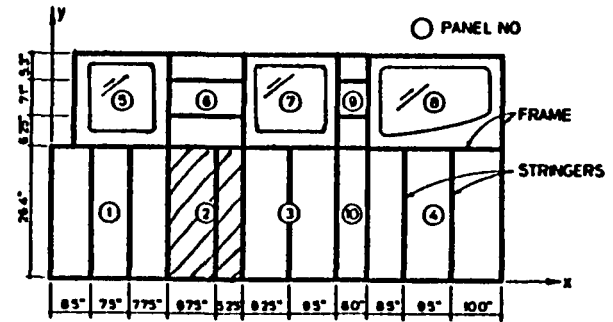
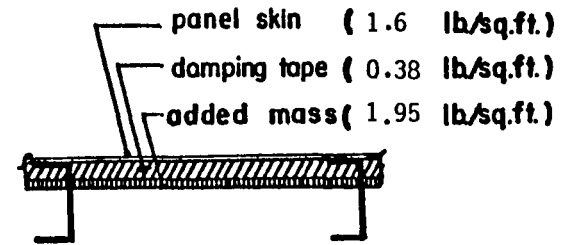
Fig. 40 Interior noise with damping tape and mass treatment (Panel No. 1)

ONE-THIRD OCTAVE BAND SOUND PRESSURE LEVEL IN dBA re 0.0002  $\mu$ bar



— baseline : OA = 92 dBA  
 --- damping tape : OA = 81 dBA  
 + added mass

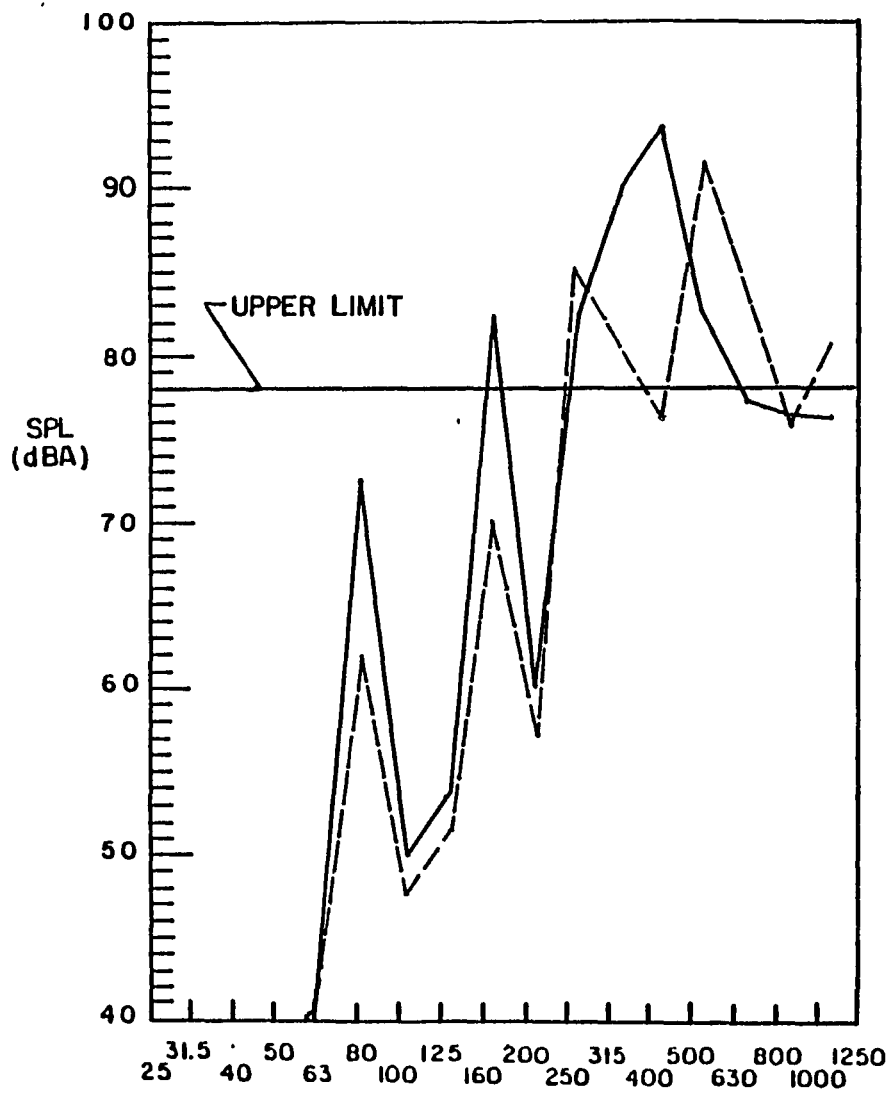
added weight = 6.41 lbs.  
 panel area = 2.75 sq.ft.



▨ - unit under study

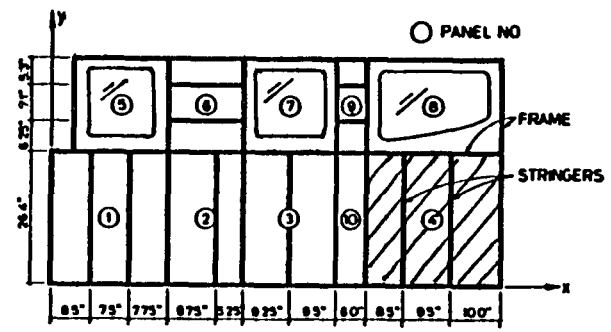
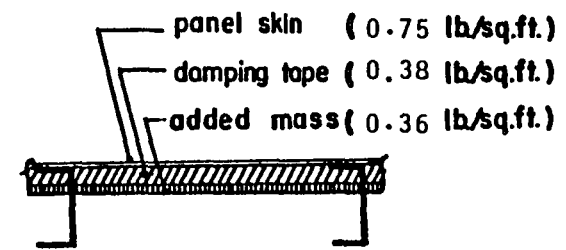
Fig. 41 Interior noise with damping tape and mass treatment (Panel No. 2)

ONE-THIRD OCTAVE BAND SOUND PRESSURE LEVEL IN dBA re 0.0002  $\mu$ bar



— baseline : OA = 95 dBA  
 --- damping tape ; OA = 92 dBA  
 + added mass

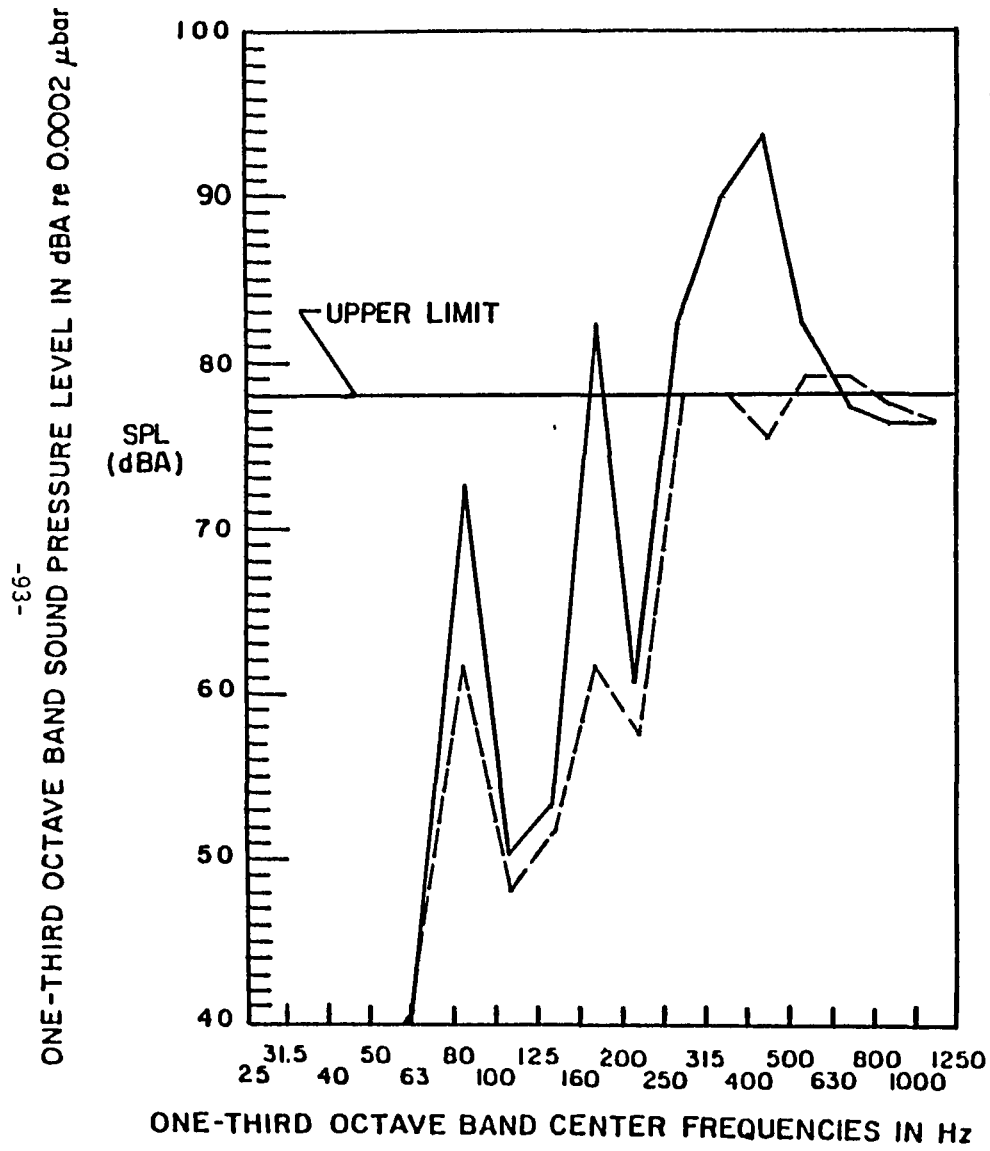
added weight = 380 lbs.  
 panel area = 5.13 sq.ft.



▨ - unit under study

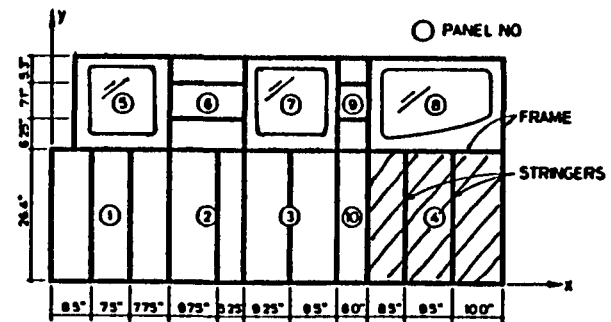
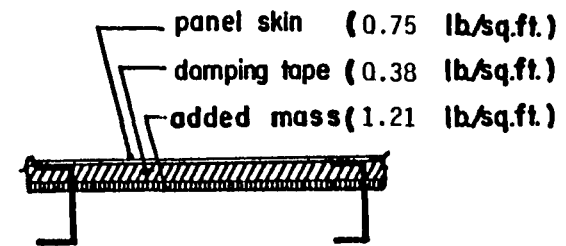
ONE-THIRD OCTAVE BAND CENTER FREQUENCIES IN Hz (cps)

Fig. 42 Interior noise with damping tape and mass treatment (Panel No. 4)



— baseline : OA = 95 dBA  
 --- damping tape : OA = 86 dBA  
 + added mass

added weight = 8.16 lbs.  
 panel area = 5.13 sq.ft.

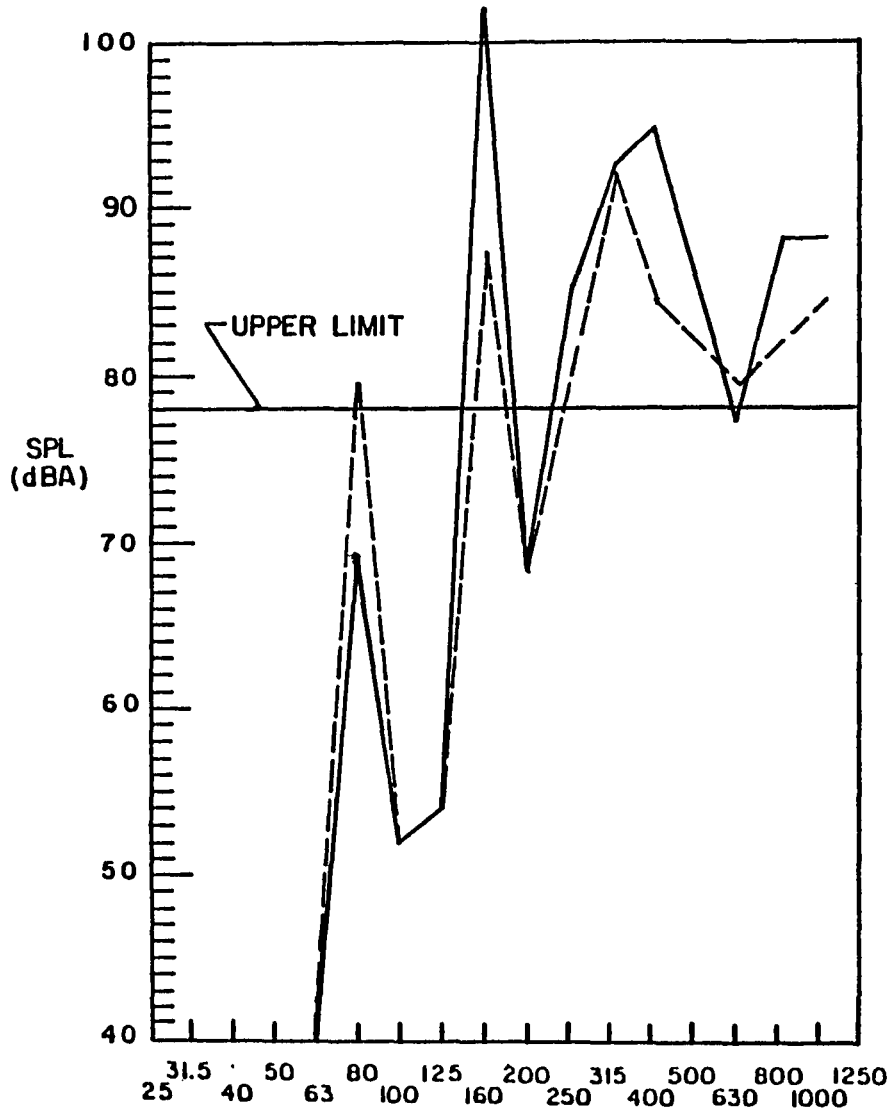


▨ - unit under study

ONE-THIRD OCTAVE BAND CENTER FREQUENCIES IN Hz (cps)

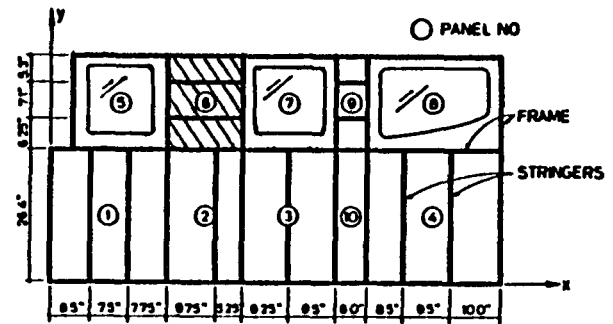
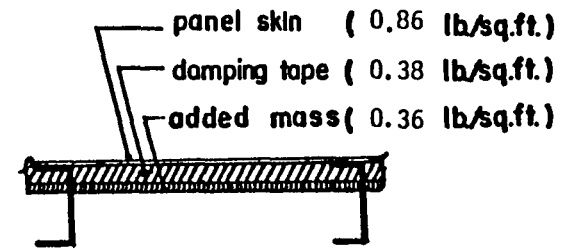
Fig. 43 Interior noise with damping tape and heavy mass treatment (Panel No. 4)

-94-  
ONE-THIRD OCTAVE BAND SOUND PRESSURE LEVEL IN dBA re 0.0002  $\mu$ bar



— baseline : OA = 106 dBA  
 - - - damping tape : OA = 95 dBA  
 + added mass

added weight = 1.44 lbs.  
 panel area = 1.94 sq.ft.



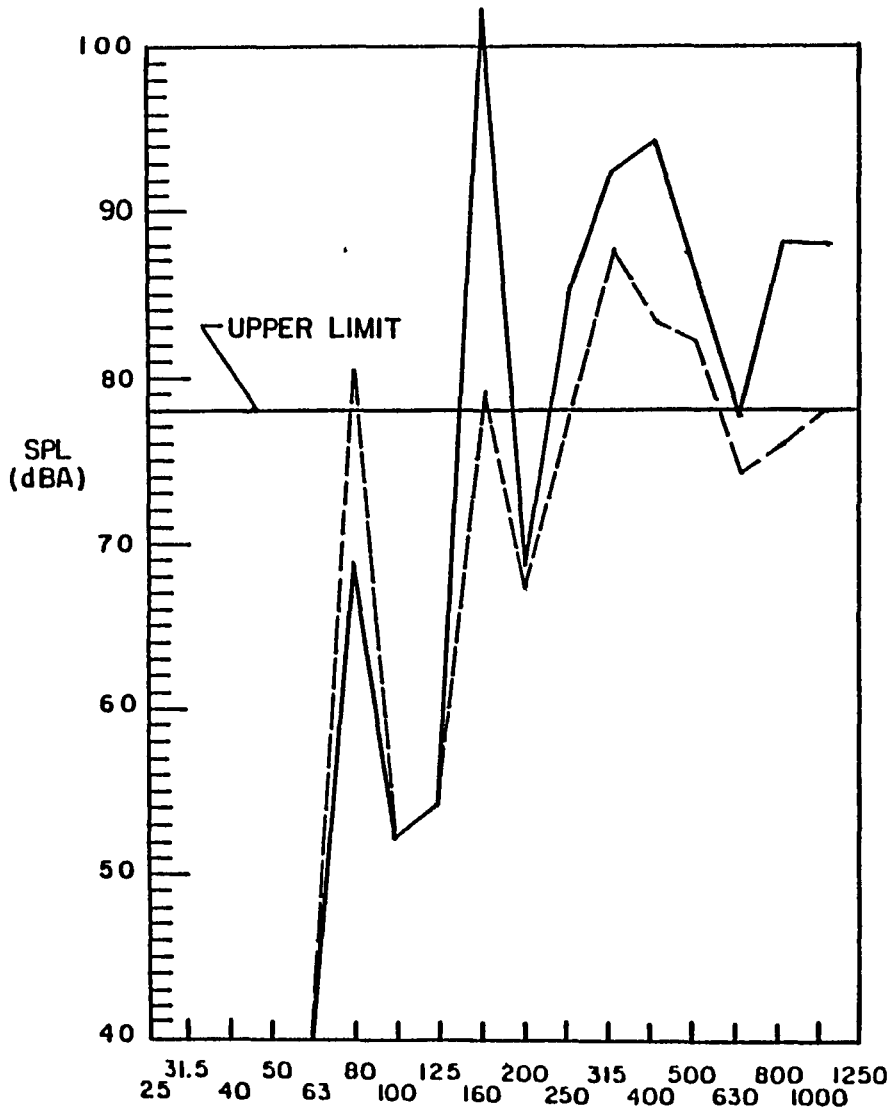
▨ - unit under study

ONE-THIRD OCTAVE BAND CENTER FREQUENCIES IN Hz (cps)

Fig. 44 Interior noise with damping tape and heavy mass treatment (Panel unit No. 6)

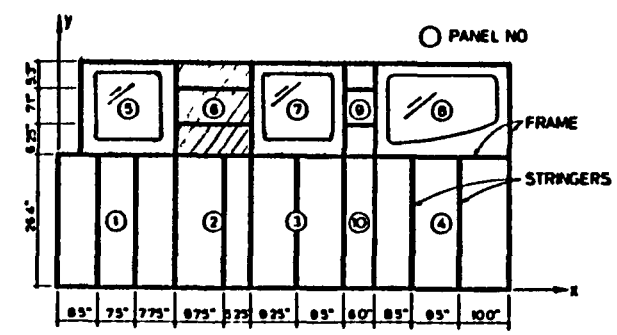
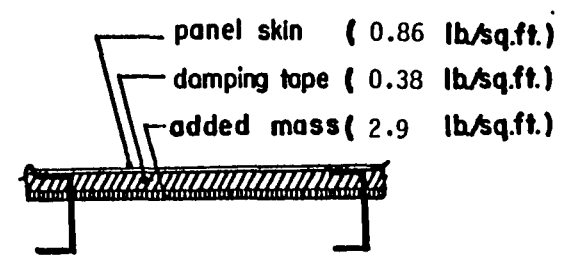
-56-

ONE-THIRD OCTAVE BAND SOUND PRESSURE LEVEL IN dBA re 00002  $\mu$ bar



— baseline : OA = 106 dBA  
 --- damping tape : OA = 91 dBA  
 + added mass

added weight = 6.36 lbs.  
 panel area = 1.94 sq.ft.

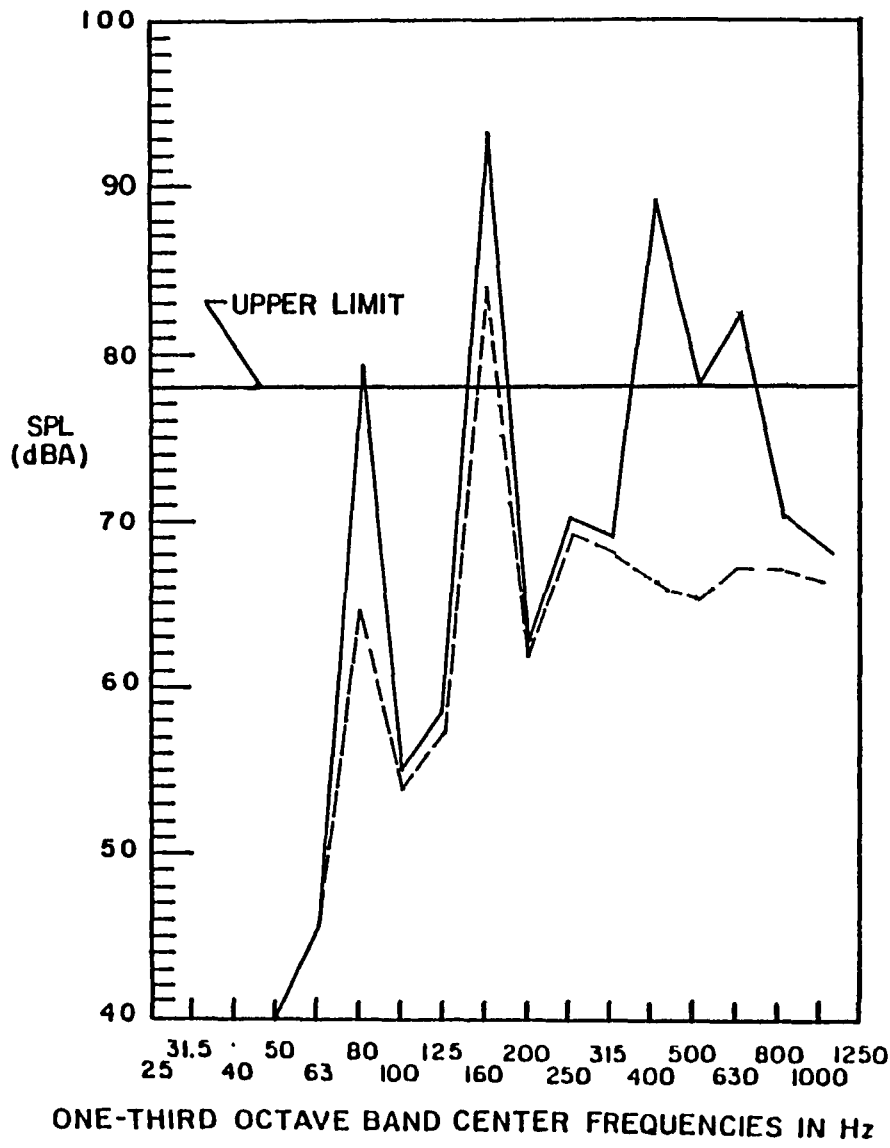


▨ - unit under study

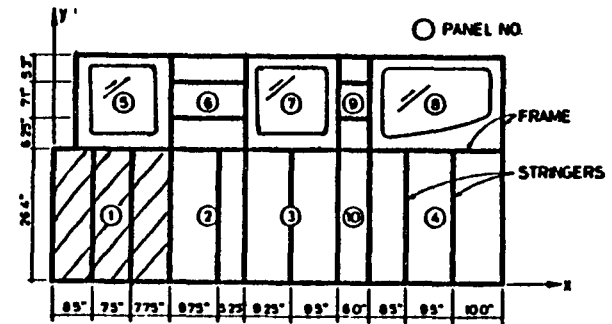
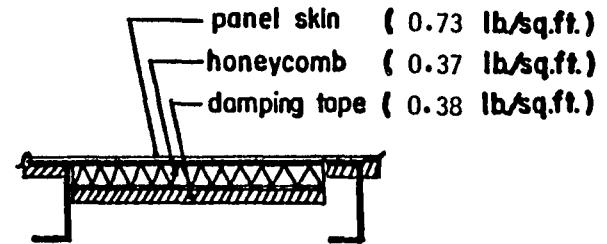
ONE-THIRD OCTAVE BAND CENTER FREQUENCIES IN Hz (cps)

Fig. 45 Interior noise with damping tape and heavy mass treatment (Panel No. 6, Add-on = 3.28 lb/ft<sup>2</sup>)

-96-  
ONE-THIRD OCTAVE BAND SOUND PRESSURE LEVEL IN dBA re 0.0002  $\mu$ bar



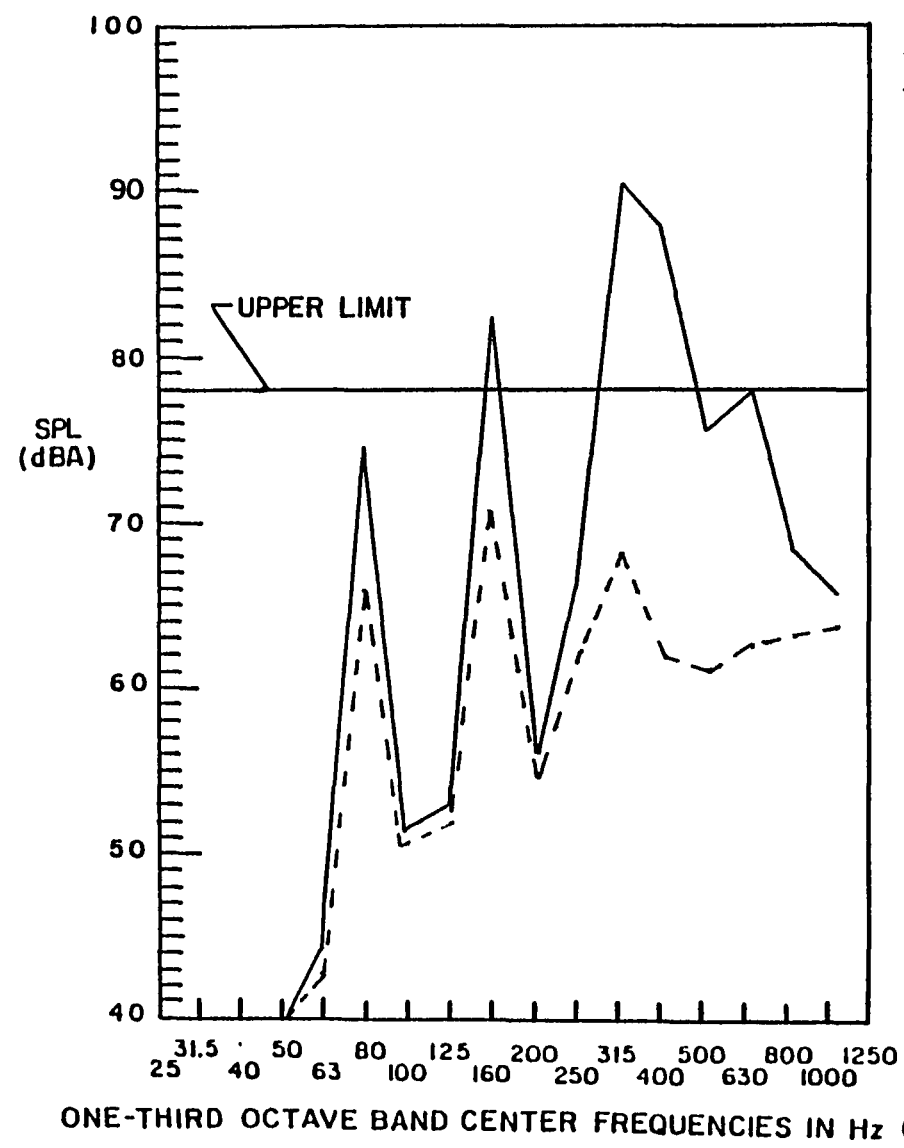
— baseline : OA = 94 dBA  
 --- honeycomb : OA = 85 dBA  
 + damping tape  
 added weight = 3.3 lbs.  
 panel area = 4.4 sq.ft.



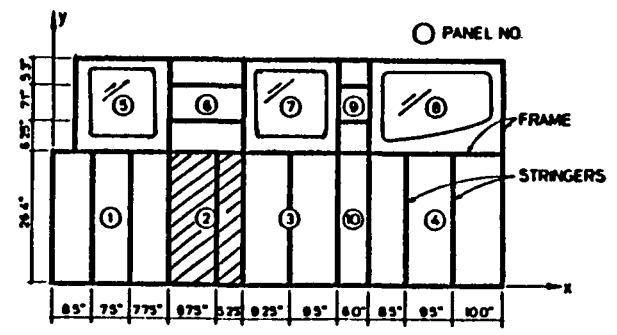
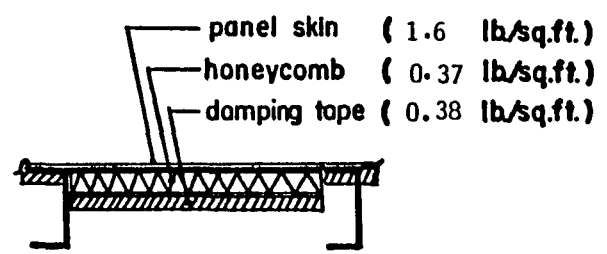
▨ - unit under study

Fig. 46 Interior noise with honeycomb-damping tape treatment (Panel No. 1)

-76-  
ONE-THIRD OCTAVE BAND SOUND PRESSURE LEVEL IN dBA re 0.0002  $\mu$ bar

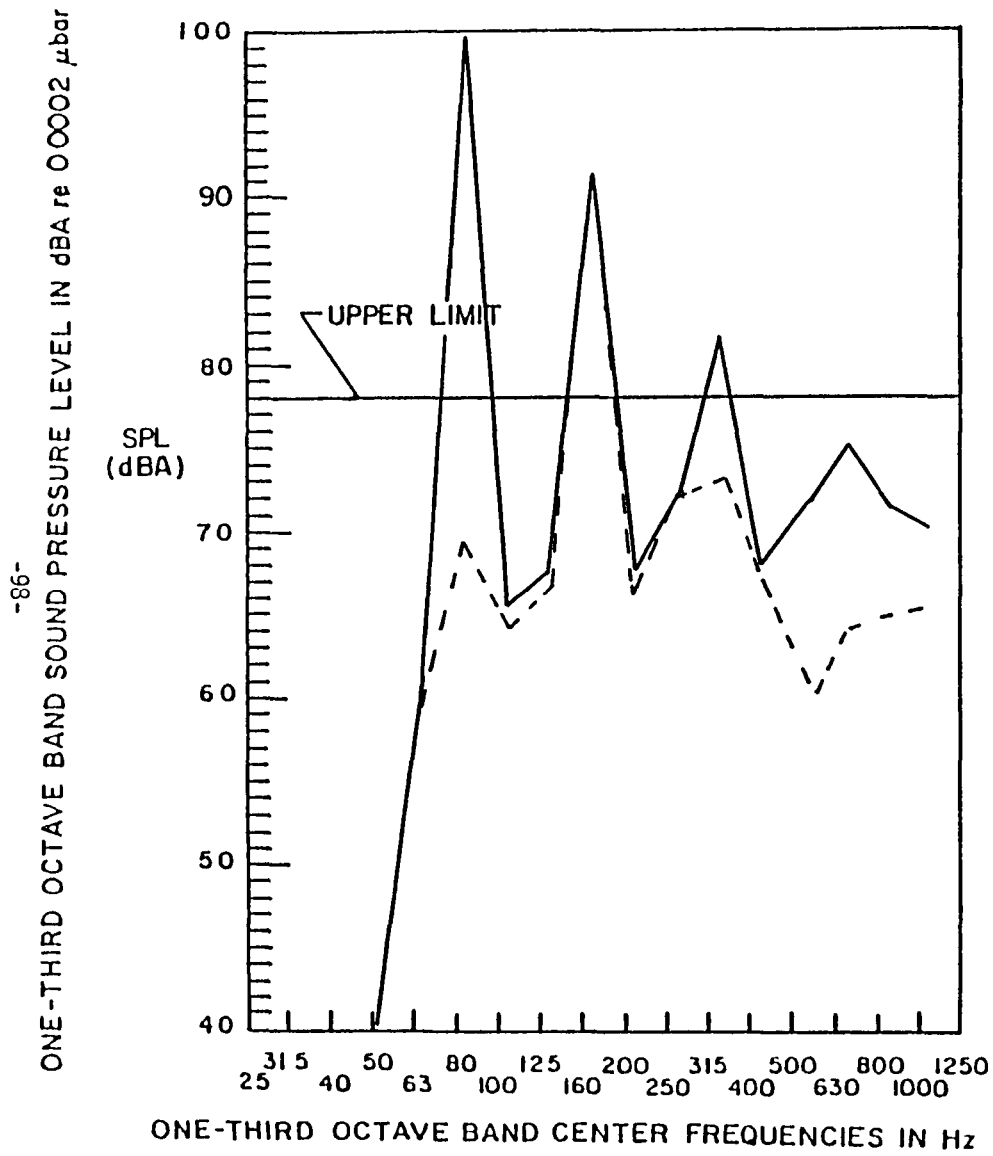


— baseline : OA = 92 dBA  
 - - - honeycomb : OA = 72 dBA  
 + damping tape  
 added weight = 2.06 lbs.  
 panel area = 2.75 sq.ft.



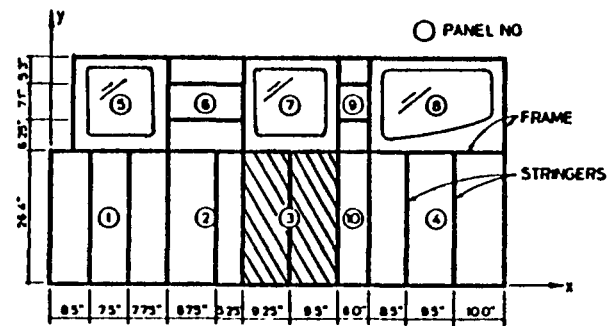
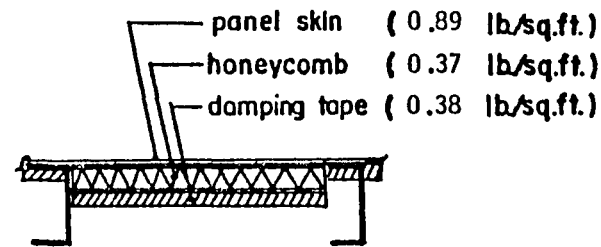
▨ - unit under study

Fig. 47 Interior noise with honeycomb-damping tape treatment (Panel No. 2)



— baseline ; OA = 102 dBA  
 - - - honeycomb ; OA = 94 dBA  
 + damping tape

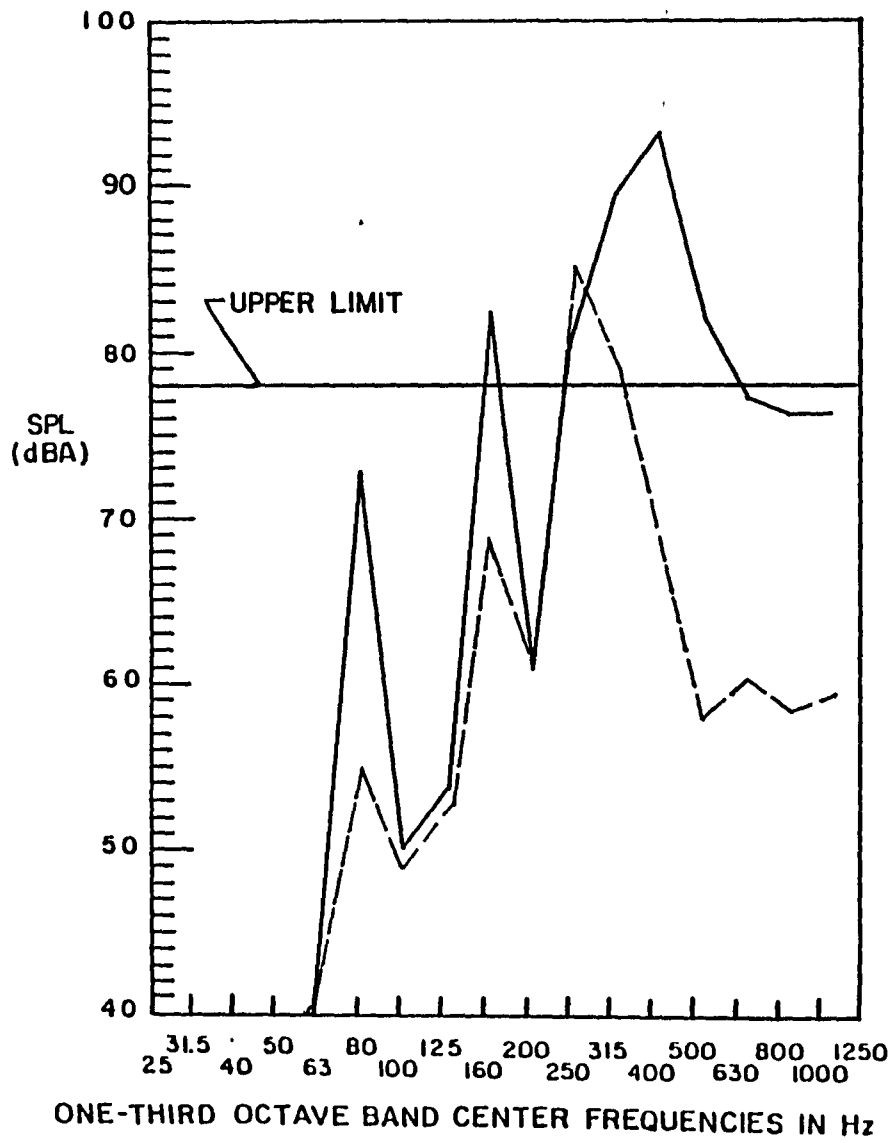
added weight = 2.58 lbs.  
 panel area = 3.44 sq.ft.



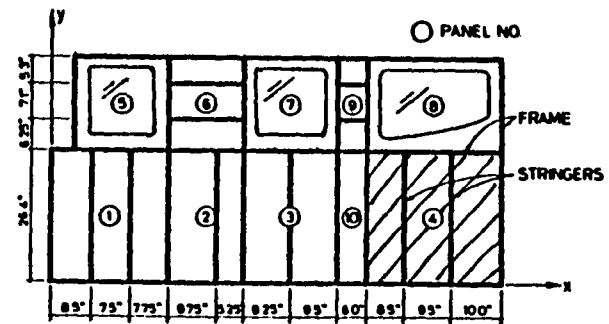
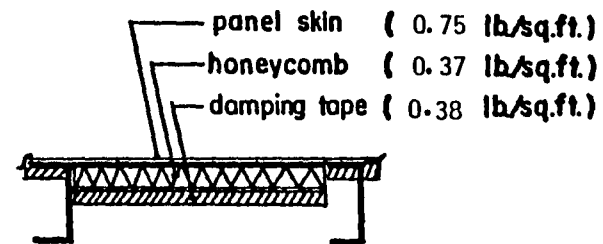
▨ - unit under study

Fig. 48 Interior noise with honeycomb-damping tape treatment (Panel No. 3)

ONE-THIRD OCTAVE BAND SOUND PRESSURE LEVEL IN dBA re 0.0002  $\mu$ bar



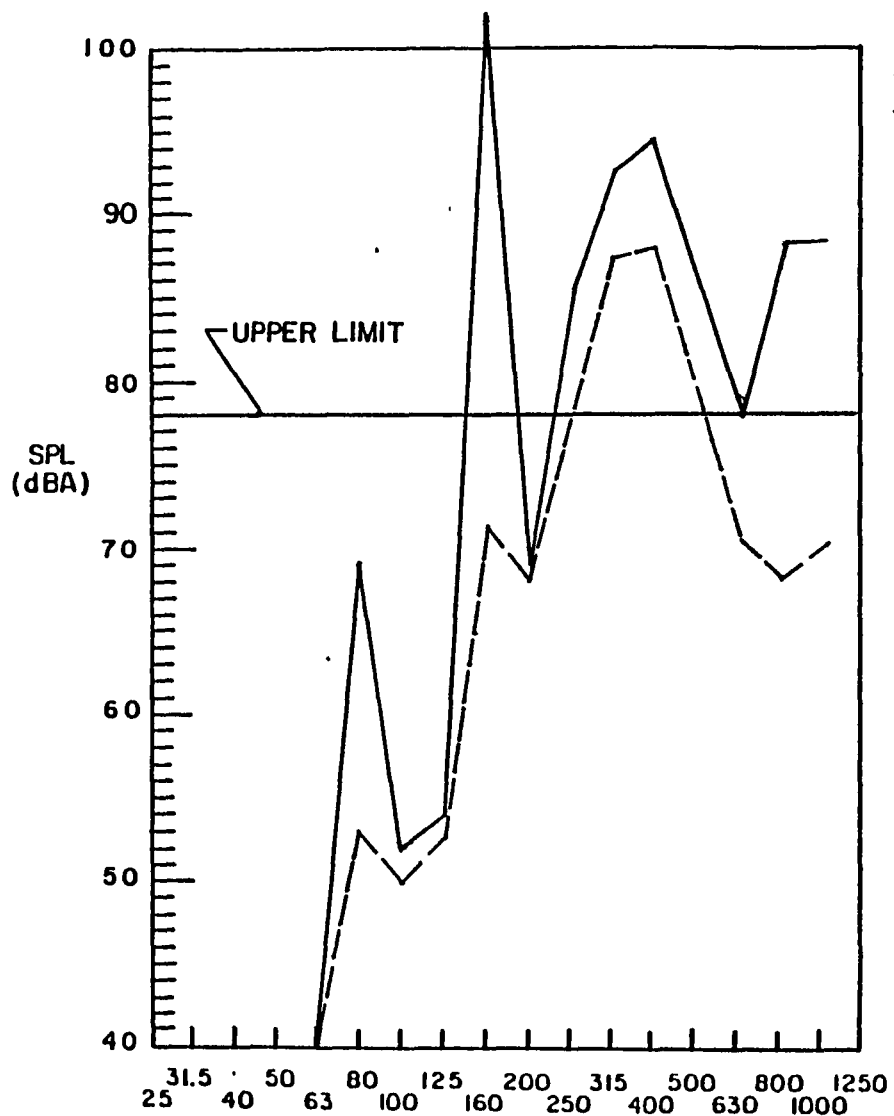
— baseline : OA = 95 dBA  
 - - - honeycomb : OA = 89 dBA  
 + damping tape  
 added weight = 3.85 lbs.  
 panel area = 5.13 sq.ft.



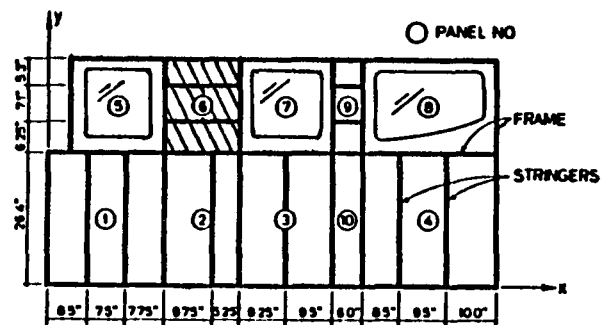
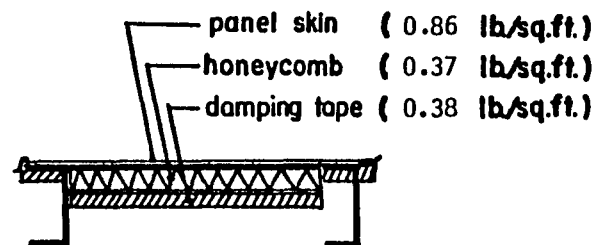
▨ - unit under study

Fig. 49 Interior noise with honeycomb-damping tape treatment (Panel No. 4)

ONE-THIRD OCTAVE BAND SOUND PRESSURE LEVEL IN dBA re 0.0002  $\mu$ bar



— baseline : OA = 106 dBA  
 - - - honeycomb : OA = 92 dBA  
 + damping tape  
 added weight = 1.46 lbs.  
 panel area = 1.94 sq.ft.

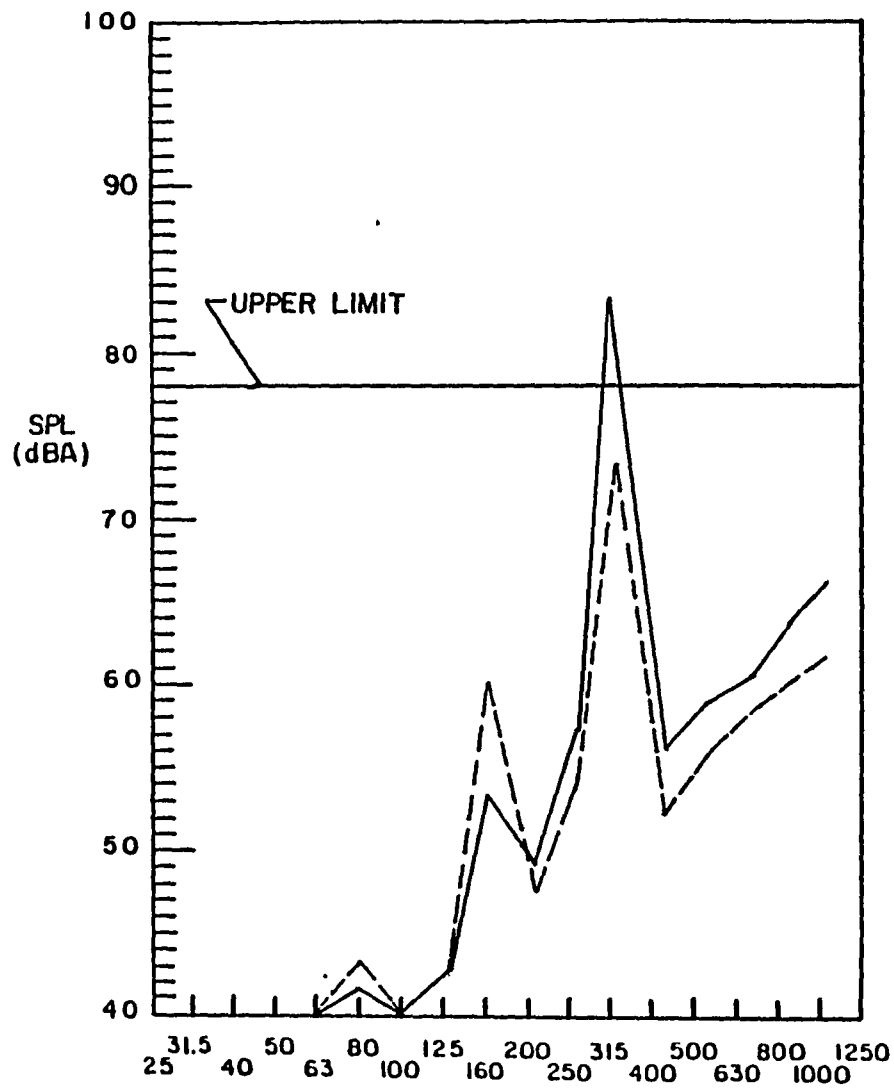


▨ - unit under study

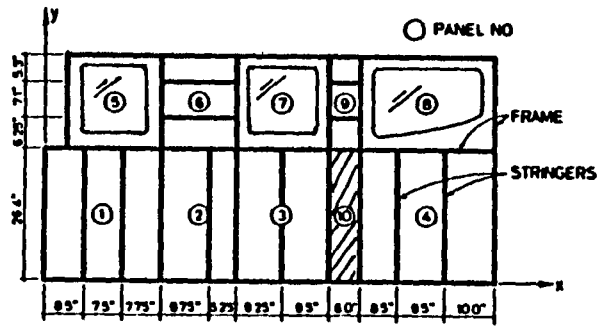
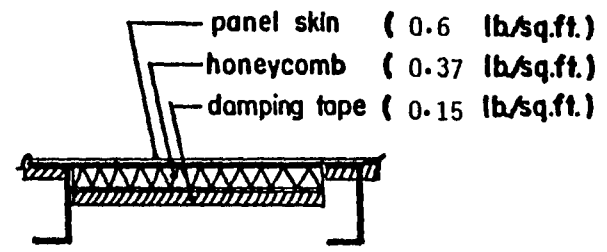
ONE-THIRD OCTAVE BAND CENTER FREQUENCIES IN Hz (cps)

Fig. 50 Interior noise with honeycomb-damping tape treatment (Pane. No. 6)

ONE-THIRD OCTAVE BAND SOUND PRESSURE LEVEL IN dBA re 0.0002  $\mu$ bar



— baseline : OA = 86 dBA  
 - - - honeycomb : OA = 75 dBA  
 + damping tape  
 added weight = 0.57 lbs.  
 panel area = 1.1 sq.ft.

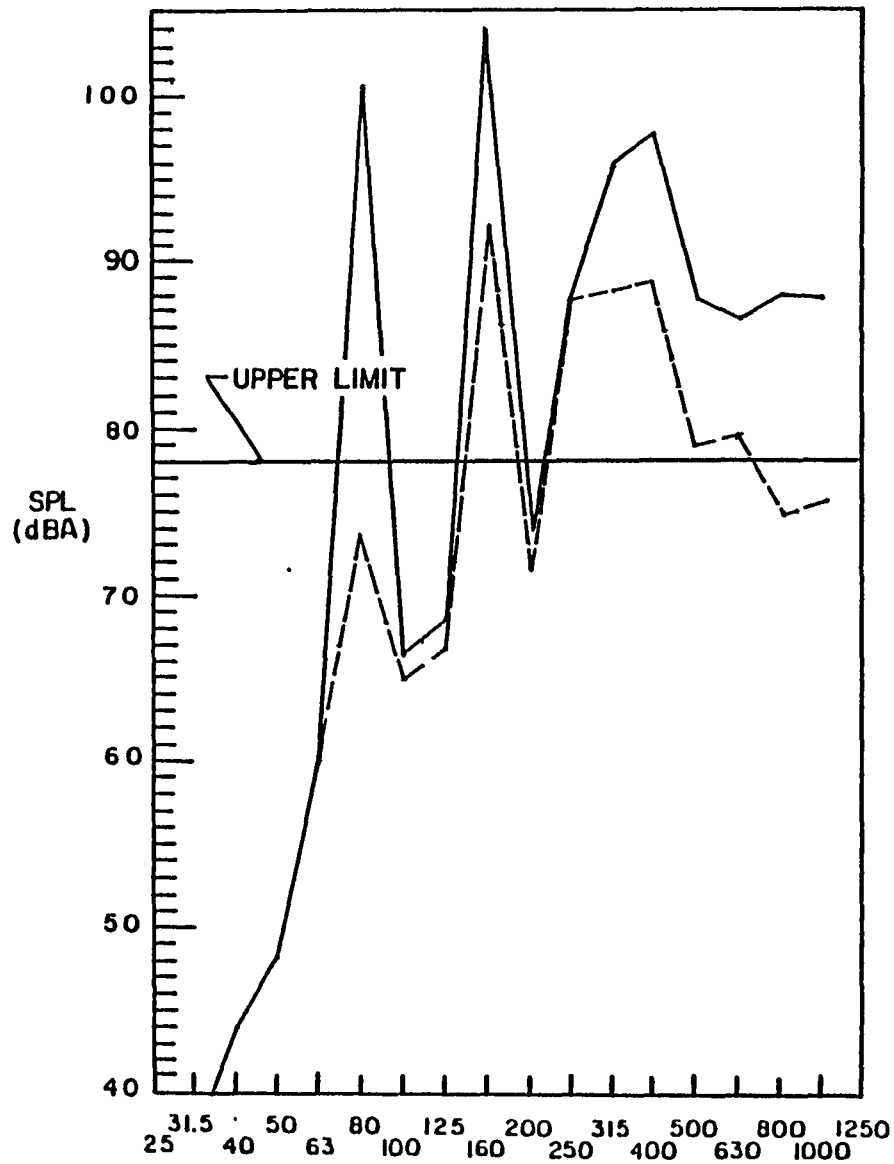


▨ - unit under study

ONE-THIRD OCTAVE BAND CENTER FREQUENCIES IN Hz (cps)

Fig. 51 Interior noise with honeycomb-damping tape treatment (Panel No. 10)

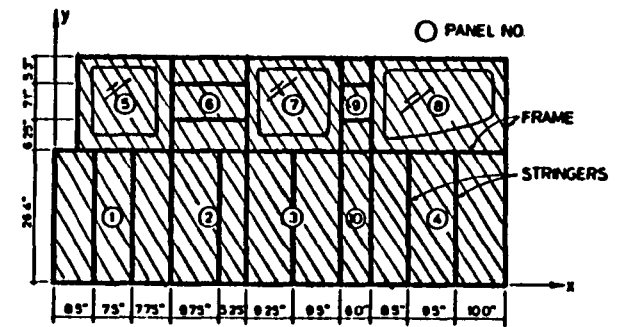
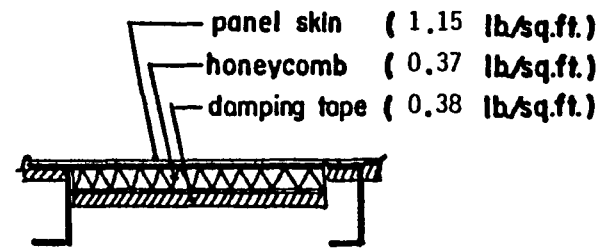
ONE-THIRD OCTAVE BAND SOUND PRESSURE LEVEL IN dBA re 00002  $\mu$ bar



ONE-THIRD OCTAVE BAND CENTER FREQUENCIES IN Hz (cps)

— baseline : OA = 107 dBA  
 - - - honeycomb : OA = 96 dBA  
 + damping tape

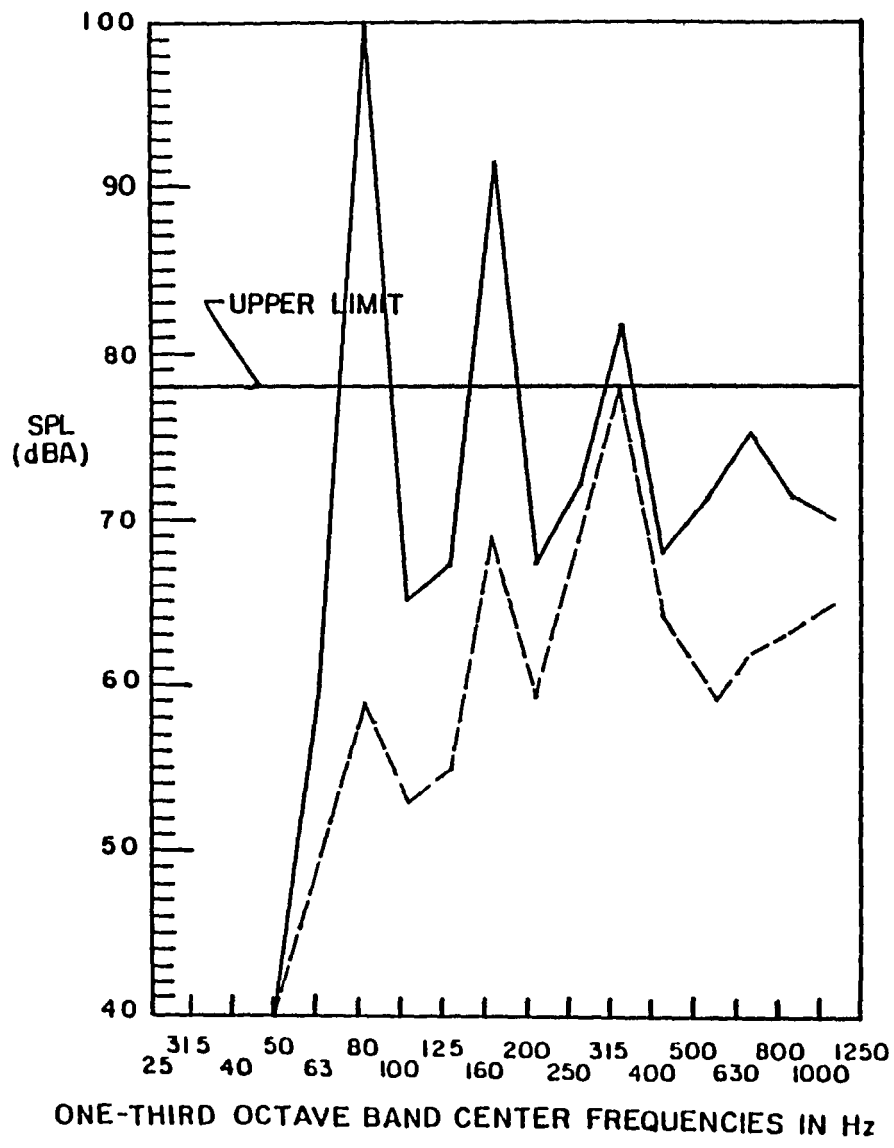
added weight = 14 lbs.  
 panel area = 29 sq.ft.



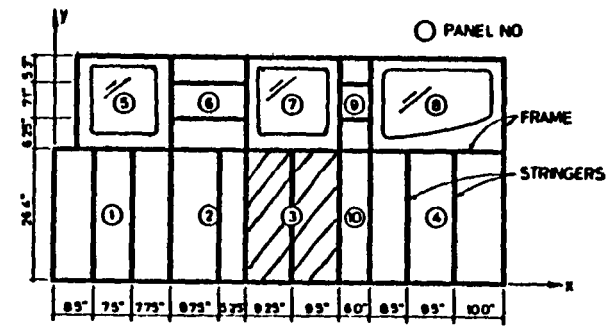
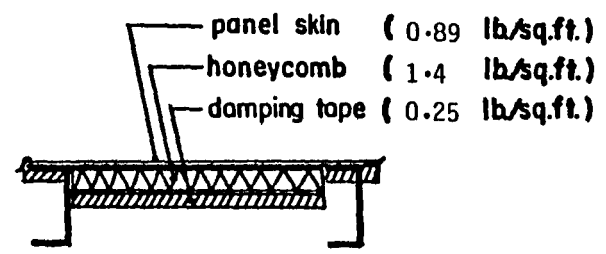
▨ - unit under study

Fig. 52 Interior noise with honeycomb-damping tape treatment (Sidewall)

-103- ONE-THIRD OCTAVE BAND SOUND PRESSURE LEVEL IN dBA re 0.0002  $\mu$ bar

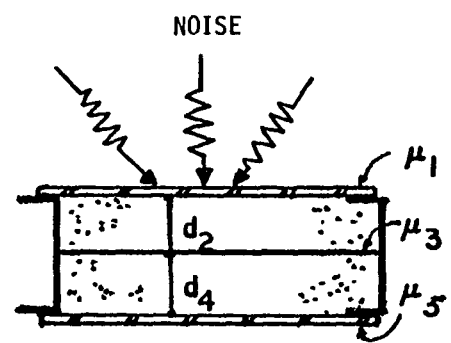
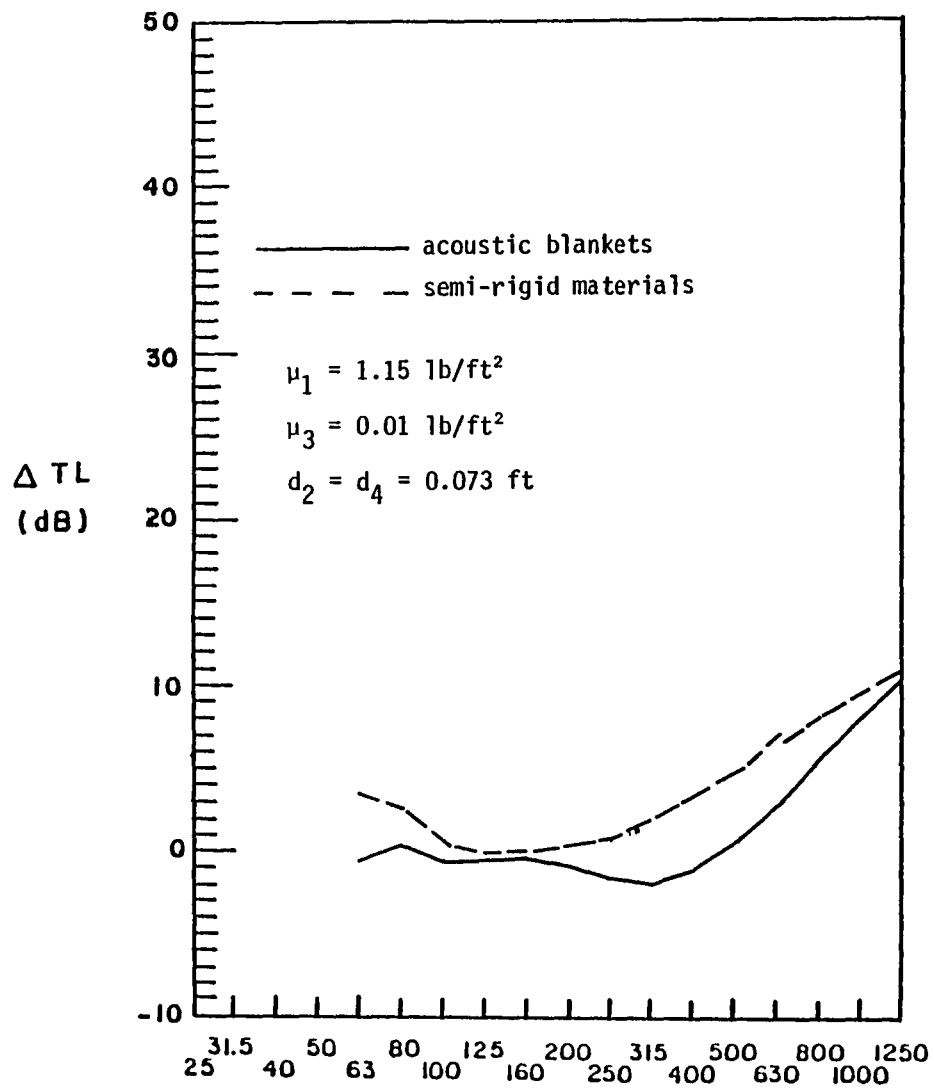


— baseline : OA = 102 dBA  
 - - - honeycomb : OA = 78 dBA  
 + damping tape  
 added weight = 5.68 lbs.  
 panel area = 3.44 sq.ft.



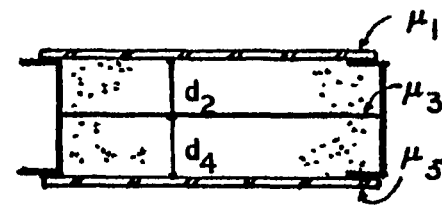
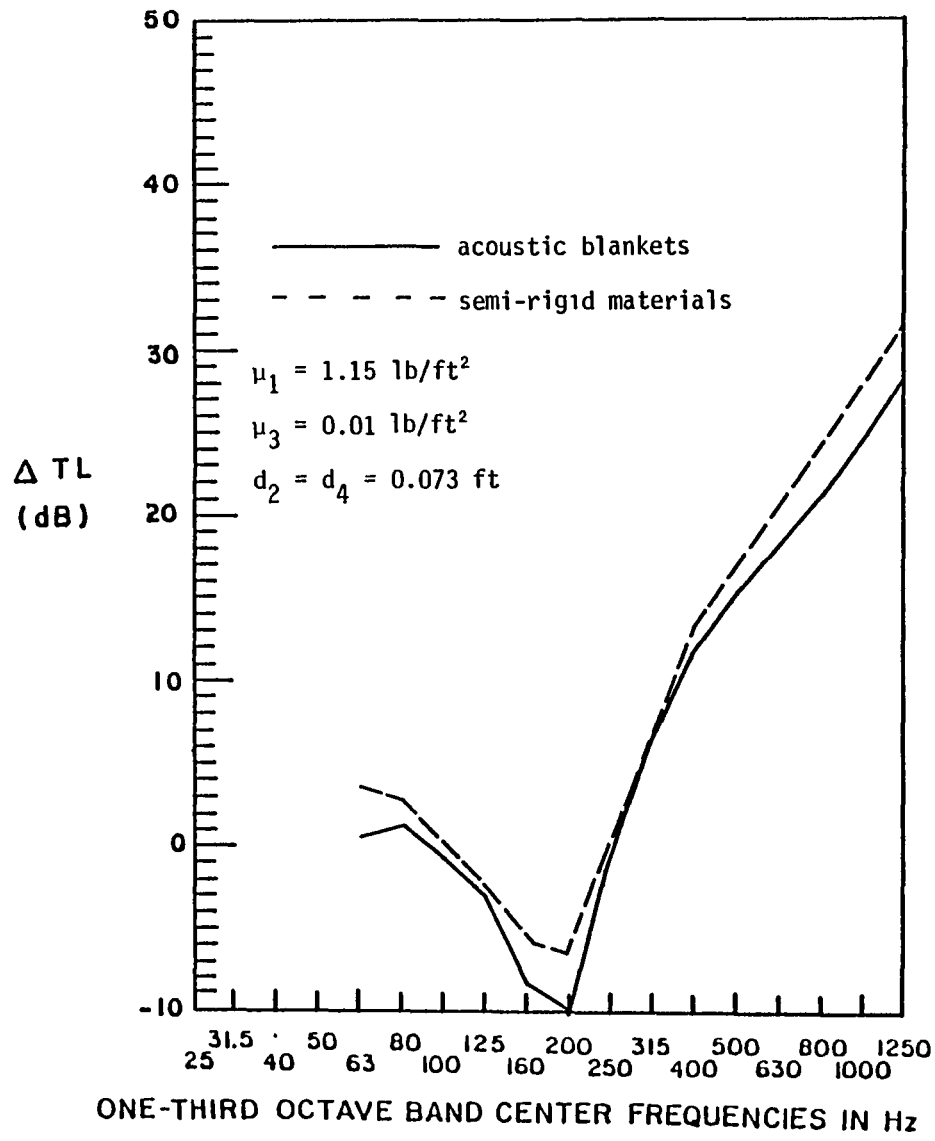
▨ - unit under study

Fig. 53 Interior noise levels with heavy honeycomb-damping tape treatment (Panel No. 3)



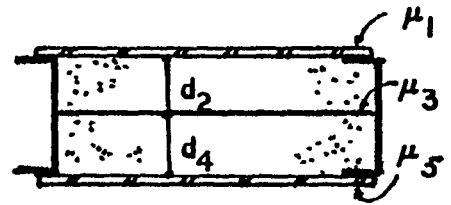
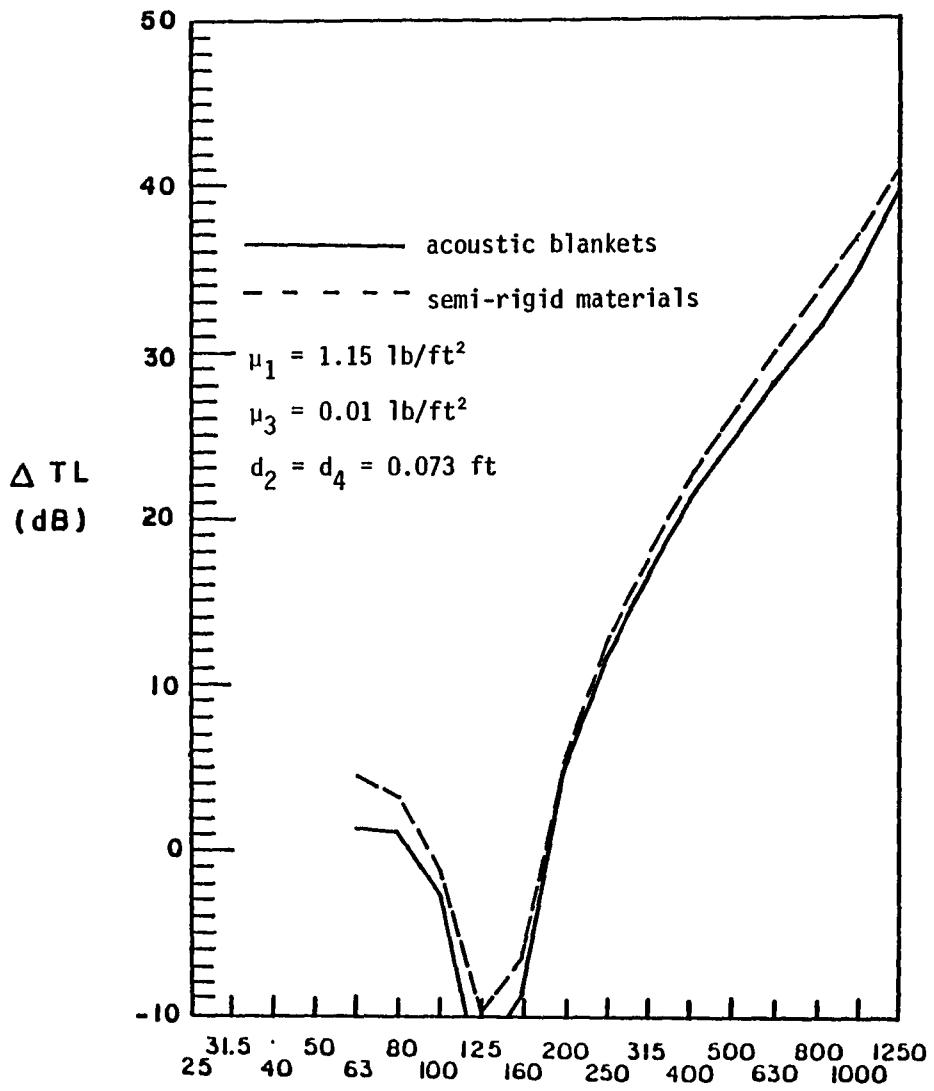
SIDEWALL SECTION

Fig. 54 Additional transmission losses for acoustic blankets and semi-rigid materials ( $\mu_5 = 0.01 \text{ lb/ft}^2$ )



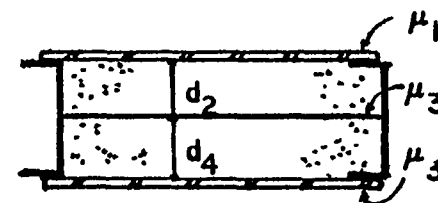
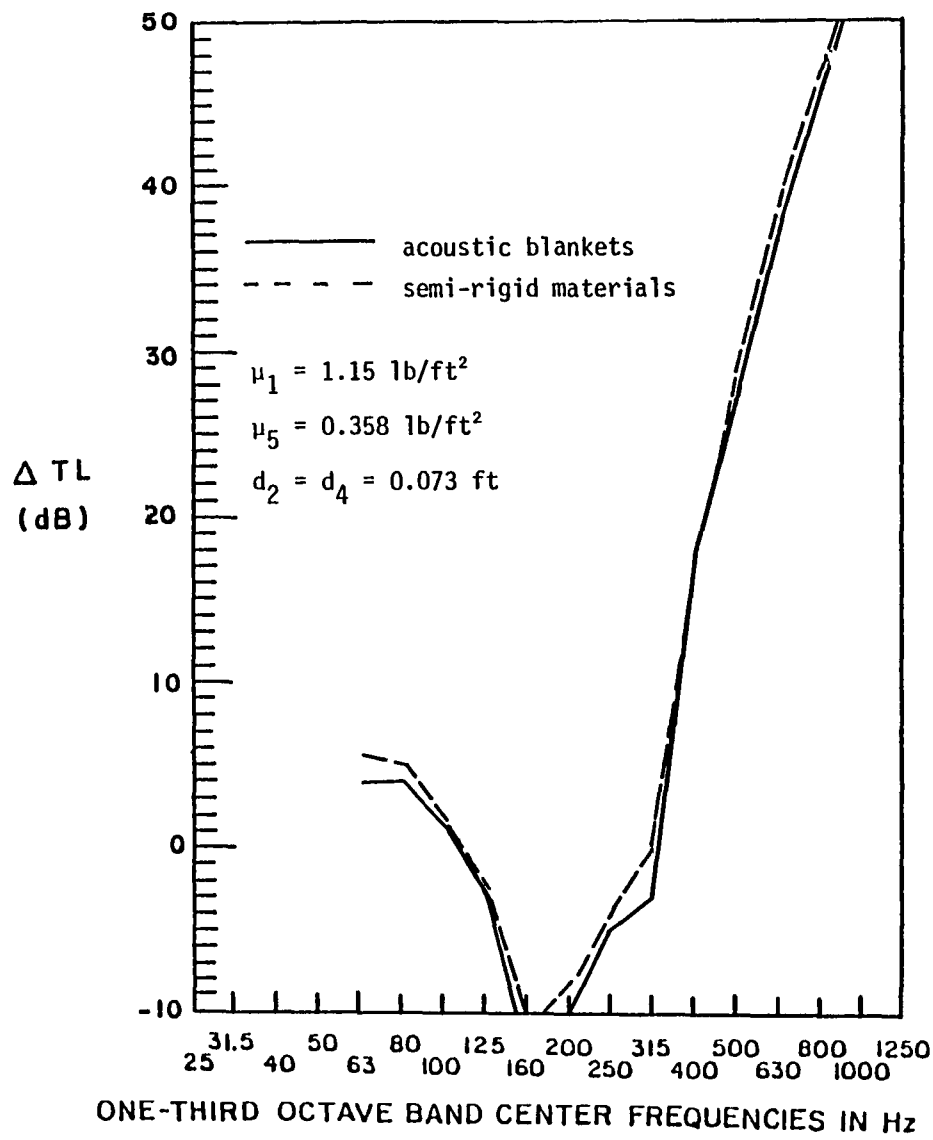
SIDEWALL SECTION

Fig. 55 Additional transmission losses for acoustic blankets and semi-rigid materials ( $\mu_5 = 0.358 \text{ lb/ft}^2$ )



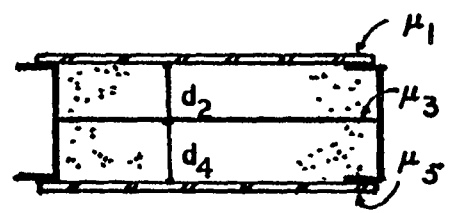
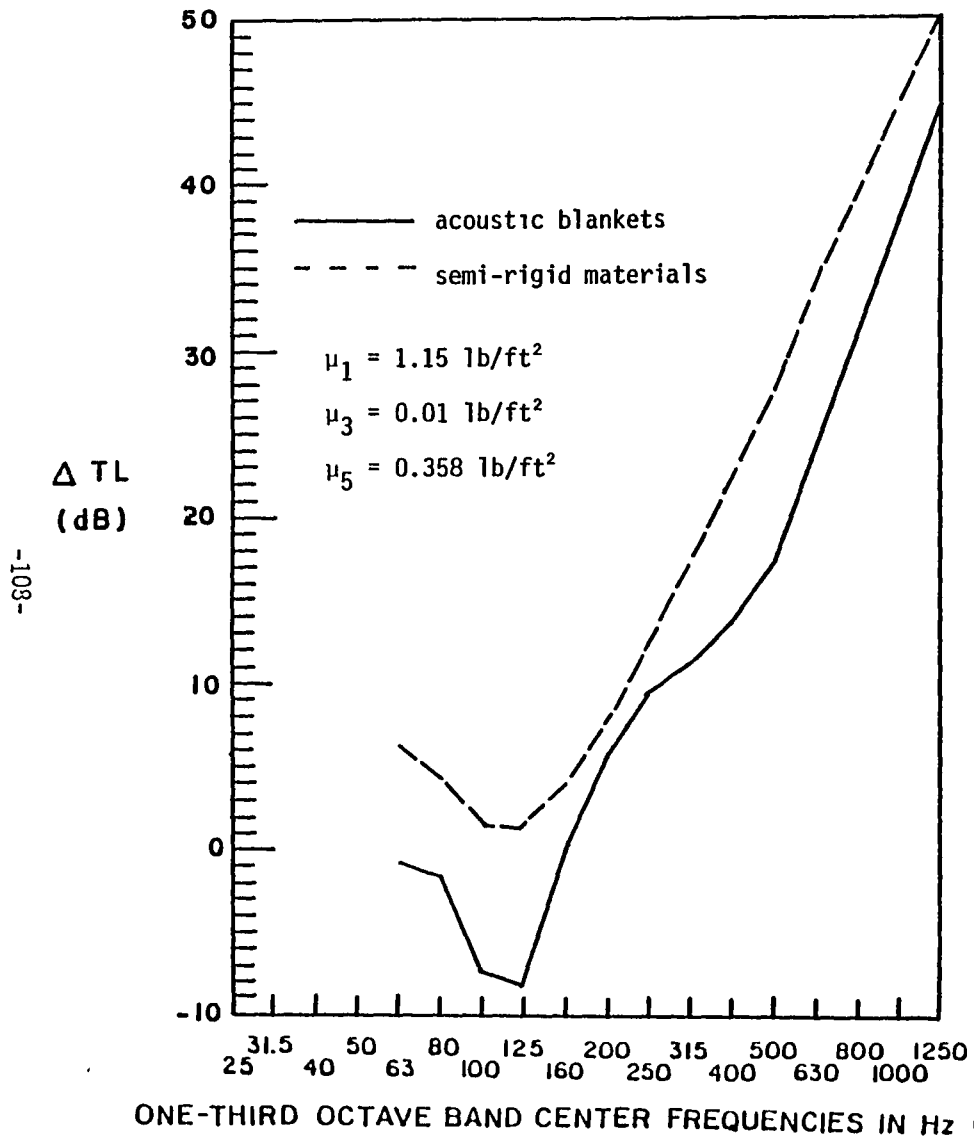
SIDEWALL SECTION

Fig. 56 Additional transmission losses for acoustic blankets and semi-rigid materials ( $\mu_5 = 1.0 \text{ lb/ft}^2$ )



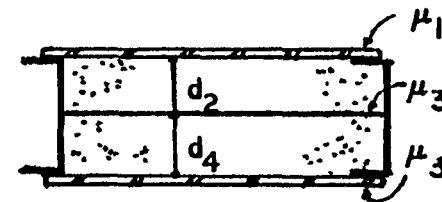
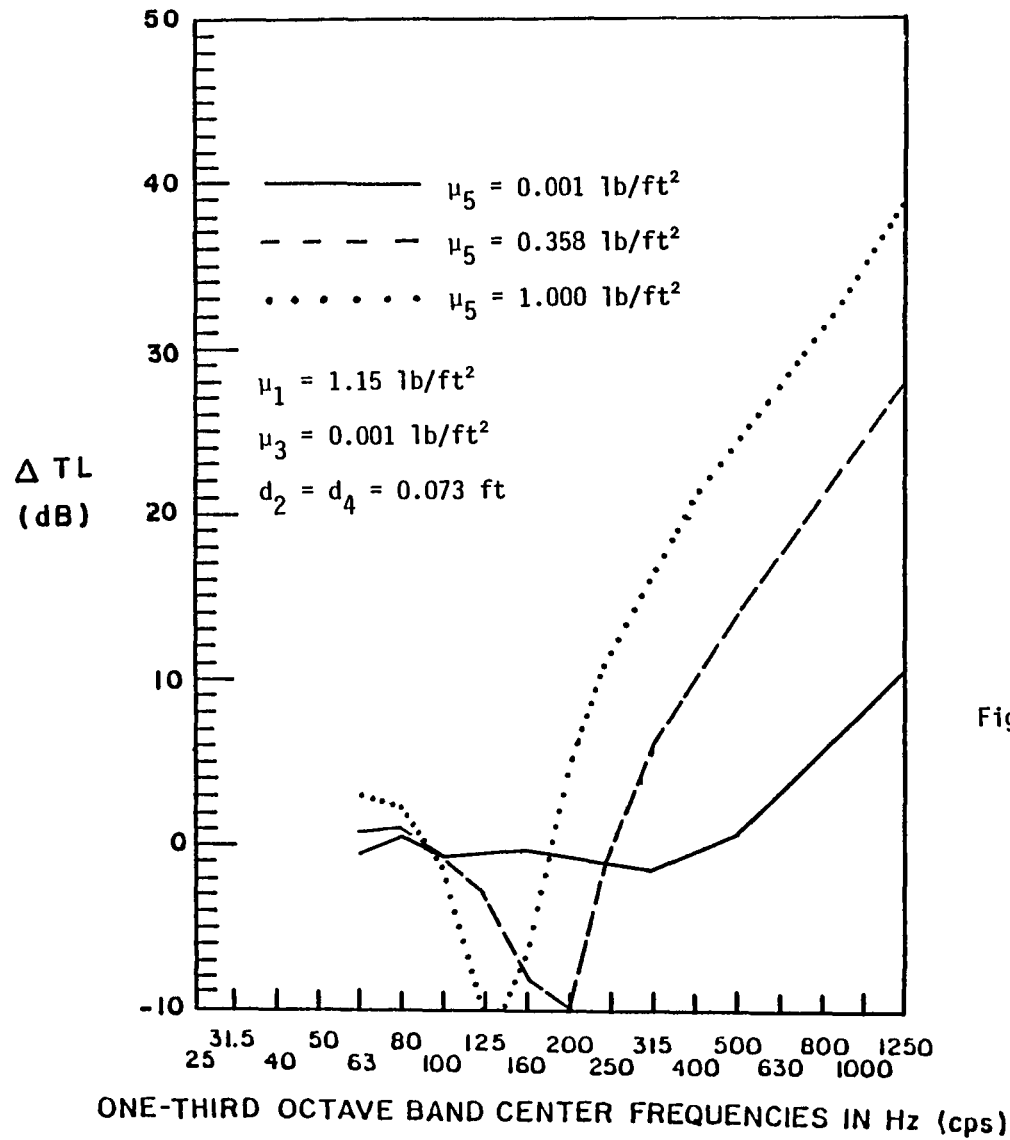
SIDEWALL SECTION

Fig. 57 Additional transmission losses for acoustic blankets and semi-rigid materials ( $\mu_3 = 1.0 \text{ lb/ft}^2$ )



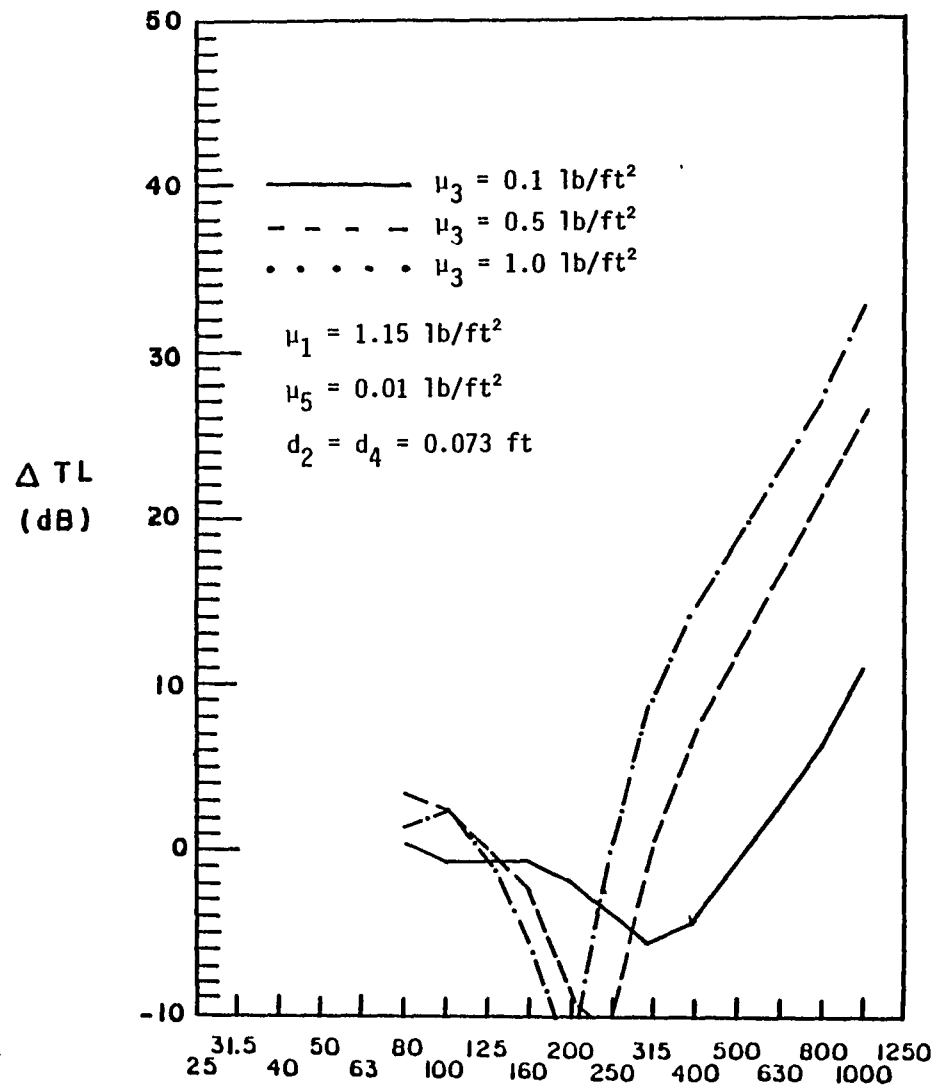
**SIDEWALL SECTION**

Fig. 58 Additional transmission losses for acoustic blankets and semi-rigid materials (  $d_2 = d_4 = 0.167 \text{ ft}$  )

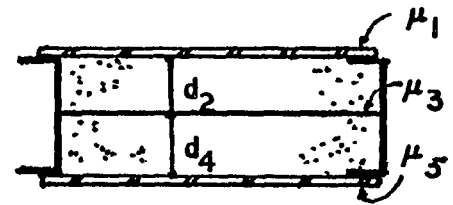


SIDEWALL SECTION

Fig. 59 Additional transmission losses for different trim panel surface densities

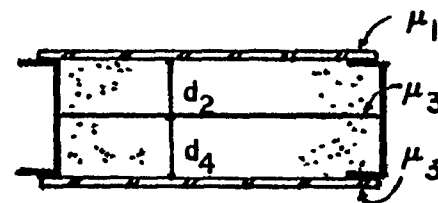
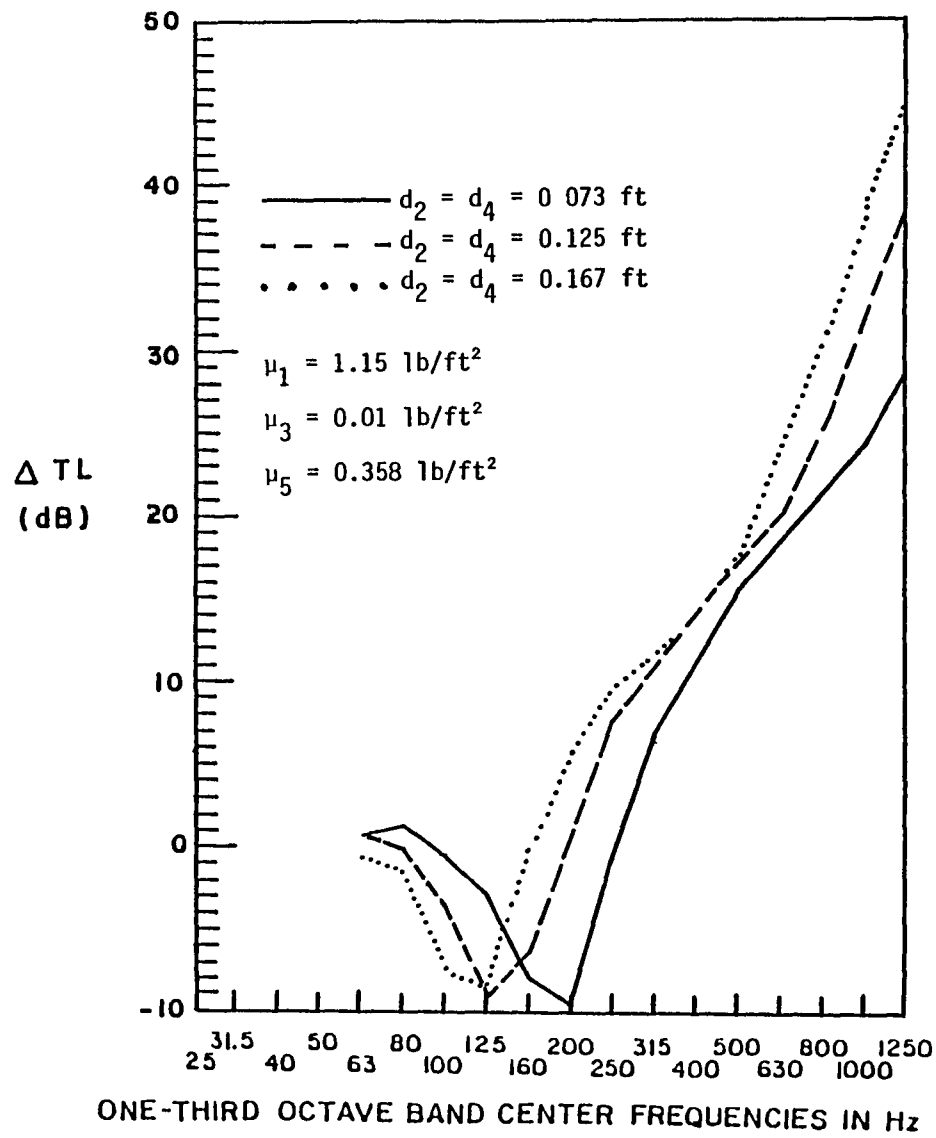


ONE-THIRD OCTAVE BAND CENTER FREQUENCIES IN Hz (cps)



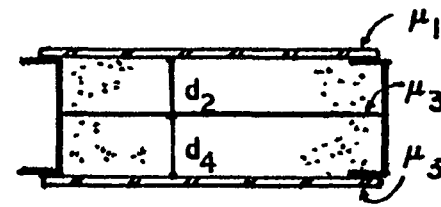
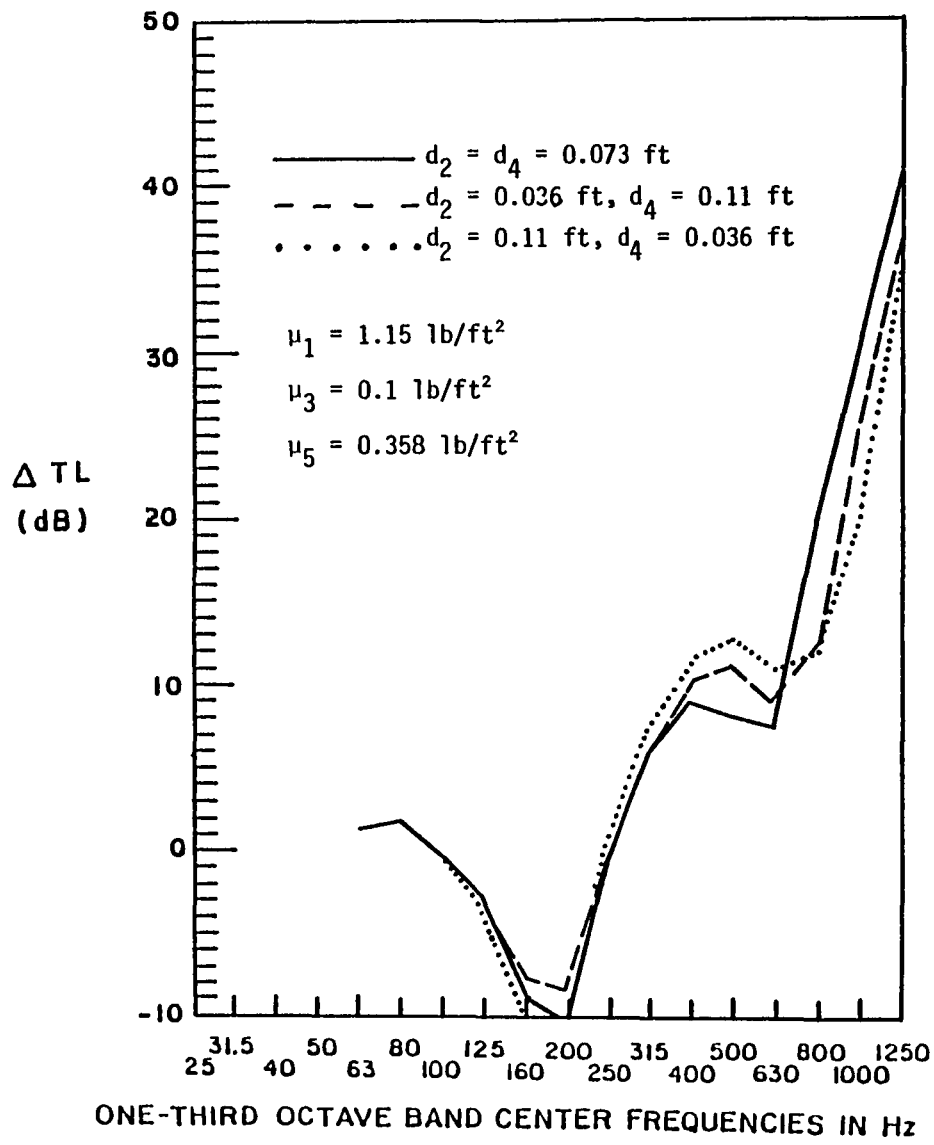
SIDEWALL SECTION

Fig. 60 Additional transmission losses for add-on treatment ( $\mu_1 = 1.15, \mu_5 = 0.01$ )



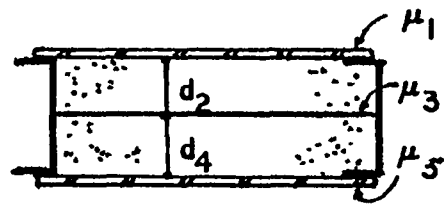
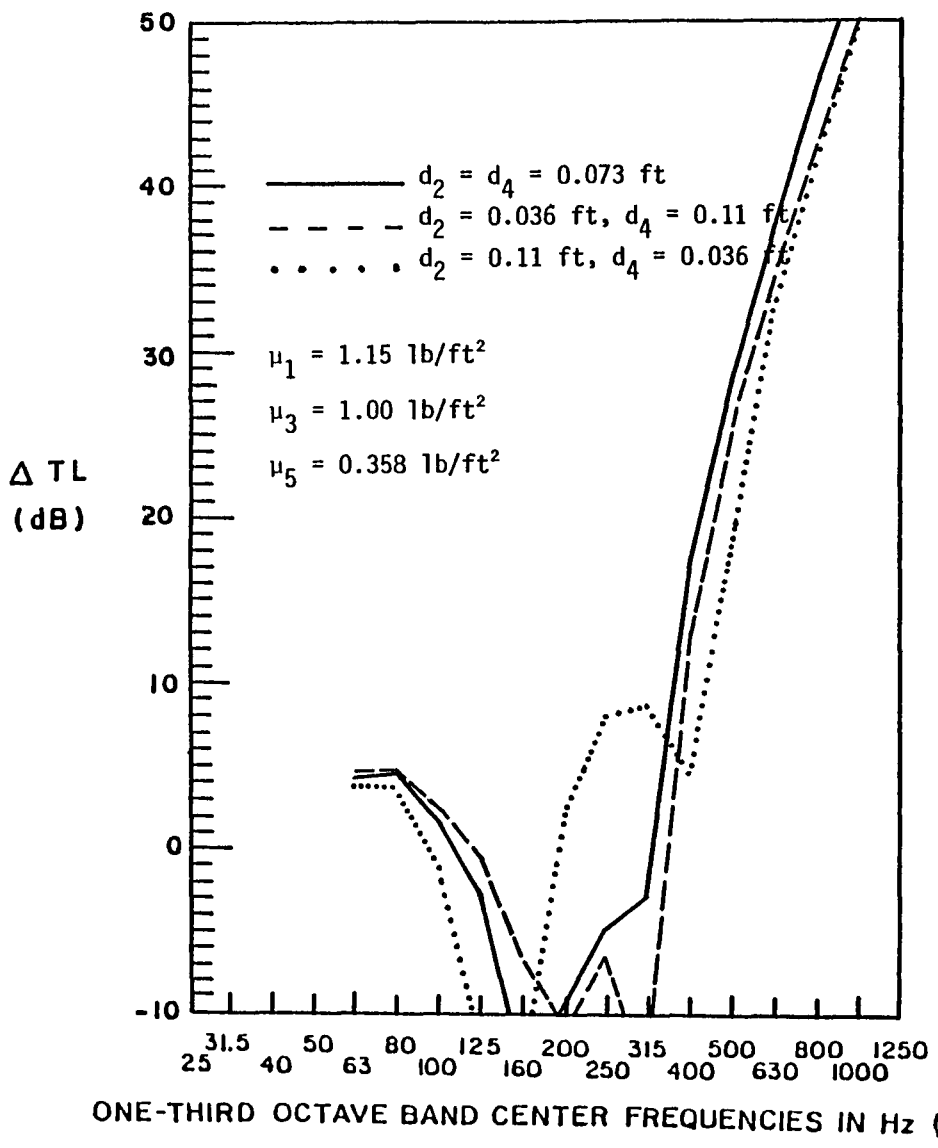
SIDEWALL SECTION

Fig. 61. Additional transmission losses for different distances between the elastic panel and the trim panel



SIDEWALL SECTION

Fig. 62 Additional transmission losses for a light septum and different distances between the elastic panel and the septum

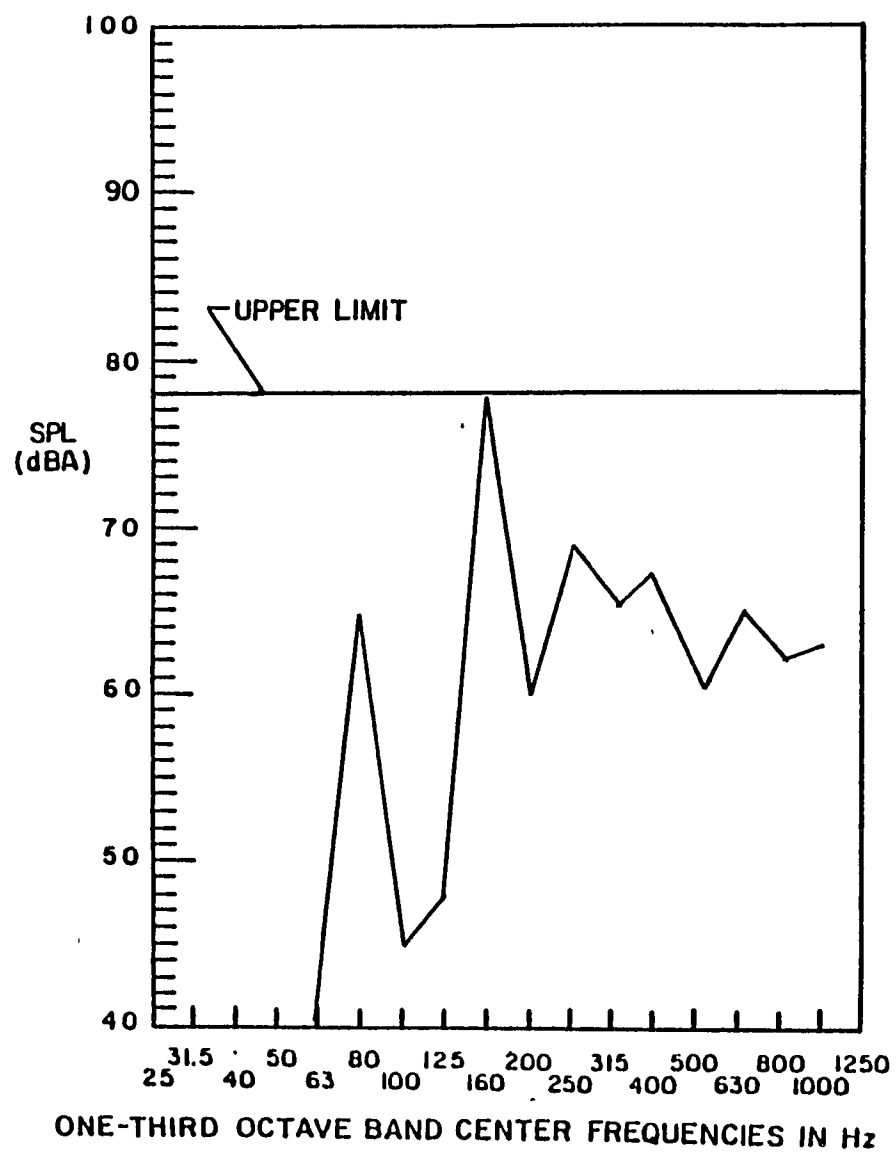


SIDEWALL SECTION

Fig. 63 Additional transmission losses for different distances between the elastic panel and the septum

ONE-THIRD OCTAVE BAND SOUND PRESSURE LEVEL IN dBA re 0.0002  $\mu$ bar

-114-



— baseline : OA = 80 dBA

added weight = 0 lbs.

panel area = 2.45 sq.ft.

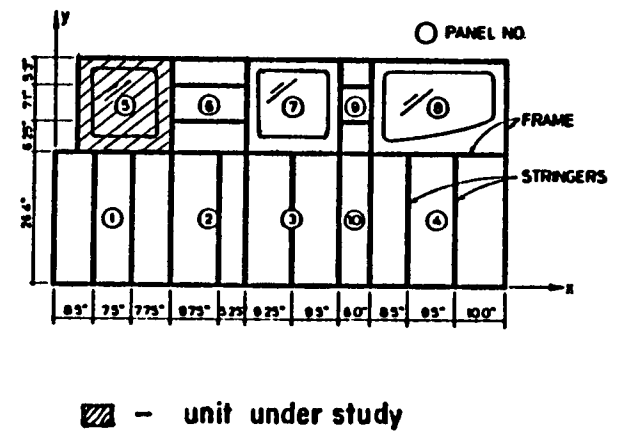
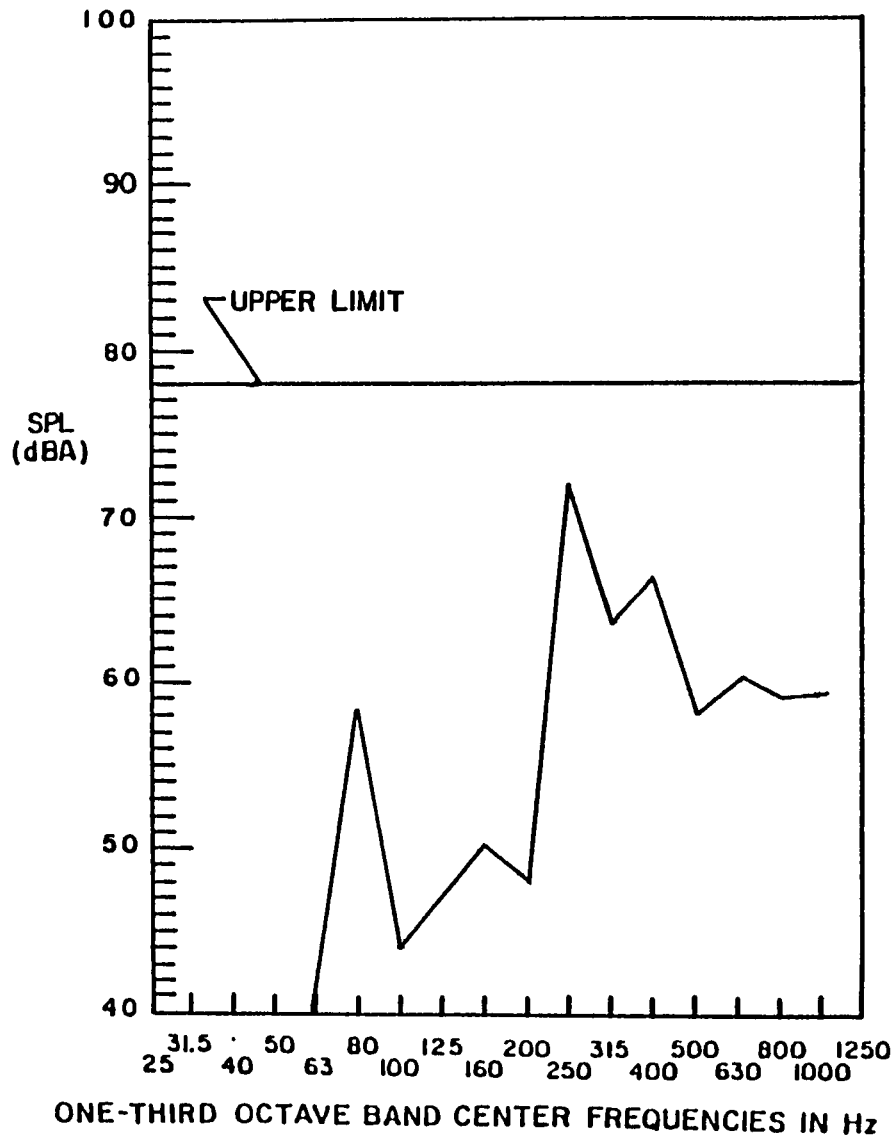


Fig. 64 Interior noise transmitted by a window (Panel No. 5)

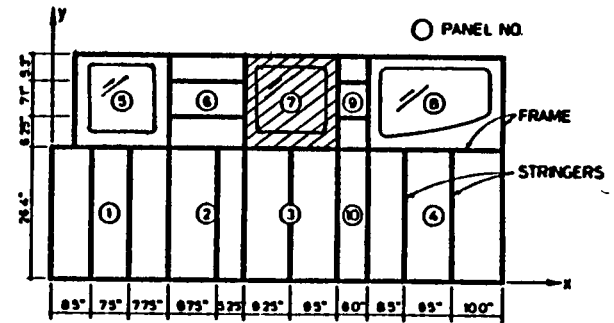
ONE-THIRD OCTAVE BAND SOUND PRESSURE LEVEL IN dBA re 0.0002  $\mu$ bar



— baseline : OA = 74 dBA

added weight = 0 lbs.

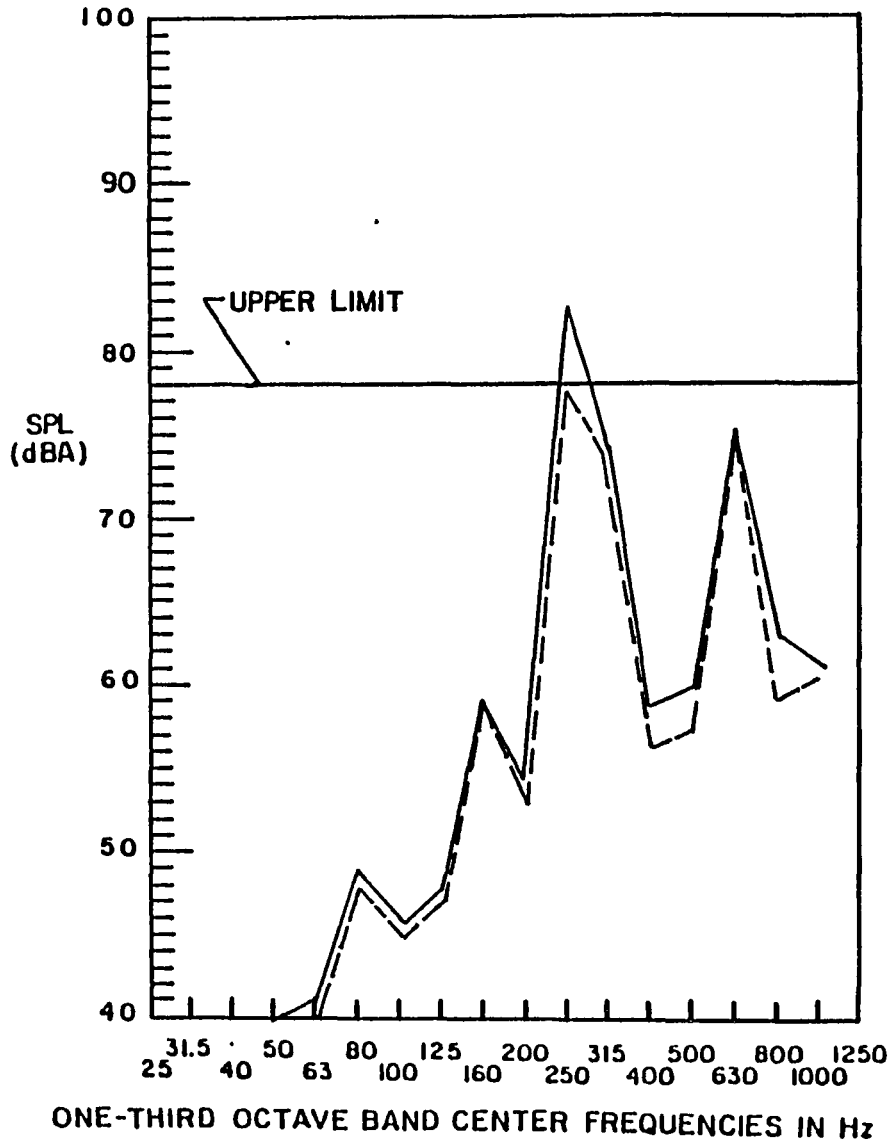
panel area = 2.45 sq.ft.



▨ - unit under study

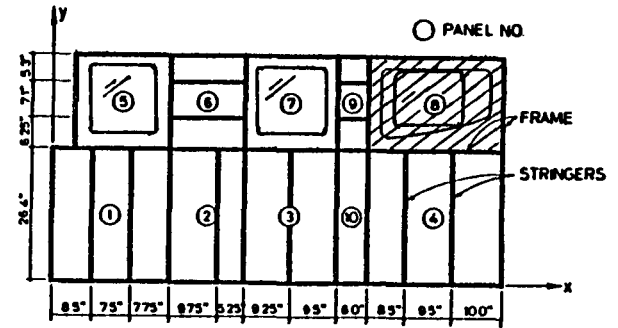
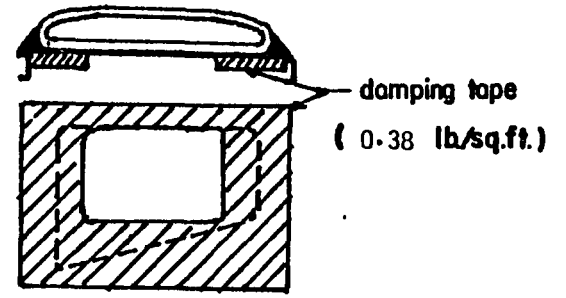
Fig. 65 Interior noise transmitted by a window (Panel No. 7)

ONE-THIRD OCTAVE BAND SOUND PRESSURE LEVEL IN dBA re 0.0002  $\mu$ bar



— baseline : OA = 85 dBA  
 - - - damping tape : OA = 80 dBA

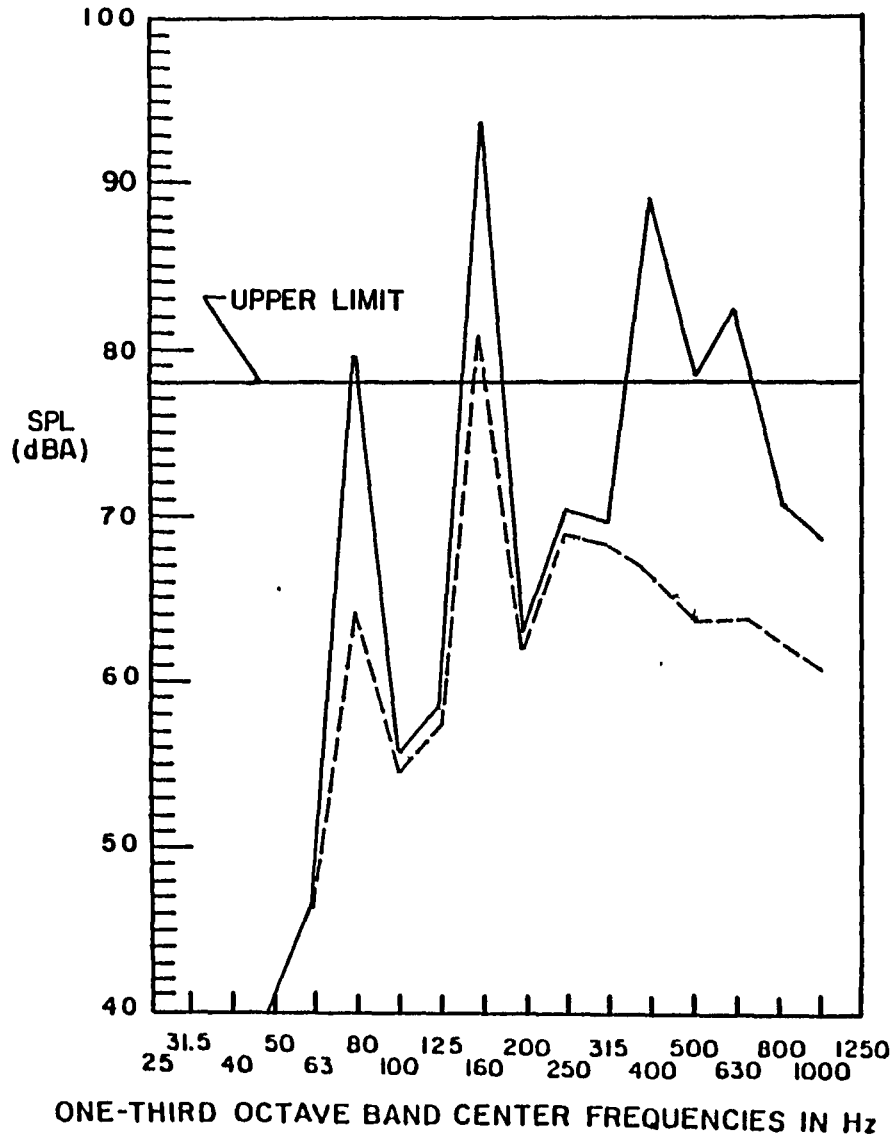
added weight = 1.0 lbs.  
 panel area = 3.6 sq.ft.



▨ - unit under study

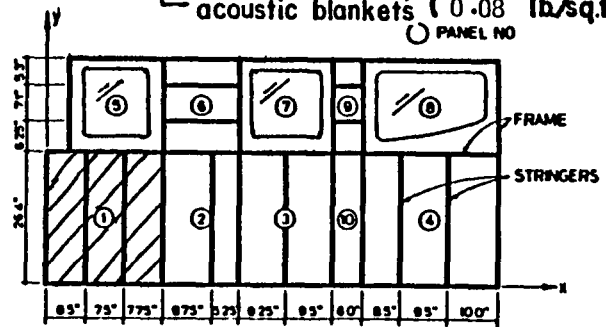
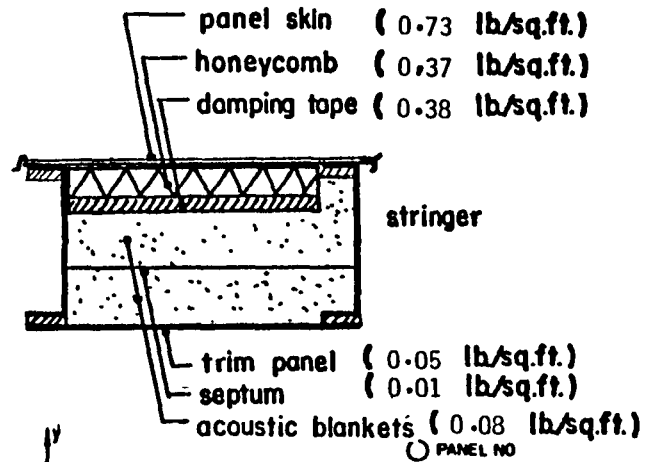
Fig. 66 Interior noise transmitted by a window (Panel No. 8)

ONE-THIRD OCTAVE BAND SOUND PRESSURE LEVEL IN dBA re 0.0002  $\mu$ bar



— baseline : OA = 94 dBA  
 --- optimized : OA = 81 dBA

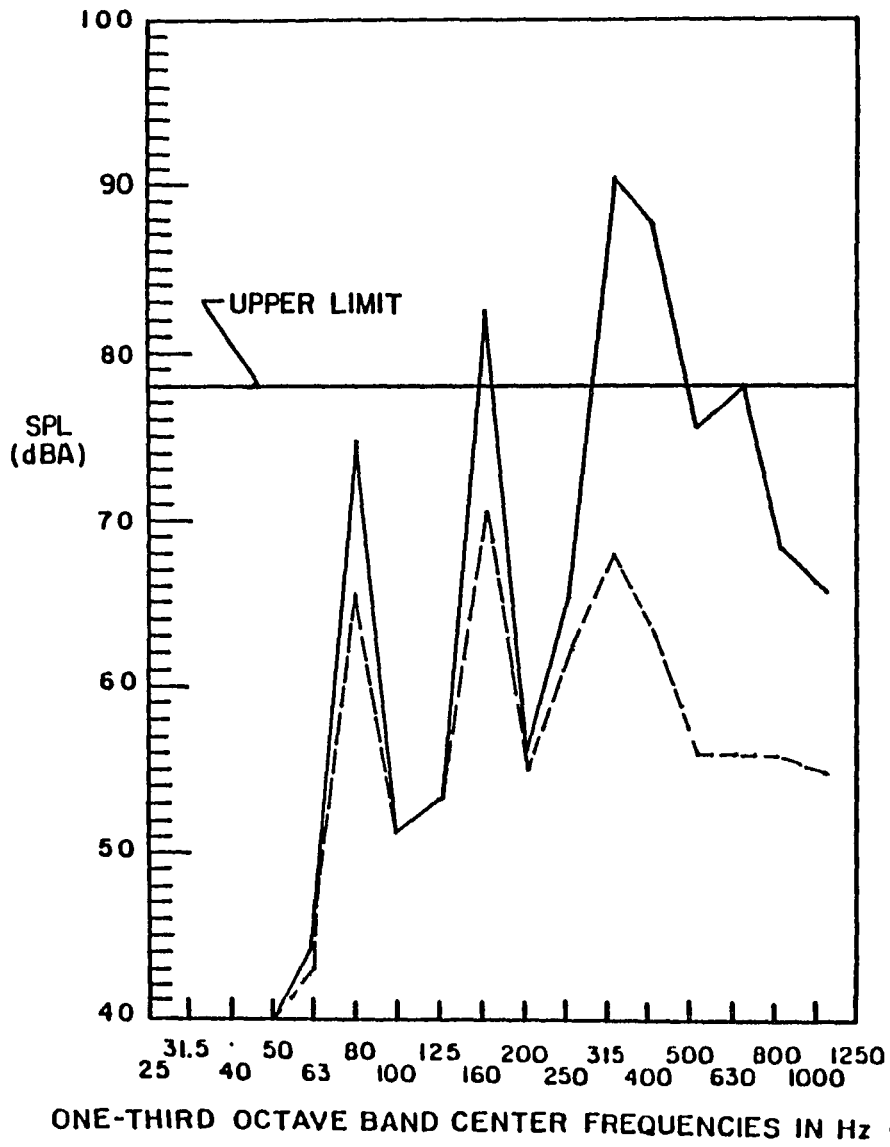
added weight = 4.5 lbs.  
 panel area = 4.4 sq.ft.



▨ - unit under study

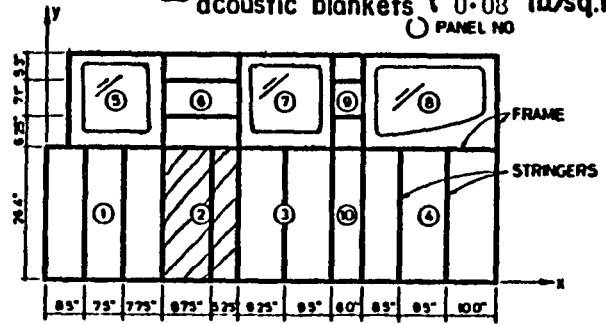
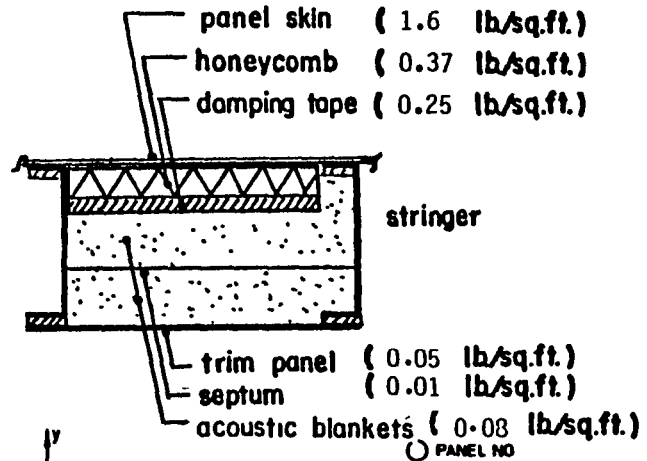
Fig. 67 Optimized interior noise (Panel No. 1)

-811-  
ONE-THIRD OCTAVE BAND SOUND PRESSURE LEVEL IN dBA re 0.0002  $\mu$ bar



— baseline ; OA = 92 dBA  
 --- optimized ; OA = 72 dBA

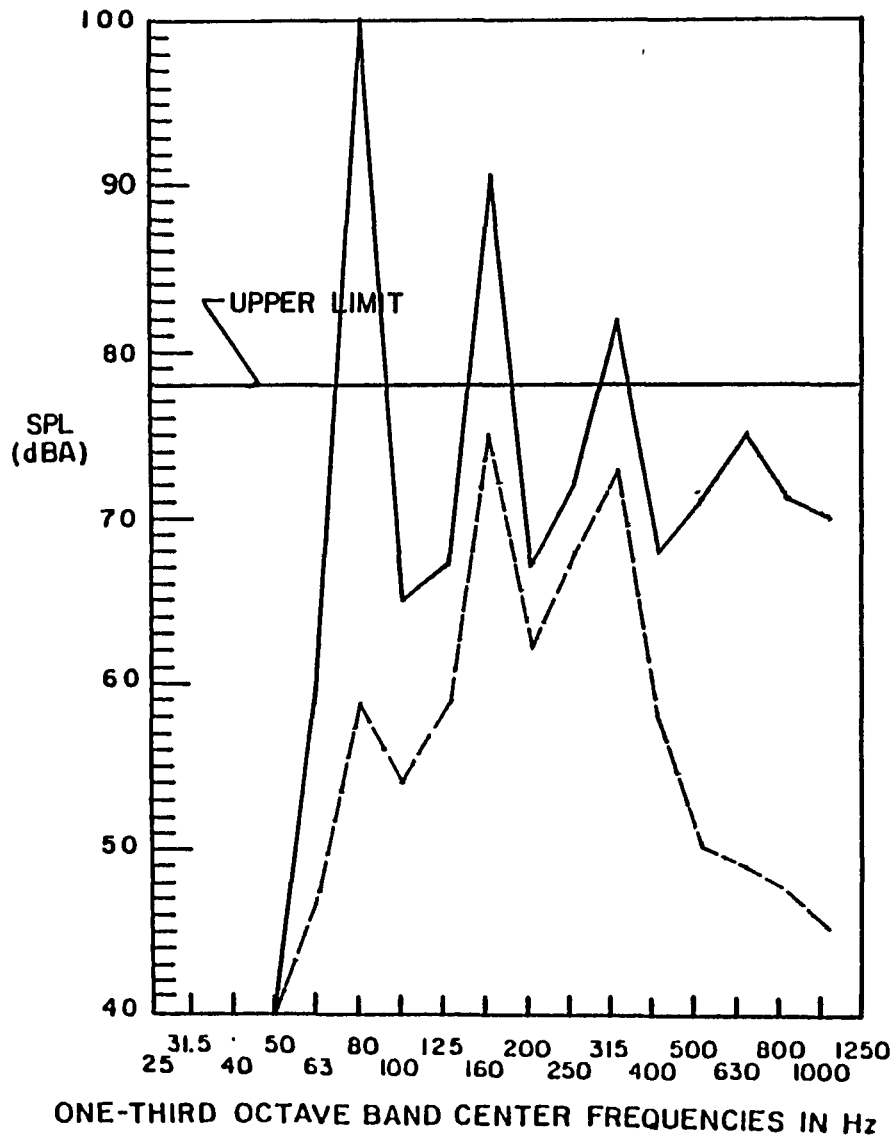
added weight = 2.43 lbs.  
 panel area = 2.75 sq.ft.



▨ - unit under study

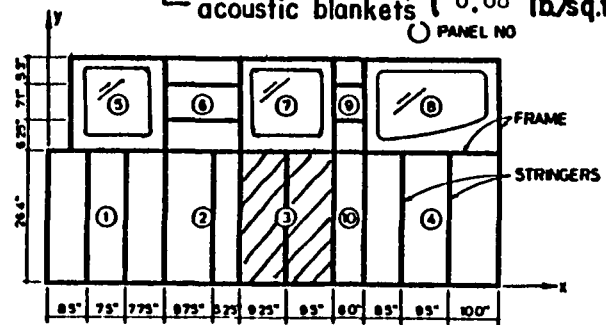
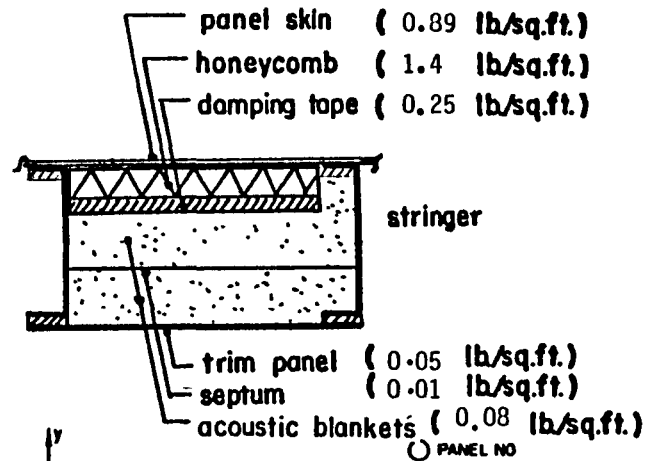
Fig. 68 Optimized interior noise (Panel No. 2)

ONE-THIRD OCTAVE BAND SOUND PRESSURE LEVEL IN dBA re 0.0002  $\mu$ bar



— baseline : OA = 102 dBA  
 --- optimized : OA = 77 dBA

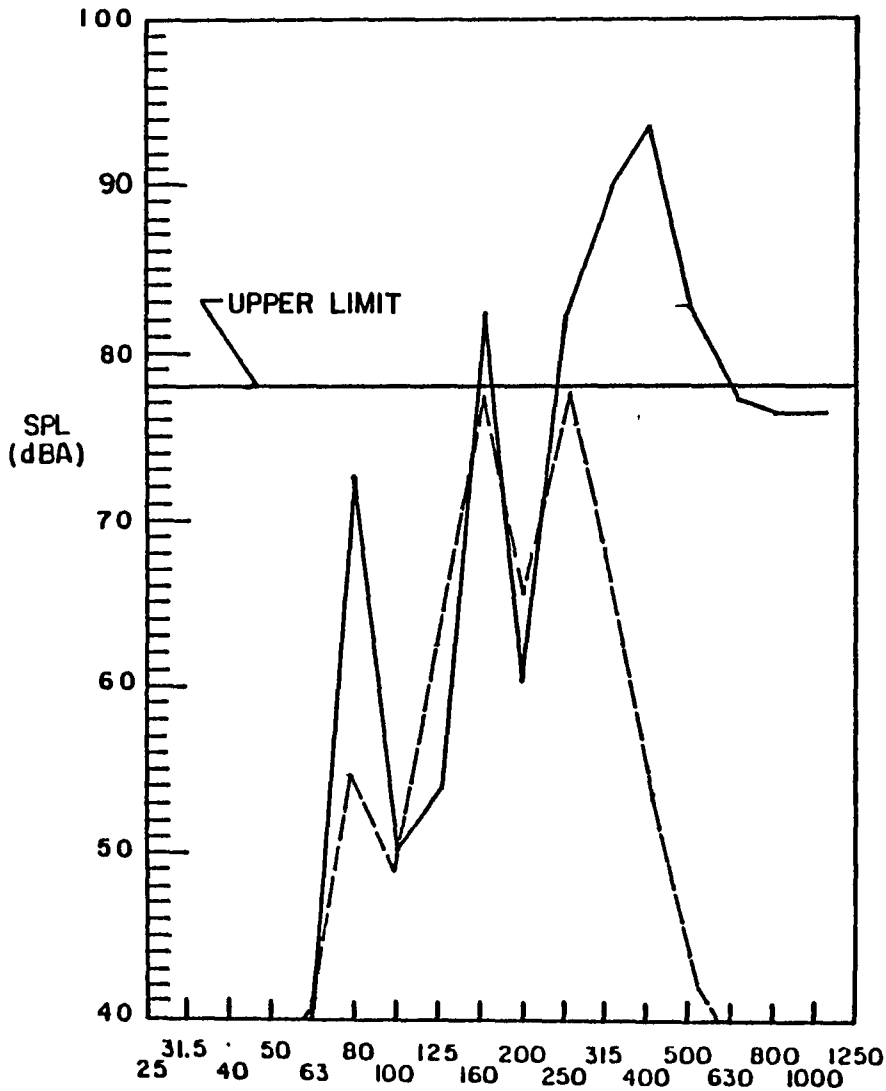
added weight = 6.75 lbs.  
 panel area = 3.44 sq.ft.



▨ - unit under study

Fig. 69 Optimized interior noise (Panel No. 3)

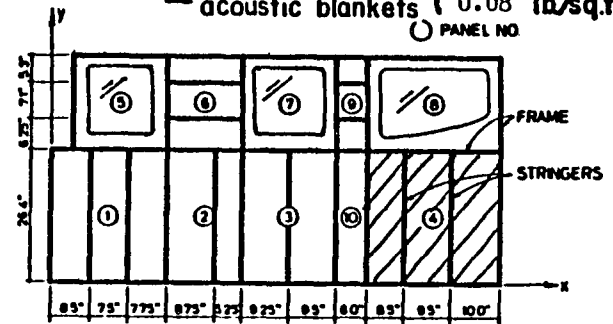
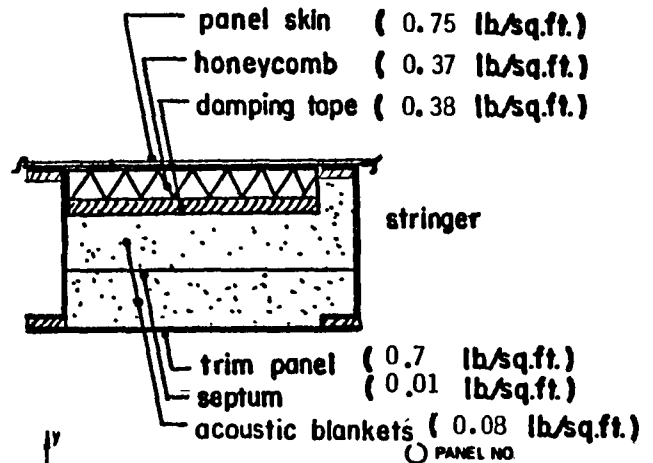
ONE-THIRD OCTAVE BAND SOUND PRESSURE LEVEL IN dBA re 0.0002  $\mu$ bar



ONE-THIRD OCTAVE BAND CENTER FREQUENCIES IN Hz (cps)

— baseline : OA = 95 dBA  
 - - - optimized : OA = 81 dBA

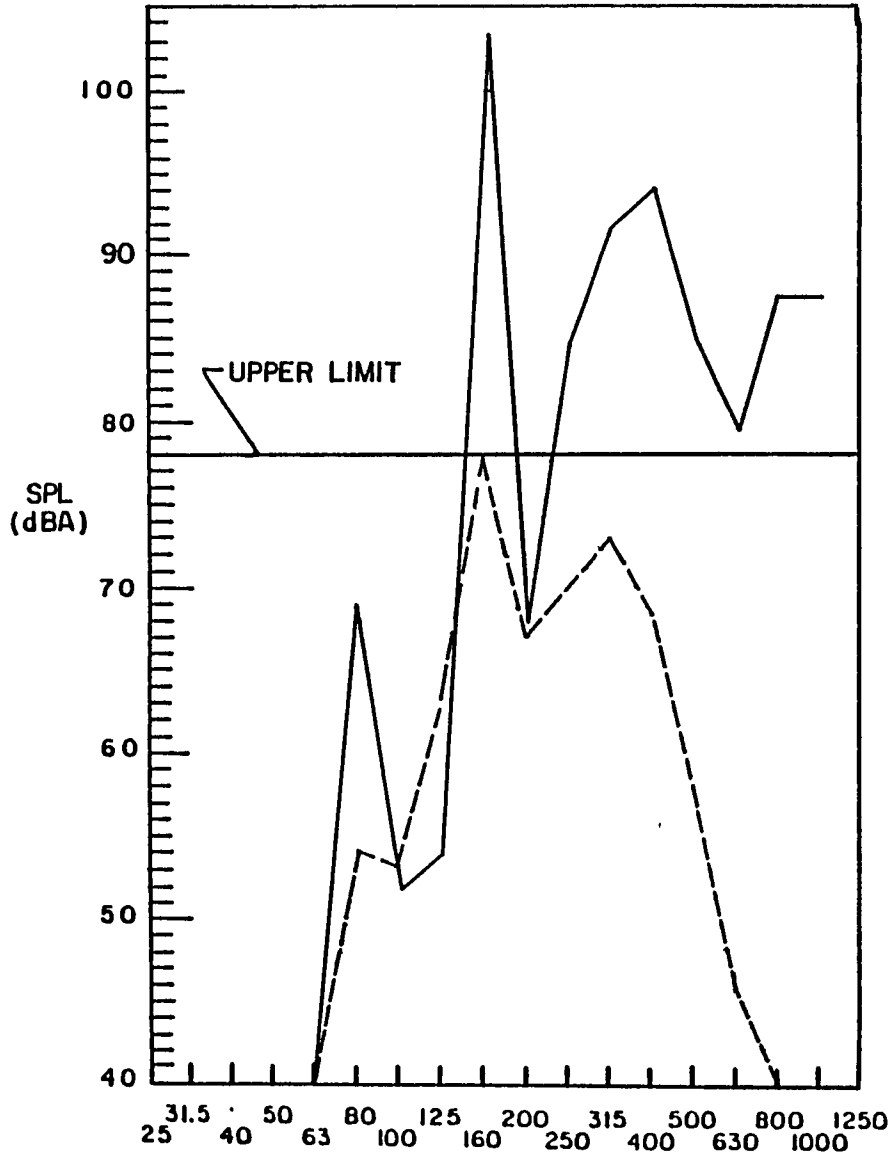
added weight = 8.73 lbs.  
 panel area = 5.13 sq.ft.



▨ - unit under study

Fig. 70 Optimized interior noise (Panel No. 4)

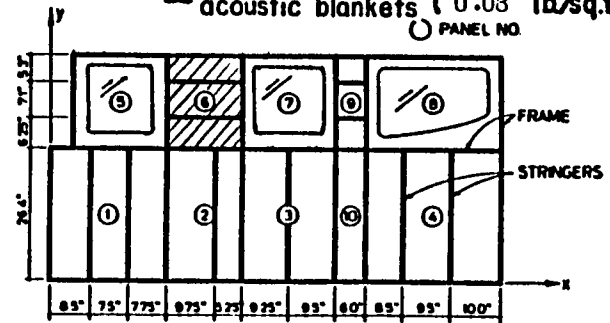
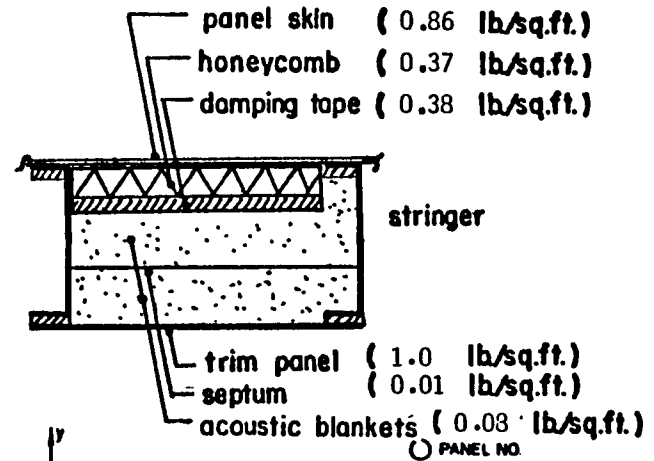
ONE-THIRD OCTAVE BAND SOUND PRESSURE LEVEL IN dBA re 0.0002  $\mu$ bar



ONE-THIRD OCTAVE BAND CENTER FREQUENCIES IN Hz (cps)

— baseline : OA = 106 dBA  
 - - - optimized : OA = 78 dBA

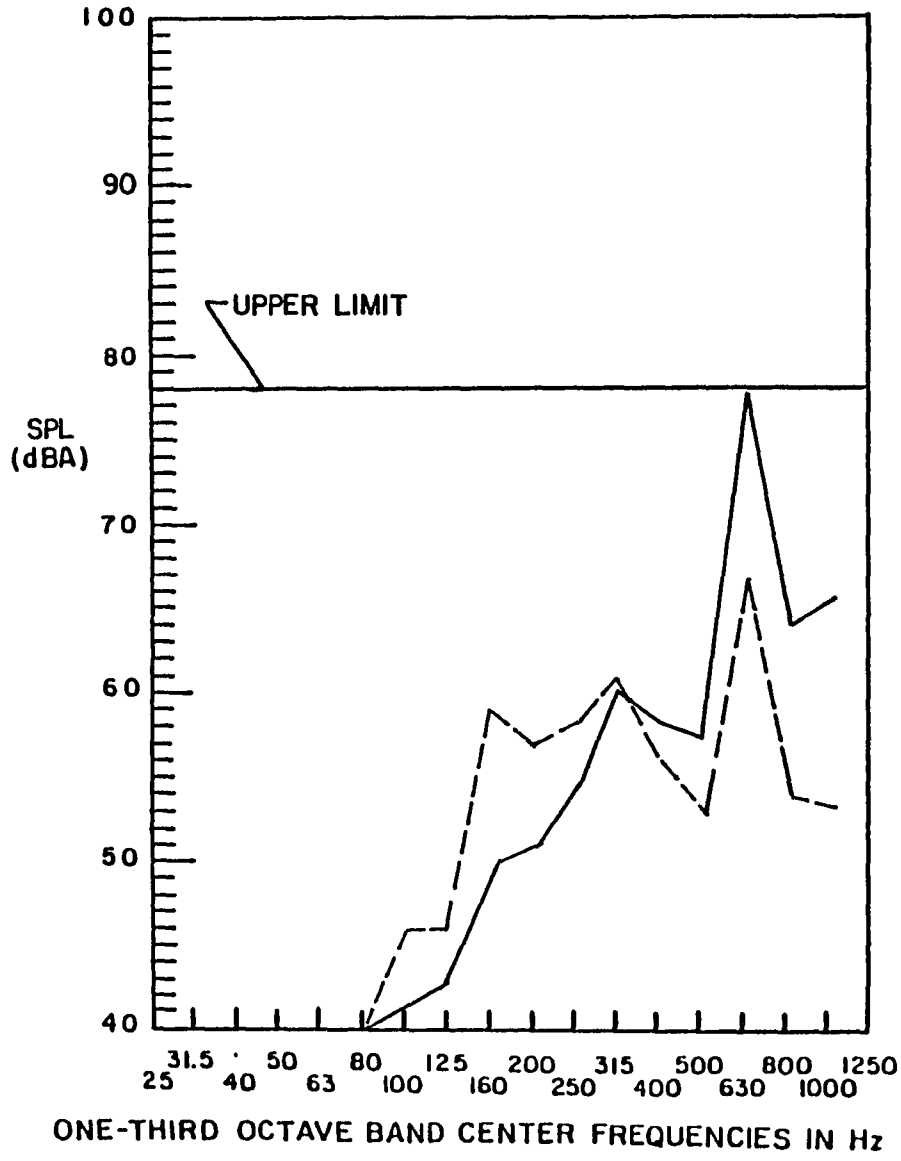
added weight = 3.91 lbs.  
 panel area = 1.94 sq.ft.



▨ - unit under study

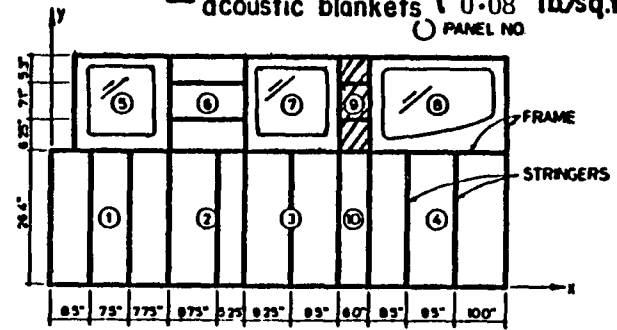
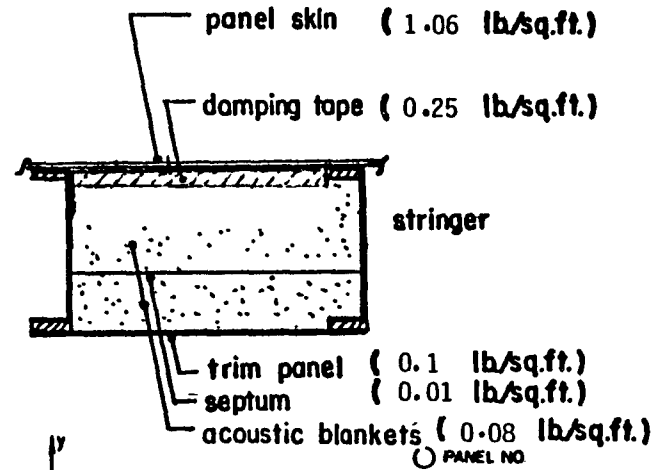
Fig. 71 Optimized interior noise (Panel No. 6)

ONE-THIRD OCTAVE BAND SOUND PRESSURE LEVEL IN dBA re 0.0002  $\mu$ bar



— baseline : OA = 78 dBA  
 --- optimized : OA = 69 dBA

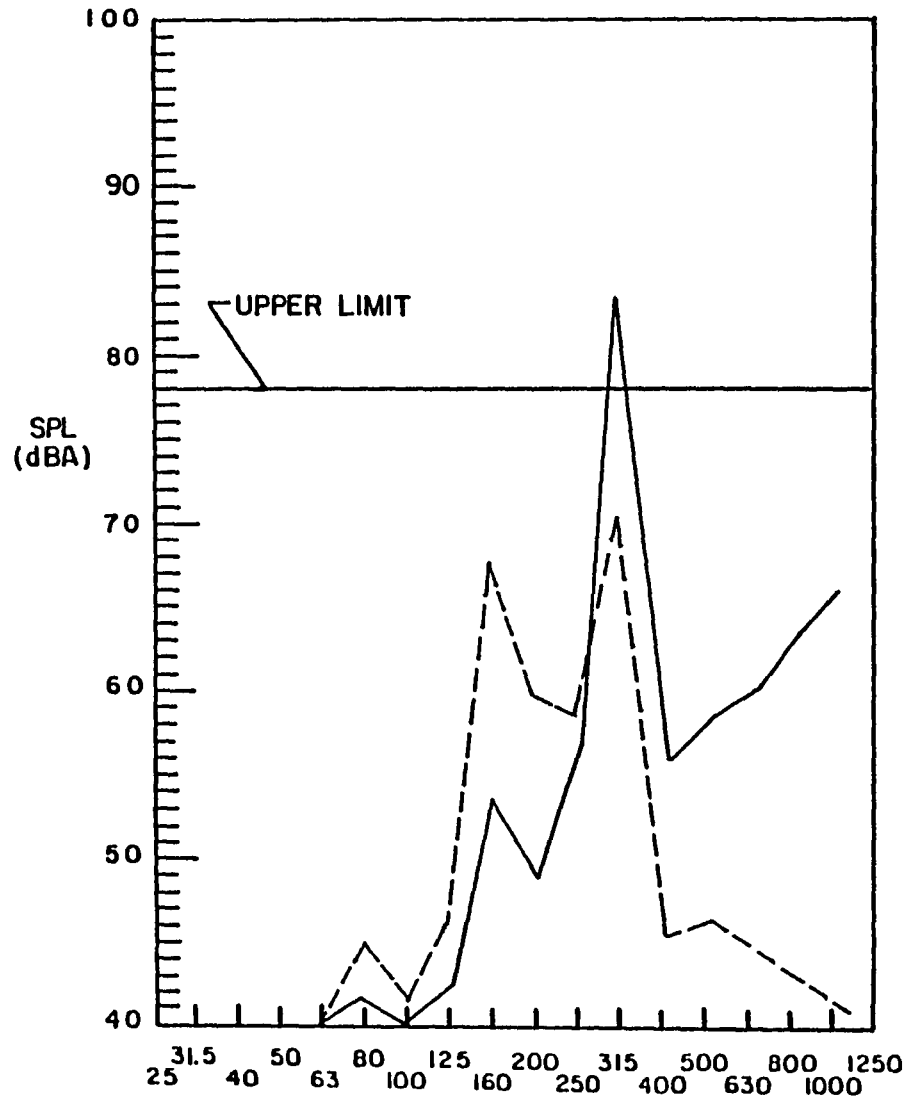
added weight = 0.42 lbs.  
 panel area = 0.77 sq.ft.



▨ - unit under study

Fig. 72 Optimized interior noise (Panel No. 9)

ONE-THIRD OCTAVE BAND SOUND PRESSURE LEVEL IN dBA re 0.0002  $\mu$ bar

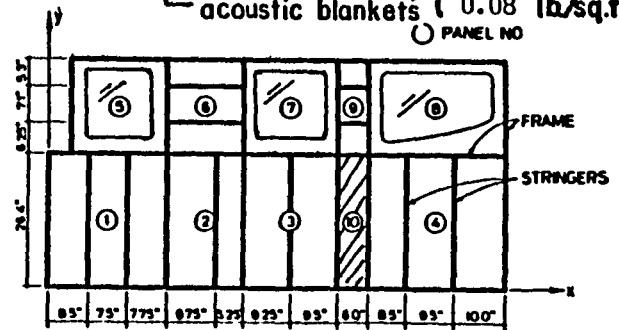
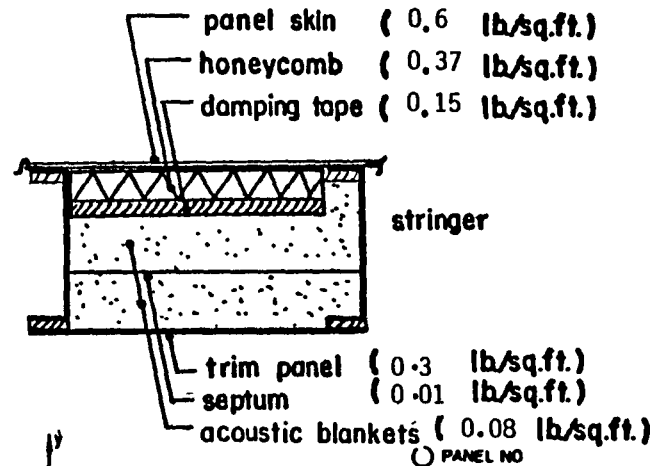


ONE-THIRD OCTAVE BAND CENTER FREQUENCIES IN Hz (cps)

Fig. 73 Optimized interior noise (Panel No. 10)

— baseline : OA = 86 dBA  
 --- optimized : OA = 73 dBA

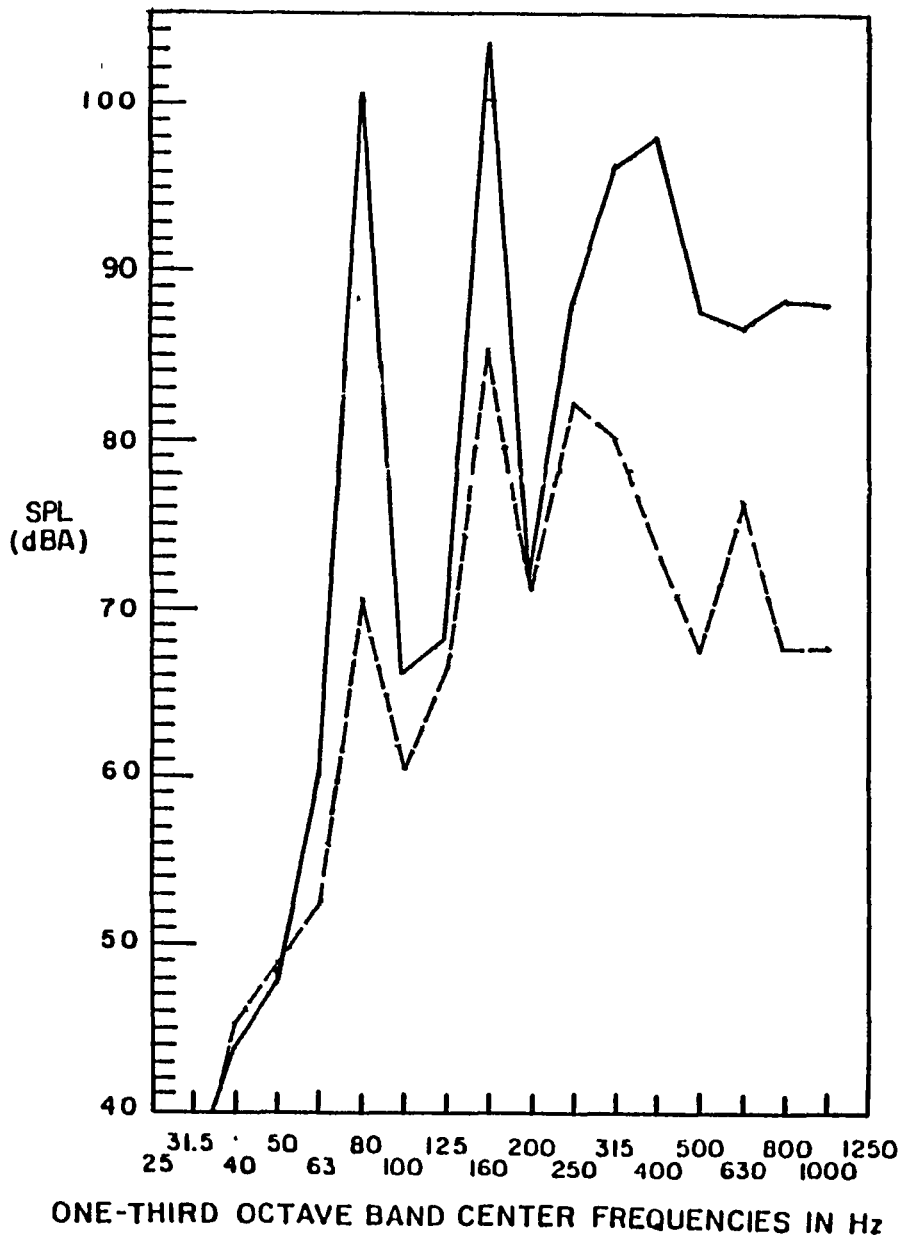
added weight = 1.14 lbs.  
 panel area = 1.1 sq.ft.



▨ - unit under study

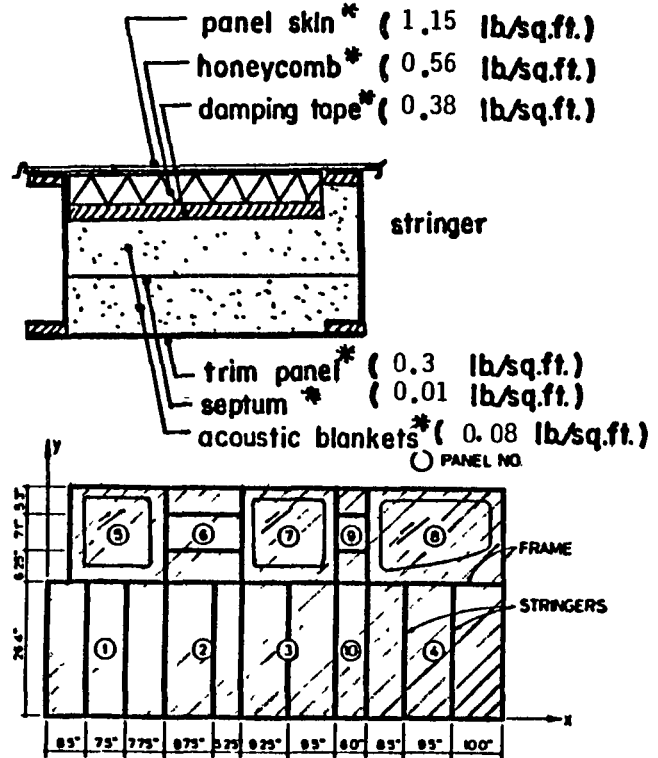
ONE-THIRD OCTAVE BAND SOUND PRESSURE LEVEL IN dBA re 0.0002  $\mu$ bar

-124-



— baseline : OA = 107 dBA  
 - - - optimized : OA = 88 dBA

added weight = 30 lbs.  
 panel area = 29 sq.ft.



▨ - unit under study  
 \* average values

Fig. 74 Optimized interior noise (Sidewall)

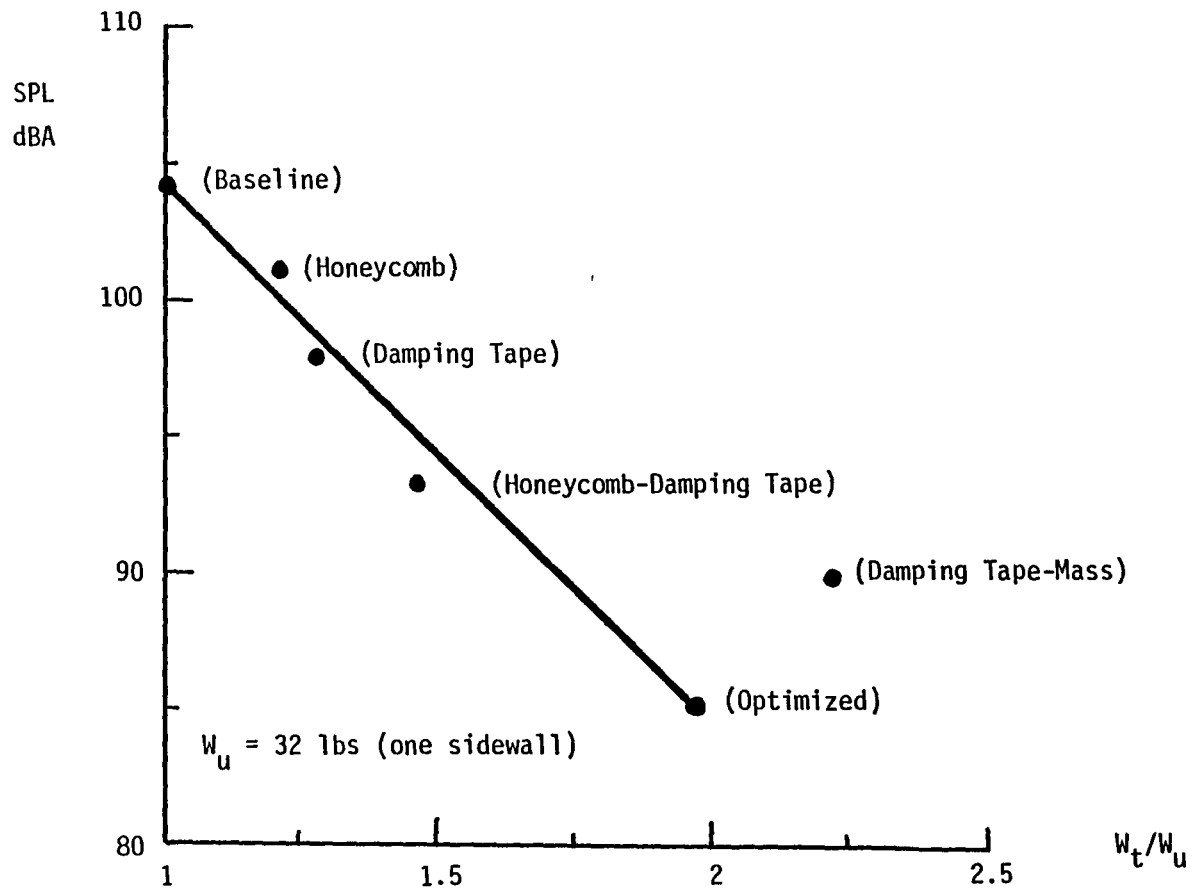


Fig. 75 Interior sound pressure levels vs the ratio of treated/untreated weight

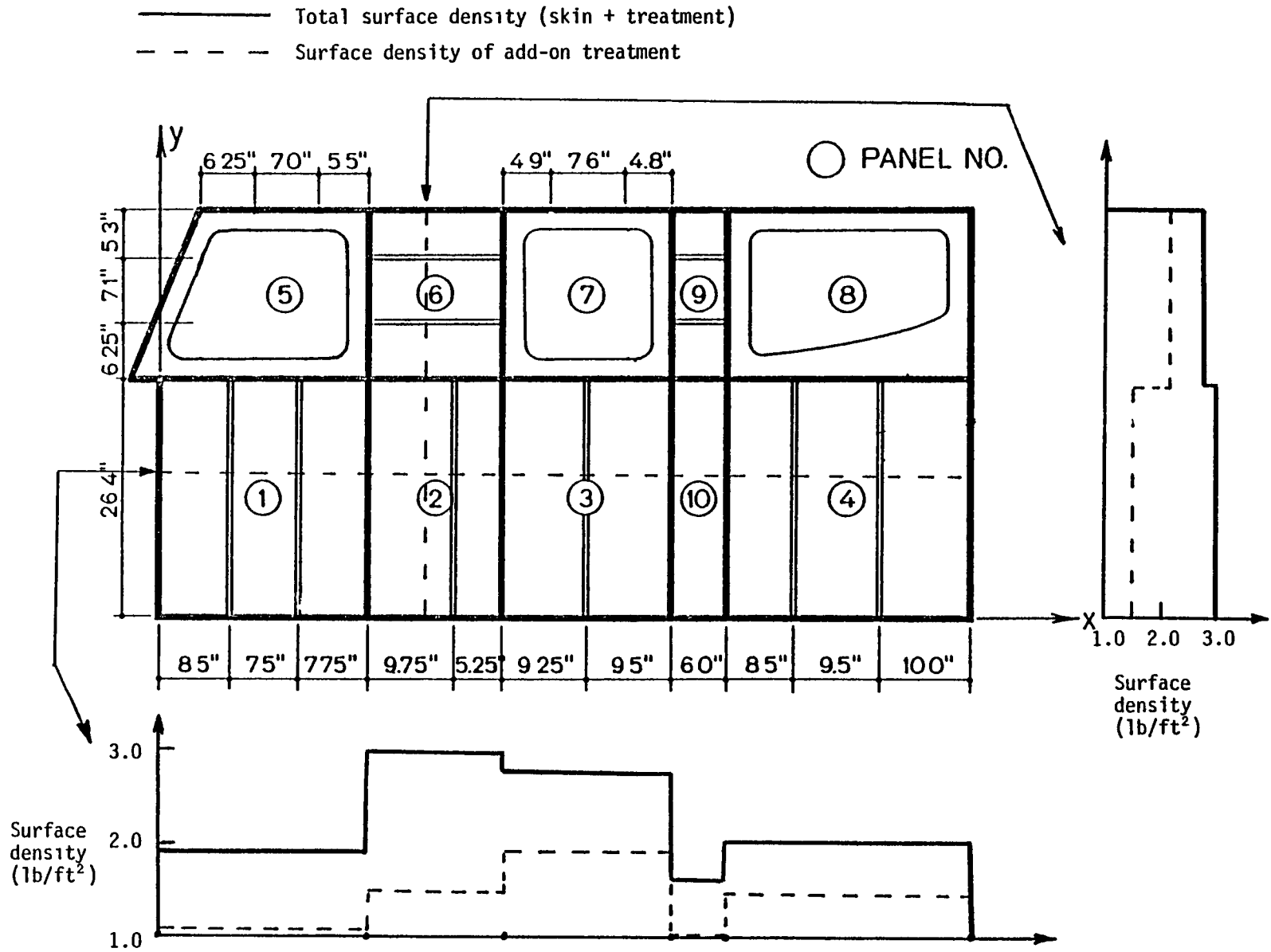
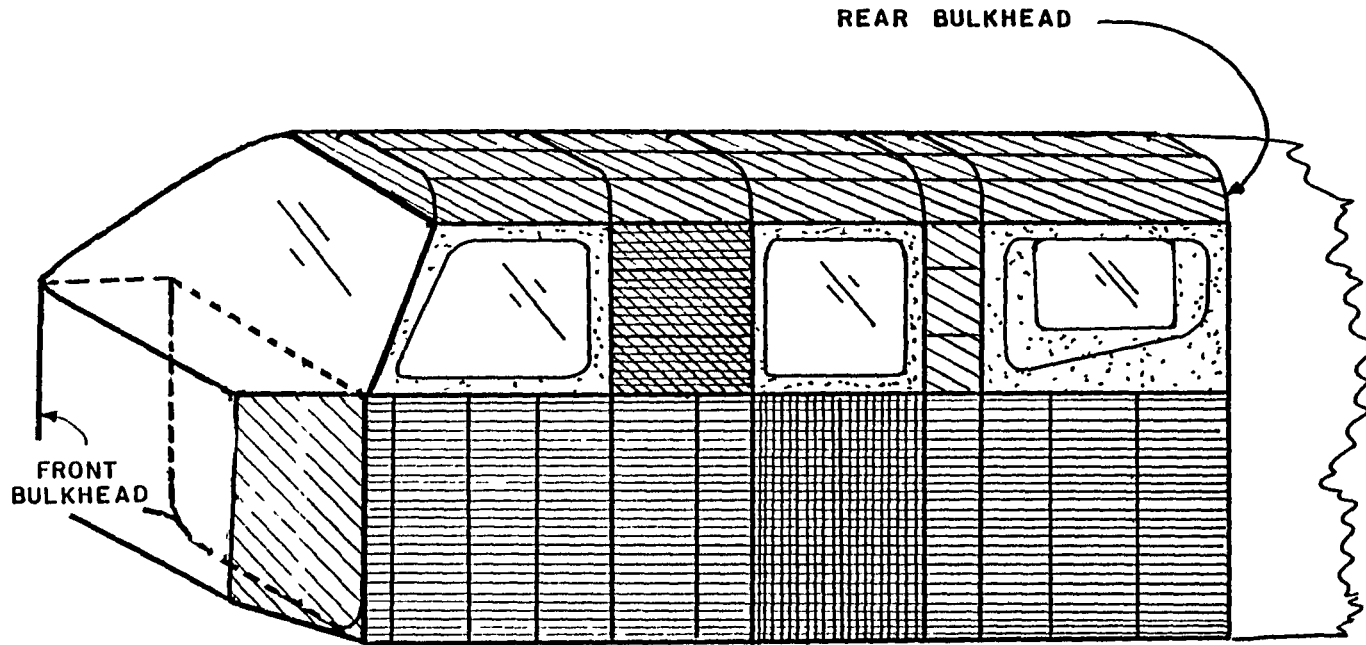


Fig. 76 Distribution of surface density

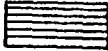


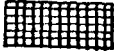
-127-

INTERIOR TREATMENT - AEROCOMMANDER

  
 Y-370  
 TNB-101-1/3  
 (0.58 lb/ft<sup>2</sup>)

  
 Y-370  
 1"AA  
 1"AA  
 Light trim  
 (0.5 lb/ft<sup>2</sup>)

  
 Honeycomb (0.37 lb/ft<sup>2</sup>)  
 Y-370  
 Soundfoil  
 1"AA  
 1"AA  
 TNB-101-1/3  
 (1.3 lb/ft<sup>2</sup>)

  
 Honeycomb (1.4 lb/ft<sup>2</sup>)  
 Y-370  
 1"AA  
 1"AA  
 Light trim  
 (1.95 lb/ft<sup>2</sup>)

  
 Honeycomb (0.37 lb/ft<sup>2</sup>)  
 Y-370  
 Soundfoil  
 1"AA  
 1"AA  
 TNB-101-1  
 (2.1 lb/ft<sup>2</sup>)

Fig. 77 The final configuration of add-on treatment for the AeroCommander aircraft

## APPENDIX A

### Elements of Transfer Matrices

The field and point matrices for the elastic stiffened panel from Ref. 16 are as follows:

(1) Point transfer matrix  $[G]$  is given for the stiffener shown in Fig. 16 by

$$[G] = \begin{bmatrix} 1 & 0 & 0 & 0 \\ 0 & 1 & 0 & 0 \\ d' & c' & 1 & 0 \\ -e' & -d' & 0 & 0 \end{bmatrix} \quad (A-1)$$

$$c' = E_S C_{WS} \left(\frac{n\pi}{L_X}\right)^4 + G_S C \left(\frac{n\pi}{L_X}\right)^2 - \rho_S I_S \omega^2 \quad (A-2a)$$

$$d' = E_S I_{\eta\xi} s_z \left(\frac{n\pi}{L_X}\right)^4 - \rho_S A c_y \omega^2 \quad (A-2b)$$

$$e' = E_S I_{\eta} \left(\frac{n\pi}{L_X}\right)^4 - \rho_S A \omega^2 \quad (A-2c)$$

where  $E_S, G_S$  and  $\rho_S$  are the modulus of elasticity, shear modulus, and mass density of the stringer, respectively. The warping constant with respect to the shear center  $C_{WS}$  is given by

$$C_{WS} = C + s_z^2 I_{\xi} \quad (A-3)$$

where  $C$  = St. Venant's constant of uniform torsion about the centroid,  $s_z$  is the perpendicular distance between the panel and an axis parallel to the  $\eta$  centroidal axis of the stiffener and passing through the shear center,  $I_{\xi}$

is the centroidal moment of inertia of the stiffener about the  $\xi$  centroidal axis of the stiffener and normal to the panel. The transformed inertia term  $I_s$  is given by

$$I_s = I_c + A[c_y^2 + (c_z - s_z)^2] \quad (A-4)$$

where  $I_c$  is the polar moment of inertia of the stiffener about the centroid,  $A$  is the area of the stiffener,  $c_y$  is the perpendicular distance between the shear center and  $\xi$  centroidal axis and  $c_z$  is the perpendicular distance between the shear center and  $\eta$  centroidal axis of the stiffener.  $I_{\eta\xi}$  is the product of inertia of the stiffener.

(2) Field matrix  $[F] = [B][R]([B]^{-1})$  where

$$[B] = \begin{bmatrix} 1 & 0 & 0 & 0 \\ 0 & 1 & 0 & 0 \\ -D\left(\frac{n\pi}{L_x}\right)^2 \nu & 0 & D & 0 \\ 0 & -D(2-\nu)\left(\frac{n\pi}{L_x}\right)^2 & 0 & D \end{bmatrix} \quad (A-5)$$

$$([B])^{-1} = \begin{bmatrix} 1 & 0 & 0 & 0 \\ 0 & 1 & 0 & 0 \\ \left(\frac{n\pi}{L_x}\right)^2 \nu & 0 & 1/D & 0 \\ 0 & (2-\nu)\left(\frac{n\pi}{L_x}\right)^2 & 0 & 1/D \end{bmatrix} \quad (A-6)$$

where  $D$  and  $\nu$  are the bending stiffness and Poisson's ratio for the panel,

respectively.

$$[R] = \begin{bmatrix} C_0 & S_{-1} & C_{-2} & S_{-3} \\ S_1 & C_0 & S_{-1} & C_{-2} \\ C_2 & S_1 & C_0' & S_{-2}' \\ S_3 & C_2 & S_1 & C_0' \end{bmatrix} \quad (A-7)$$

where

$$\begin{aligned} C_{-2} &= (\cosh\sigma_1 y_j - \cos\sigma_2 y_j)/s^2 \\ C_0 &= (\sigma_2^2 \cosh\sigma_1 y_j + \sigma_1^2 \cos\sigma_2 y_j)/s^2 \\ C_0' &= (\sigma_1^2 \cosh\sigma_1 y_j + \sigma_2^2 \cos\sigma_2 y_j)/s^2 \\ C_2 &= \sigma_1^2 \sigma_2^2 (\cosh\sigma_1 y_j - \cos\sigma_2 y_j)/s^2 \\ S_{-3} &= \{(1/\sigma_1) \sinh\sigma_1 y_j - (1/\sigma_2) \sin\sigma_2 y_j\}/s^2 \end{aligned} \quad (A-8)$$

$$\begin{aligned} S_{-1}' &= (\sigma_1 \sinh\sigma_1 y_j + \sigma_2 \sin\sigma_2 y_j)/s^2 \\ S_1 &= \sigma_1 \sigma_2 (\sigma_2 \sinh\sigma_1 y_j + \sigma_1 \sin\sigma_2 y_j)/s^2 \\ S_1' &= (\sigma_1^3 \sinh\sigma_1 y_j - \sigma_2^3 \sin\sigma_2 y_j)/s^2 \\ S_3 &= \sigma_1^2 \sigma_2^2 (\sigma_1 \sinh\sigma_1 y_j + \sigma_2 \sin\sigma_2 y_j)/s^2 \end{aligned}$$

$$s^2 = \sigma_1^2 + \sigma_2^2 \quad (A-9)$$

$$\sigma_1^2 = \{ \sqrt{\rho_p h_p / D} + (n\pi / L_x)^2 \}$$

$$\sigma_2^2 = \{ \sqrt{\rho_p h_p / D} - (n\pi / L_x)^2 \}$$

(A-10)

## APPENDIX B

### List of Symbols

A	= stringer cross-sectional area
a	= cabin dimension
$a_0, b_0$	= distances from x and y axes, respectively, to panel location
b	= cabin dimension
$b_2, b_4$	= propagation constants in porous materials 2 and 4, respectively, $b = \alpha + j\beta$
C	= Saint-Venant constant of uniform torsion
$C_w$	= warping constant of stringer cross-section
$C_{ws}$	= $C_w + I_\zeta s^2$
$c_y, c_z$	= distances defined in Fig. 16
c	= speed of sound
$c_1, \dots, c_6$	= speed of sound in regions 1, ..., 6, respectively
D	= elastic panel stiffness
$D_t$	= stiffness of honeycomb panel
$D_x, D_y$	= bending rigidities of skin-stringer panels
d	= cabin dimension
$d_2$	= distance between elastic panel and septum barrier
$d_4$	= distance between septum barrier and trim panel
E	= elastic modulus of the panel
$E_s$	= elastic modulus of the stringer
$E_1, E_2$	= elastic moduli of the facings of the honeycomb panel
[F]	= field transfer matrix
[G]	= point transfer matrix
$G_s$	= shear modulus of the stringer
H	= cross-rigidity of skin-stringer panel

$H_{mn}$	= frequency response function of the panel
$h$	= thickness of honeycomb core
$h_p$	= elastic panel thickness
$I_c$	= polar moment of inertia about stringer centroid
$I_\eta, I_\xi, I_{\eta\xi}$	= stringer cross-section polar moments of inertia and product of inertia, respectively, about the $\xi$ and $\eta$ axes
$I_s$	= transformed polar moment of inertia about point of attachment
$i$	= $\sqrt{-1}$
$i, j, k, \ell, m, n, r, s$	= indices
$K_2, K_4$	= compressibility ratios in regions 2 and 4, respectively
$L_{ijmn}$	= acoustic-structural modal coupling terms
$L_x, L_y$	= longitudinal and transverse dimensions of a panel, respectively
$M_{mn}$	= generalized mass
$M_n$	= bending moment amplitude
$m_s$	= panel mass per unit area
NR	= noise reduction
$p_{mn}^r$	= generalized random forces
$p$	= acoustic pressure
$p_0$	= reference acoustic pressure
$\bar{p}$	= Fourier transform of acoustic pressure
$\bar{p}^r$	= Fourier transform of input random pressure
$Q_n$	= shear amplitude of panel motions
$\bar{q}_{mn}$	= generalized coordinates of the panel
$R(\omega)$	= resistance of acoustic material
$R_1$	= flow resistivity of the porous material
$S_F$	= surface of a flexible wall
$S_i$	= spectral density of input noise for the $i$ -th panel

$S_{mnrs}$	= cross-spectral densities of generalized random forces
$S_p$	= spectral density of acoustic pressure
$S_w$	= deflection response spectral density of the panel
$S^e$	= cross-spectral density of pressure
$S_p^e$	= spectral density of external pressure
$S_p^i$	= spectral density of sound pressure transmitted by the i-th panel
SPL	= sound pressure levels
SPL <sup>T</sup>	= total sound pressure levels transmitted by all panels
$s_z$	= distance defined in Fig. 16
[T]	= transfer matrix
t	= time
$t_{ij}$	= elements of transfer matrix
$t'_1, t_2$	= thicknesses of honeycomb panel facings
V	= volume of airplane cabin
$V_x, V_y$	= convection velocities of propeller noise corresponding to direction along propeller rotation and perpendicular to it, respectively
$\{W_n\}$	= state vector
w	= panel deflection
$\bar{w}$	= Fourier transform of panel deflection
$X(\omega)$	= reactance of porous material
$X_{ij}$	= acoustic longitudinal-transverse modes
x,y,z	= spatial coordinates
$\bar{x}$	= spatial separation along the x axis, $\bar{x} = x_1 - x_2$
$Y_{mn}$	= structural modes
$Y_2, Y_4$	= porosity for porous materials in regions 2 and 4, respectively
$y_q$	= local coordinate

$\bar{y}$	= spatial separation along the y axis, $\bar{y} = y_1 - y_2$
Z	= impedance
$Z_A$	= acoustic impedance
$Z_p$	= impedance of untreated panel
$Z_2, Z_4$	= impedance of porous acoustic blankets in regions 2 and 4, respectively
$Z_3, Z_5$	= septum impedances
$Z_6$	= termination impedance
$\alpha_2, \alpha_4$	= real parts of propagation constants $b_2$ and $b_4$ , respectively
$\beta$	= acoustic damping coefficient
$\beta_2, \beta_4$	= imaginary parts of propagation constants $b_2$ and $b_4$ , respectively
$\Delta\omega$	= frequency bandwidth
$\Delta TL$	= additional noise transmission losses
$\delta_n$	= deflection amplitude
$\zeta$	= structural damping coefficient
$\zeta_{mn}$	= structural modal damping coefficients
$\theta_n$	= slope amplitude of panel motions
$\theta_1, \dots, \theta_6$	= incidence angles for different media
$\eta$	= loss factor of the sidewall
$\mu_1, \mu_3, \mu_5$	= surface densities of elastic panel, septum barrier, and trim panel, respectively
$\nu$	= Poisson's ratio
$\xi_0$	= acoustic damping coefficient
$\xi_{ij}$	= acoustic modal damping coefficients
$\rho$	= air density
$\rho_1, \dots, \rho_6$	= air densities for regions 1, ..., 6, respectively
$\rho_p$	= material density of the panel

$\rho_s$  = material density of the stringer  
 $\tau$  = transmission coefficient of add-on sidewall treatment  
 $\phi$  = azimuthal angle  
 $\omega$  = angular frequency  
 $\omega_{ij}$  = acoustic modal frequencies  
 $\omega_{mn}$  = structural modal frequencies

1 Report No NASA CR-165833		2. Government Accession No		3 Recipient's Catalog No	
4 Title and Subtitle Study of Cabin Noise Control for Twin Engine General Aviation Aircraft				5 Report Date February 1982	
				6 Performing Organization Code	
7 Author(s) R. Vaicaitis and M. Slazak				8 Performing Organization Report No 1	
				10 Work Unit No	
9 Performing Organization Name and Address Modern Analysis Inc. 825 Norgate Drive Ridgewood, N.J. 07450				11 Contract or Grant No NAS1-16117	
				13 Type of Report and Period Covered Contractor Report February 26, 1980 - pres.	
12 Sponsoring Agency Name and Address National Aeronautics and Space Administration Washington, D.C. 20546				14 Sponsoring Agency Code	
15 Supplementary Notes Langley Technical Monitor: Dr. John S. Mixson					
16 Abstract An analytical model based on modal analysis has been developed to predict the noise transmission into a twin-engine light aircraft. The model has been applied to optimize the interior noise to an A-weighted level of 85 dBA. To achieve the required noise attenuation, add-on treatments in the form of honeycomb panels, damping tapes, acoustic blankets, septum barriers and limp trim panels were added to the existing structure. The added weight of the noise control treatment is about 1.1% of the total gross take-off weight of the aircraft.					
17 Key Words (Suggested by Author(s)) Aircraft Interior Noise Propeller Noise Noise Optimization Add-On Treatments			18 Distribution Statement Unclassified - Unlimited Subject Category 71		
19 Security Classif (of this report) Unclassified		20 Security Classif (of this page) Unclassified		21 No of Pages 136	22 Price